

10th HIGH-TECH RESEARCH CENTER INTERNATIONAL SYMPOSIUM

“Supramolecular Science-Based Organic Materials and Devices”

Research Center for Materials with Integrated Properties, Toho University, Funabashi, Japan
*Supported Program for Strategic Research Foundation at Private Universities (2012–2016),
Ministry of Education, Culture, Sports, Science and Technology, Japan*

Narashino Campus
Toho University, Funabashi, Chiba 274-8510, Japan

December 9-11, 2016



Toho University

Welcome to International Symposium on Supramolecular Science Based on Organic Devices and Materials

It is our great pleasure to welcome to the International Symposium on Supramolecular Science Based on Organic Devices and Materials, which is held in Funabashi, Chiba, Japan on December 9-11, 2016.

The International Symposium on “Supramolecular Science Based on Organic Devices and Materials” is organized by the Research Center for Materials with Integrated Properties (RCMIP), Toho University. The RCMIP was established as an interdepartmental research center by researchers in Chemistry, Physics, and Molecular Biology Departments in 2005 under the financial support from the Ministry of Education, Culture, Sports, Science and Technology (MEXT). After the five years in “The High-tech Research Center Project (2005-2009)” had finished, the RCMIP obtained a grant “The supported Program for Strategic Research Foundation at Private Universities” from the MEXT again. The project entitled “Creation and Evaluation of Rare Earth Metal-alternative Organic Materials Based on Supramolecular Science” started from 2012. Supramolecular science covers a wide variety of science, and the purpose of this project is to develop new materials and devices using supramolecular systems which are a kind of new knowledge and technology. The project has accelerated not only individual works, but also collaboration works between researchers in different fields.

The symposium has been planned to summarize our five years outcomes as well as offer a forum for encouraging the communications among the various scientific communities. We invited fifteen outstanding guest speakers from France, Korea, Russia, Spain, the United States, and domestic. We hope that all the participants including graduate and undergraduate students may enjoy the two days program.

Finally, I would like to thank all the staffs, students, and some companies for supporting the symposium.



Yoichi Habata. Ph.D.
Director of RCMIP
Toho University

10th HIGH-TECH RESEARCH CENTER INTERNATIONAL SYMPOSIUM

“Supramolecular Science-Based Organic Materials and Devices”

Research Center for Materials with Integrated Properties, Toho University, Funabashi, Japan
*Supported Program for Strategic Research Foundation at Private Universities (2012–2016),
Ministry of Education, Culture, Sports, Science and Technology, Japan*

Narashino Campus
Toho University, Funabashi, Chiba 274-8510, Japan

December 9–11, 2016

Conference Chair:

Y. Habata (Toho Univ.)

T. Kawarabayashi (Toho Univ.)

Organizer:

Research Center for Materials with Integrated Properties, Toho University, Funabashi, Japan

Co-organizer:

Faculty of Science, Toho University, Funabashi, Japan

Sponsors:

FEI Company Japan Ltd.

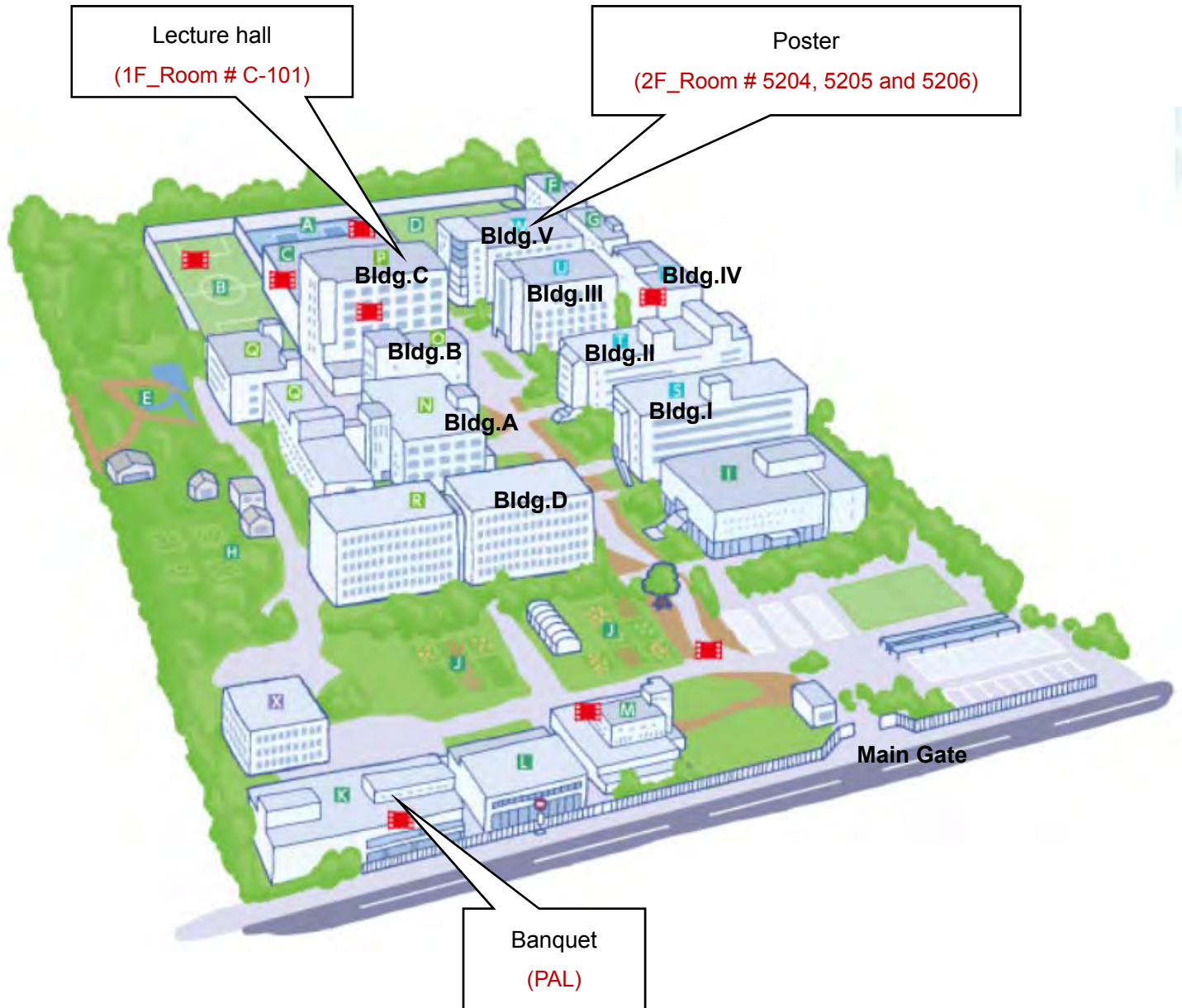
Wavefunction, Inc.

Bruker AXS K.K.

KANTO CHEMICAL CO., INC.



Toho Univ. Narashino Campus Map



Program (Saturday, December 10)

ORAL PRESENTATIONS 1 (Room #C-101)

Chairman: *Kawarabayashi (Toho Univ.)*

10:00–10:10 [Opening Remarks] Y. Habata (Toho Univ.)

10:10–10:20 [Welcome Remarks] J. Yamazaki (President of Toho Univ.)

Chairman: *T. Kawarabayashi (Toho Univ.)*

10:20–10:40 [Lecture-1] **J. Ohe (Toho Univ.)**

"Topologically protected spin-wave propagation in magnonic crystals"

Chairman: *T. Kitazawa (Toho Univ.)*

10:40–11:10 [Invited lecture-1] **K. Maryunina (Hiroshima Univ.)**

"Pressure/temperature induced magnetic anomalies in Cu(II)-nitroxides complexes"

11:10–11:20 Coffee break

Chairman: *R. Saito (Toho Univ.)*

11:20–12:10 [Plenary lecture-1] **K. Kim (POSTECH, S. Korea)**

"Nanostructured materials by covalent self-assembly"

12:10–13:30 Lunch

13:30–14:30 **POSTER SESSION (Room # 5204, 5205 and 5206)**

[Invited Poster Presenters] K.-M. Park (Gyeongsang National Univ. S. Korea)
E. Lee (Gyeongsang National Univ. S. Korea)
H. Ju (Gyeongsang National Univ. S. Korea)

ORAL PRESENTATIONS 2 (Room #C-101)

Chairman: *N. Tajima (Toho Univ.)*

14:40–15:00 [Lecture-2] **E. Wada (Toho Univ.)**

"Interfacial frustration originating from quantum well formation in epitaxial Fe/Ag/Cr trilayers"

Chairman: *N. Tajima (Toho Univ.)*

15:00–15:30 [Invited lecture-2] **M. Mizuguchi (Tohoku Univ.)**

"Artificial Synthesis of Magnetically Anisotropic Materials in Iron Meteorite by Atomic Building Blocks"

15:30–15:40 Coffee break

Chairman: *T. Sugai (Toho Univ.)*

15:40–16:10 [Invited lecture-3] **T. Naito (Ehime Univ.)**

"Optical Control of Carriers and Spins in Molecular Materials"

Chairman: *T. Sugai (Toho Univ.)*

16:10–16:40 [Invited lecture-4] **K. Suenaga (AIST)**

"Hetero-structures of low-dimensional materials studied by atomic resolution STEM"

Chairman: *T. Kitazawa (Toho Univ.)*

16:40–17:10 [Invited lecture-5] **J. A. Rodríguez-Velamazán**

(Institut Laue-Langevin, Grenoble, France)

"New molecular materials studied by neutron scattering"

17:20–19:00 Banquet (PAL)

Program (Sunday, December 11)

ORAL PRESENTATIONS 3 (Room #C-101)

Chairman: T. Sugai (Toho Univ.)

- 10:10–10:40 [Invited lecture-6] **T. Ishida (Univ. of Electro-Communications)**
"Exchange-Coupled Heavy-Lanthanoid and Nitroxide Molecular Magnets"
Chairman: T. Sugai (Toho Univ.)
- 10:40–11:10 [Invited lecture-7] **H. Yoshikawa (Kwansei Gakuin Univ.)**
"Solid-state electrochemistry of coordination compounds"
- 11:10–11:20 Coffee break
Chairman: N. Tajima (Toho Univ.)
- 11:20–12:10 [Plenary lecture-2] **R. Kato (RIKEN)**
"Molecular quantum spin liquid"
- 12:10–13:20 Lunch
- 13:20–14:20 **POSTER SESSION (Room # 5204, 5205 and 5206)**

ORAL PRESENTATIONS 4 (Room #C-101)

Chairman: N. Hirayama (Toho Univ.)

- 14:20–14:40 [Lecture-3] **T. Sugai (Toho Univ.)**
"Development of multi-stage ion trap ion mobility measurement system"
Chairman: T. Sugai (Toho Univ.)
- 14:40–15:10 [Invited lecture-8] **Alexandre A. Shvartsburg (Wichita State Univ. USA)**
"High-resolution FAIMS for proteomics, lipidomics, and structural elucidation based on isotopologic shifts"
- 15:10–15:20 Coffee break
Chairman: N. Hirayama (Toho Univ.)
- 15:20–15:50 [Invited lecture-9] **T. Mochida (Kobe Univ.)**
"Ionic liquids from metal complexes: physical properties and chemical reactivities"
Chairman: R. Saito (Toho Univ.)
- 15:50–16:20 [Invited lecture-10] **M. Nakamura (Toho Univ.)**
"New insight into the electronic and magnetic structures of iron porphyrin complexes"
Chairman: J. Ishii (Toho Univ.)
- 16:20–16:40 [Lecture-4] **M. Hasegawa (Toho Univ.)**
"Liquid-crystalline Polymers with Benzoxazole Units for Application as Thermally Conductive Films"
- 16:40–17:10 [Closing Ceremony] T. Kawarabayashi (Toho Univ.)

Posters (December 10, 11)

(Room # 5204)

IP_1. "Calix[4]arene-based Metal-Organic Frameworks (CalixMOFs) & Metallopolycapsular Networks"

Eunji Lee, Huiyeong Ju, Suk-Hee Moon,[†] and Ki-Min Park^{*}

Research Institute of Natural Science and Department of Chemistry, Gyeongsang National University, Jinju 52828, Republic of Korea., [†] Department of Food and Nutrition, Kyungnam College of Information and Technology, Busan 47011, Republic of Korea.

IP_2. "Cation-Selective and Anion-Controlled Fluorogenic Behaviors of a Benzothiazole-Attached Macrocyclic That Correlate with Structural Coordination Modes"

Huiyeong Ju,^a Duk Jin Chang,^{a,b} Seulgi Kim,^a Hyunsoo Ryu,^a Eunji Lee,^a In-Hyeok Park,^a Mari Ikeda,^c Yoichi Habata,^{*,d} and Shim Sung Lee^{*,a}

^aDepartment of Chemistry, Gyeongsang National University, Jinju 52828, S. Korea, ^bBongilcheon High School, Paju 10938, S. Korea, ^cEducation Center, Faculty of Engineering, Chiba Institute of Technology, Japan, ^dDepartment of Chemistry, Faculty of Science, Toho University, Japan

IP_3. "Metallation-Mediated Adaptive Guest Binding: Formation of Cascade Complexes with Pillar[5]-bis-thiacrown as a New Fused Macrocyclic"

Eunji Lee and Shim Sung Lee^{*}

Department of Chemistry, Gyeongsang National University, S. Korea

(Room # 5204)

P_1. "Aggregation and disaggregation of highly water-soluble phthalocyanines"

H. Isago and H. Fujita

National Institute for Materials Science (NIMS)

P_2. "Structure and Thermodynamics of Bis(tetra-armed cyclen)/Ag⁺ Complex"

M. Iwase^{*}, C. Kachi-Terajima^{*,**}, M. Ikeda^{***}, S. Kuwahara^{*,**}, and Y. Habata^{*,**}

^{}Department of Chemistry, Faculty of Science, Toho University, ^{**}Research Center for Materials with Integrated Properties, Toho University, ^{***}Department of Chemistry, Education Centre, Faculty of Engineering, Chiba Institute of Technology*

P_3. "Synthesis of Cylindrical Cyclen-Based Cryptands and Allosteric Property of their Ag⁺ Complexes"

S. Kamo^{*}, Y. Nihei^{*}, M. Ikeda^{**}, S. Kuwahara^{*,***}, and Y. Habata^{*,***}

^{} Department of Chemistry, Faculty of Science, Toho University, ^{**} Education Centre, Faculty of Engineering, Chiba Institute of Technology, ^{***} Research Centre for Materials with Integrated Properties, Toho University*

P_4. "Synthesis of Dendrimer-type Penta Cyclen"

F. Nemoto^{*}, M. Iwase^{*}, M. Ikeda^{**}, S. Kuwahara^{*,***}, and Y. Habata^{*,***}

^{}Department of Chemistry, Faculty of Science, Toho University, ^{**}Department of Chemistry, Education Centre, Faculty of Engineering, Chiba Institute of Technology, ^{***}Research Center for Materials with Integrated Properties, Toho University,*

P_5. "Ionic liquid chelate extraction of trivalent metals using 2-mercaptopyridine N-oxide"

Ayano Eguchi^{*}, Kotaro Morita^{*}, and Naoki Hirayama^{*,**}

^{} Department of Chemistry, Faculty of Science, Toho University, ^{**} Research Center for Materials with Integrated Properties, Toho University*

P_6. “Anion-exchange transport behavior of zinc(II) as its thiocyanato complex through ionic liquid supported liquid membrane”Aika Suda^{*}, Kotaro Morita^{*}, and Naoki Hirayama^{*,**}^{*} Department of Chemistry, Faculty of Science, Toho University, ^{**} Research Center for Materials with Integrated Properties, Toho University**P_7. “Extraction behavior of Fe(II) and Fe(III) in ionic liquid triphasic extraction system using 2,2'-bipyridine and TOPO”**Mizuki Toita^{*}, Kotaro Morita^{*}, and Naoki Hirayama^{*,**}^{*} Department of Chemistry, Faculty of Science, Toho University, ^{**} Research Center for Materials with Integrated Properties, Toho University**P_8. “Ionic liquid chelate extraction of divalent metals using 1-(2-pyridylazo)-2-naphthol”**Wataru Tsuzaki^{*}, Kotaro Morita^{*}, and Naoki Hirayama^{*,**}^{*} Department of Chemistry, Faculty of Science, Toho University, ^{**} Research Center for Materials with Integrated Properties, Toho University**P_9. “Cadmium(II) cyanide complexes containing 2-alkoxyethanol”**Takeshi Kawasaki^{*} and Takafumi Kitazawa^{*,#}^{*} Department of Chemistry, Faculty of Science, Toho University, [#] Research Center for Materials with Integrated Properties, Toho University**P_10. “Multistep Spin-Crossover Complex Fe(4-methylpyrimidine)₂[Au(CN)₂]₂”**Kosuke Kitase¹, Jun Okabayashi², and Takafumi Kitazawa^{*1,3},¹ Department of Chemistry, Faculty of Science, Toho University, ² Research Center for Spectrochemistry, The University of Tokyo, ³ Research Center for Materials with Integrated Properties, Toho University**P_11. “The designing of spin crossover behavior by controlling cooperativity by using Hoffman-like structural system”**T. Kosone^{*}, T. Kawasaki^{**}, J. Okabayashi and T. Kitazawa^{***}^{*} Department of Creative Technology Engineering, National Institute of Technology, Anan College, ^{**} Department of Chemistry, Faculty of Science, Toho University, ^{***} Research Center for Spectrochemistry, University of Tokyo**P_12. “Spin Crossover Coordination Polymer based [Au(III)(CN)₄]⁻ unit”**Kouhei Mitani¹, and Takafumi Kitazawa^{1,2}¹ Department of Chemistry, Faculty of Science, Toho University, ² Research Center for Materials with Integrated Properties, Toho University**P_13. “Spin Crossover in Fe^{II} compounds based on the [M(CN)₄]²⁻ (M = Ni, Pd, Pt) units”**Suzue Saito¹, Takafumi Kitazawa^{1,2}¹ Department of Chemistry, Faculty of Science, Toho University, ² Research Center for Materials with Integrated Properties, Toho University**P_14. “Spin crossover behavior in 2 dimensional MOF; Fe(Ethyl Isonicotinate)₂M(CN)₄ (M = Ni, Pd, Pt)”**Hitomi Shiina¹, Jun Okabayashi², Masashi Takahashi^{1,3}, and Takafumi Kitazawa^{1,3}¹ Department of Chemistry, Faculty of Science, Toho University, ² Research Center for Spectrochemistry, The University of Tokyo, ³ Research Center for Materials with Integrated Properties, Toho University**(Room # 5205)****P_15. “Spin Crossover MOF Materials with 4-(5-Nonyl)pyridine”**Tomoyuki Shimoide¹, Takafumi Kitazawa^{1,2}¹ Department of Chemistry, Faculty of Science, Toho University, ² Research Center for Materials with Integrated Properties, Toho University

P_16. “Synthesis of Fe(II)-Au(I) 2D Hofmann-type spin crossover compounds using n-Ethynylpyridine”

Shiho Suzuki¹, Takafumi Kitazawa^{1,2}

¹ Department of Chemistry, Faculty of Science, Toho University, ² Research Center for Materials with Integrated Properties, Toho University

P_17. “Correlation between Guest molecules and 2D Hofmann-type Spin crossover complexes”

Yusuke Ueki¹, Jun Okabayashi², and Takafumi Kitazawa^{1,3}

¹ Department of Chemistry, Faculty of Science, Toho University, ² Research Center for Spectrochemistry, The University of Tokyo, ³ Research Center for Materials with Integrated Properties, Toho University

P_18. “Numerical study of irrational charges in fermion vortex systems”

R.Itagaki, Y.Hatsugai *, H.Aoki**, T.Kawarabayashi

Toho University, *Institute of physics, University of Tsukuba, ** Department of Physics, University of Tokyo, and Advanced Industrial Science and Technology(AIST)

P_19. “The effect of spin-orbit interaction on the spin current in helimagnets”

Koujiro Hoshi, Jun-ichiro Ohe

Department of Physics, Toho University

P_20. “Internal deformation of magnetic skyrmion due to excitation of exchange spin-wave mode”

Yuhki Shimada and Jun-ichiro Ohe

Department of Physics, Toho University

P_21. “Acceleration of micromagnetics simulation using GPU”

Takumi Sugiura, Junichiro Ohe

Department of Physics, Toho University

P_22. “ α -Methylphenacyl thioesters as convenient thioacid precursors”

T. Hatanaka*, R. Yuki*, R. Saito*** and K. Sasaki*

* Department of Chemistry, Faculty of Science, Toho University, ** Research Center for Materials with Integrated Properties, Toho University

P_23. “Structure-activity relationship study on the inhibition of aldose reductase by botryllazine B analogues having bicyclic heterocycles on the C6 position”

A. Kato*, K. Sasaki**, and R. Saito**, ***

*Grad. School of Toho University, ** Department of Chemistry, Faculty of Science, Toho University, *** Research Center for Materials with Integrated Properties, Toho University

P_24. “Synthesis of acetamidopyrazine dendrimer as fluorescent chemosensor”

R. Saito*, **

* Department of Chemistry, Faculty of Science, Toho University, ** Research Center for Materials with Integrated Properties, Toho University

P_25. “Structure-activity relationship study of (Z)-4-arylmethylidene-1H-imidazol-5(4H)-ones as aldose reductase inhibitors”

A. Kato* and R. Saito**, ***

*Grad. School of Toho University, ** Department of Chemistry, Faculty of Science, Toho University, *** Research Center for Materials with Integrated Properties, Toho University

P_26. “Synthesis of fluorescent dendrimer having 2,5-bis(benzimidazol-2-yl)pyrazine core”

Y. Suzuki^{*}, K. Sasaki^{**}, and R. Saito^{**}, ^{***}

^{*}Grad. School of Toho University, ^{**} Department of Chemistry, Faculty of Science, Toho University, ^{***} Research Center for Materials with Integrated Properties, Toho University

P_27. “Synthesis of glycosyl donors bearing the 2,6-lactam moiety”

M. Tatsuta^{*}, Y. Hashimoto^{*}, R. Saito^{**}, ^{***} and K. Sasaki^{*}

^{*} Department of Chemistry, Faculty of Science, Toho University, ^{**} Research Center for Materials with Integrated Properties, Toho University

P_28. “Control of fluorescence color of 2,5-bis(benzimidazol-2-yl)pyrazines with substituent effects”

T. Yanagiba^{*}, K. Sasaki^{**}, and R. Saito^{**}, ^{***}

^{*}Grad. School of Toho University, ^{**} Department of Chemistry, Faculty of Science, Toho University, ^{***} Research Center for Materials with Integrated Properties, Toho University

P_29. “Improved gram-scale synthesis of shikonin derivatives”

M. Ono^{*}, K. Sasaki^{**}, and R. Saito^{**}, ^{***}

^{*}Grad. School of Toho University, ^{**} Department of Chemistry, Faculty of Science, Toho University, ^{***} Research Center for Materials with Integrated Properties, Toho University

P_30. “Synthesis of propeller shaped triple[5]helicene derivatives”

Hiroaki Hiyama,¹ Tomoya Matsushima,^{1,2} Soichiro Watanabe^{1,2}

¹ Department of Biomolecular Science, Faculty of Science, Toho University, ² Research Center for Materials with Integrated Properties, Toho University

P_31. “Synthesis of Triple Helicene Cage”

Tomoya Matsushima, Soichiro Watanabe

Department of Biomolecular Science, Faculty of Science, Toho University, Research Center for Materials with Integrated Properties, Toho University

(Room # 5206)

P_32. “Dissociative Ionization Processes of Molecules by Scattered Electron–Ion Coincidence Measurements”

T. Hasegawa, K. Takahashi, K. Homma, S. Oomori, N. Miyauchi, and Y. Sakai

Department of Physics, Faculty of Science, Toho University

P_33. “Development of a Time-of-Flight Mass Spectrometer Combined with an Ion Attachment Method”

Y. Motegi^{*}, K. Takeuchi^{*}, C. Mori^{*}, K. Takahashi^{*}, and Y. Sakai^{**}, ^{***}

^{*} Department of Physics, Faculty of Science, Toho University, ^{**} Research Center for Materials with Integrated Properties, Toho University

P_34. “Production and characterization of fluorescent gold nanoclusters”

Y. Hamano, and T. sugai

Department of Chemistry, Faculty of Science, Toho University

P_35. “Flow rate dependence of production of double-wall carbon nanotubes by high-temperature pulsed-arc discharge”

Yuto Hikichi, Toshiki Sugai

Department of Chemistry, Faculty of Science, Toho University

P_36. “Production and characterization of graphene quantum dots”H. Morita, and T. sugai*Department of Chemistry, Faculty of Science, Toho University***P_37. “Coulomb Interaction in Hole-Doped Molecular Dirac Fermion Systems”**Y. Akita¹, E. Tsuboi¹, S. Hayashi¹, K. Ogawa¹, N. Tajima^{1,2}, Y. Kawasugi², M. Suda³, H. M. Yamamoto^{2,3}, R. Kato², Y. Nishio¹ and K. Kajita¹¹ Department of Physics, Faculty of Science, Toho University, ² RIKEN, ³Institute for Molecular Science**P_38. “Angle dependent interlayer magnetoresistance in multilayered Dirac fermion systems”**K. Ogawa¹, S. Hayashi¹, Y. Akita¹, N. Tajima^{1,2}, Y. Kawasugi², M. Suda³, H. M. Yamamoto^{2,3}, R. Kato², Y. Nishio¹ and K. Kajita¹¹ Department of Physics, Faculty of Science, Toho University, ² RIKEN, ³Institute for Molecular Science**P_39. “Polyimides derived from Novel Cycloaliphatic Tetracarboxylic Dianhydride.”**Hiroki SATO, Shuichi TAKAHASHI, Junichi ISHII, Masatoshi HASEGAWA*Department of Chemistry, Faculty of Science, Toho University***P_40. “In-plane Orientation in Colorless Polyimides as Induced by Solution Casting from Polyimide Varnishes (20)”**Shinya TAKAHASHI, Soichi TSUKUDA, Junichi ISHII, Masatoshi HASEGAWA*Department of Chemistry, Faculty of Science, Toho University***P_41. “Polyalkylfluorene incorporating azomethine units for OLED applications”**Yoshifumi KURIHARA, Junichi ISHII, Masatoshi HASEGAWA*Department of Chemistry, Faculty of Science, Toho University***P_42. “Polybenzoxazoles with Low Coefficient of Thermal Expansion. Effect of Amide-containing Bis(o-aminophenol)”**Ryosuke WATANABE, Junichi ISHII, Masatoshi HASEGAWA*Department of Chemistry, Faculty of Science, Toho University***P_43. “Effect of chemical substitution on the relaxation time distribution for a spin ice compound Dy₂Ti₂O₇”**Akira Horikawa^A, Masaki Azuma^A, Eiji Wada^B, Daisuke Akahoshi^{A,B}, and Toshiaki Saito^{A,B}^ADept. of Phys., Toho Univ., ^BResearch Center for Materials with Integrated Properties, Toho Univ.**P_44. “Effect of random anisotropy on critical lines in H-T plane for a RKKY Heisenberg-type spin glass amorphous GdSi system”**Koki Kato^A, Ryosuke Motoki^A, Hiroshi Kobayashi^A, Kazuya Nakazawa^A, Eiji Wada^B, Daisuke Akahoshi^{A,B}, and Toshiaki Saito^{A,B}^ADept. of Phys., Toho Univ., ^BResearch Center for Materials with Integrated Properties, Toho Univ.**P_45. “Effect of R-site randomness on the physical properties near the multicritical point in ordered RBaMn₂O₆”**Norihisa Tanikawa^A, Hiroki Takada^A, Miyuki Hori^A, Eiji Wada^B, Ryo Oda^C, Hideki Kuwahara^C, Daisuke Akahoshi^{A,B}, and Toshiaki Saito^{A,B}^ADept. of Phys., Toho Univ., ^BResearch Center for Materials with Integrated Properties, Toho Univ., ^CDept. of Phys., Sophia Univ.

P_46. “Magnetoelectric properties for perovskite-type oxide $\text{EuTi}_{1-x}\text{Al}_x\text{O}_3$ ($0 \leq x \leq 1$)”

Shuto Koshikawa^A, Takuro Nagase^A, Eiji Wada^B, Kosuke Nishina^C, Ryo Kajihara^C, Hideki Kuwahara^C,
Daisuke Akahoshi^{A,B}, and Toshiaki Saito^{A,B}

^ADept. of Phys., Toho Univ., ^BResearch Center for Materials with Integrated Properties, Toho Univ., ^CDept. of Phys., Sophia Univ.

P_47. “Effect of random uniaxial anisotropy on critical lines in H-T plane for a RKKY Heisenberg spin glass amorphous GdDySi system”

Ryosuke Motoki^A, Koki Kato^A, Hiroshi Kobayashi^A, Kazuya Nakazawa^A, Masaya Mitsuishi^A, Eiji Wada^B,
Daisuke Akahoshi^{A,B}, and Toshiaki Saito^{A,B}

^ADept. of Phys., Toho Univ., ^BResearch Center for Materials with Integrated Properties, Toho Univ.

P_48. “Dependence of Ag/Cr interfacial frustration on the growth temperature for epitaxial Fe/Ag/Cr trilayers:”

Kyosuke Yokoyama^A, Eiji Wada^B, Kento Kato^A, Daisuke Akahoshi^{A,B}, and Toshiaki Saito^{A,B}

^ADept. of Phys., Toho Univ., ^BResearch Center for Materials with Integrated Properties, Toho Univ.

Plenary Lectures

(50 min. inc. discussion)

Nanostructured materials by covalent self-assembly

Kimoon Kim

*Center for Self-assembly and Complexity, Institute for Basic Science, Pohang, Korea
and
Department of Chemistry, Pohang University of Science and Technology, Pohang, Korea
E-mail: kkim@postech.ac.kr*

Keywords: self-assembly, nanomaterials, covalent bond

One of the most exciting developments in chemistry during the last two decades is construction of nanostructured objects or materials from small building blocks by self-assembly. However, most of these studies utilize weak noncovalent interactions between building blocks, which allow a reversible process ultimately leading to the formation of thermodynamically most stable species. However, due to the weak and reversible nature of noncovalent interactions quite often, the resulting nanostructures are not robust enough to be useful for practical applications. An intriguing question is whether we use strong (and therefore quite likely irreversible) covalent bonds for self-assembly. Over the last 10 years, despite skepticism, we successfully demonstrated that we can indeed construct robust nanostructured objects from small building blocks in a one-pot synthesis through *strong (therefore likely to be irreversible) covalent bond formation* without the aid of templates.

What we first demonstrated was the direct synthesis of nanometer-sized polymer hollow spheres without needs for any pre-organized structures or templates, and core-removal.^[1] In this work, flat and rigid-core tectons with multiple functional groups isotropically predisposed in all directions were cross-linked with linear linkers through irreversible covalent bond formation. These polymer capsules are useful in many applications including targeted drug delivery, photodynamic therapy, catalysis, and imaging. Extending this

work, we also demonstrated the synthesis and isolation of micrometer-scale 2D polymer sheets of single-molecular thickness,^[2] which may find interesting applications including separation and sensor. Very recently, this strategy has also been extended to synthesize other nanostructured materials including hollow nanotubular toroidal polymer microrings.^[3] These are rare examples of covalent self-assembly under kinetic control,^[4] and some of recent progress will be presented.

References

- [1] (a) D. Kim et al. *Angew. Chem. Int. Ed.* **2007**, *46*, 3471, (b) E. Kim et al. *Angew. Chem. Int. Ed.* **2010**, *49*, 4405, (c) D. Kim et al. *J. Am. Chem. Soc.* **2010**, *132*, 9908, (d) R. Hota et al. *Chem. Sci.* **2013**, *4*, 339, (e) G. Yun et al. *Angew. Chem. Int. Ed.*, **2014**, *53*, 6414, (f) J. Kim et al. *Angew. Chem. Int. Ed.*, **2015**, *54*, 2693, (g) I. Roy et al. *Angew. Chem. Int. Ed.* **2015**, *50*, 15152, (h) K. I. Min et al. *Angew. Chem. Int. Ed.*, **2016**, *54*, 6925.
- [2] (a) K. Baek et al. *J. Am. Chem. Soc.* **2013**, *135*, 6523, (b) K. Baek et al. *Chem. Comm.* **2016**, *52*, 9676, (c) I. Roy et al, submitted for publication
- [3] J. Lee et al. *Nature Chem.* **2014**, *6*, 97.
- [4] K. Baek et al. *Acc. Chem. Res.* **2015**, *48*, 2221.

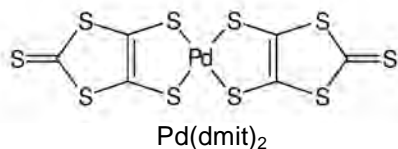
Molecular quantum spin liquid

Reizo Kato

Condensed Molecular Materials Laboratory, RIKEN

Keywords: Molecular conductor, Quantum spin liquid, Strongly correlated electron system, Valence bond formation

Quantum spin liquid (QSL) proposed by P. W. Anderson in 1973 exhibits the absence of magnetic or valence bond solid order among entangled quantum spins even at zero temperature [1]. Although this third fundamental state for magnetism is a long-sought state of matter that has attracted much theoretical attention, the ground state and low-energy excitations of the $S=1/2$ antiferromagnetic triangular lattice are still far from full understanding and furthermore there are few candidates of real materials [2]. In a series of anion radical salts of a metal complex $\text{Pd}(\text{dmit})_2$ ($\text{dmit} = 1,3\text{-dithiol-2-thione-4,5-dithiolate}$) [3], we found that $\beta\text{-EtMe}_3\text{Sb}[\text{Pd}(\text{dmit})_2]_2$ with a quasi triangular lattice of $[\text{Pd}(\text{dmit})_2]_2^-$ dimers is a promising candidate for QSL [4, 5, 6].



The ground state of the $\text{Pd}(\text{dmit})_2$ salts, $X[\text{Pd}(\text{dmit})_2]_2$ (X : monovalent cation) is classified by the anisotropy of the triangular lattice that can be tuned by the choice of the counter cation X . In the cation effect on the degree of frustration, the arch-shaped distortion of the $\text{Pd}(\text{dmit})_2$ molecule plays an important role [7]. Although an origin of this arch-shaped distortion remains an open question, this is a unique example where the molecular degree of freedom operates on the electronic state.

The QSL phase is near the Mott transition and is situated between the antiferromagnetic (AF) phase and the charge order (CO) phase. The AF phase in the vicinity of the QSL phase exhibits very small magnetic moment. The AF state in the $\text{Pd}(\text{dmit})_2$ salts is accompanied by intramolecular antiparallel spin configuration and charge disproportionation.

On the other hand, the CO state in the $\text{Et}_2\text{Me}_2\text{Sb}$ and Cs salts is understood in terms of the formation of a closed shell octamer composed of two charge-rich dimers and two charge-poor dimers [8]. The valence bond order (VBO) state observed in the EtMe_3P salts is characterized by the formation of a closed shell tetramer composed of two dimers with intradimer charge disproportionation [9]. These results indicate an importance of the *extended* charge distribution on the closed shell "supramolecule" (tetramer or octamer). Vibrational spectra of the QSL salt indicate competition between the tetramerization and octamerization, suggesting that the charge degree of freedom is important for the emergence of the QSL state.

References

1. P. W. Anderson, *Mater. Res. Bull.* **8**, 153 (1973).
2. L. Balents, *Nature*, **464**, 199 (2010).
3. R. Kato, *Chem. Rev.*, **104**, 5319 (2004).
4. (a) K. Kanoda and R. Kato, *Annu. Rev. Condens. Matter Phys.*, **2**, 167 (2011). (b) R. Kato, *Bull. Chem. Soc. Jpn.*, **87**, 355 (2014).
5. (a) T. Itou, et al., *Phys. Rev. B*, **77**, 104413 (2008). (b) M. Yamashita, et al., *Science*, **328**, 1246 (2010). (c) T. Itou, et al., *Nature Phys.*, **6**, 673 (2010). (d) S. Yamashita, et al., *Nature Commun.*, **2**, 275 (2011). (e) D. Watanabe, et al., *Nature Commun.*, **3**, 1090 (2012).
6. (a) T. Tsumuraya, et al., *J. Phys. Soc. Jpn.*, **82**, 033709 (2013). (b) H. Seo, et al., *J. Phys. Soc. Jpn.*, **84**, 044716 (2015).
7. R. Kato and H. Cui, *Crystals*, **2**, 861 (2012).
8. T. Yamamoto et al., *J. Phys. Soc. Jpn.*, **85**, 104711 (2016).
9. T. Yamamoto et al., *J. Phys. Soc. Jpn.*, **83**, 053703 (2014).

Invited Lectures

(30 min. inc. discussion)

Pressure/temperature induced magnetic anomalies in Cu(II)-nitroxides complexes

K. Maryunina*, S. Nishihara***, K. Inoue***, G. Romanenko***, V. Ovcharenko***

* Department of Chemistry, Graduate School of Science and Center for Chiral Science, Hiroshima University,
1-3-1, Kagamiyama, Higashi Hiroshima, Hiroshima, 739-8526, Japan

** Institute for Advanced Materials Research, Natural Science Center for Basic Research and Development,
Hiroshima University, 1-3-1 Kagamiyama, Higashi Hiroshima, 739-8526, Japan

*** International Tomography Center SB RAS,
Institutskaya Str. 3A, Novosibirsk, 630090, Russian Federation

Keywords: pressure effect, spin crossover, nitroxide, copper(II)

The complexes of Cu(II) with nitroxyl radicals are unique objects for detailed studies of thermally, pressure, and light induced phase transitions. In the course of a thermally induced structural rearrangements of Cu(II) coordination units, the energy of exchange interaction between the odd electrons of the Cu(II) and coordinated nitroxide groups changes, leading to magnetic anomalies similar to spin crossover (SCO) [1].

We analyzed pressure induced phenomena for number of complexes $[\text{Cu}(\text{hfac})_2\text{NN-PzR}]$ with pyrazolyl-substituted nitronyl nitroxides (NN-PzR) undergoing various magnetic anomalies. It was shown that SCO-like phenomenon in Cu(II)-nitroxide complexes is extremely sensitive to pressure: the most considerable changes of magnetic properties take place in pressure interval 10^{-4} -0.20 GPa [2]. Increasing

pressure has different effect for different types of magnetic anomalies (suppressing or initiating of specific changes at $\mu_{\text{eff}}(T)/\chi T(T)$ dependences, change the type of magnetic anomaly, increasing critical temperature, Fig 1). Both pressure induced and temperature induced phenomena provide valuable information on the spin state in heterospin solid and could serve as a new type of a pressure and temperature sensor.

References

1. V. I. Ovcharenko, E. G. Bagryanskaya, in *Spin-Crossover Materials: Properties and Applications*, ed. M. Halcrow, John Wiley & Sons Ltd., 239 (2013).
2. Maryunina, K. Yu.; Zhang, X.; Nishihara, S.; Inoue, K.; Morozov, V. A.; Romanenko, G. V.; Ovcharenko, V. I. *J. Mater. Chem. C*, 3, 7788 (2015)

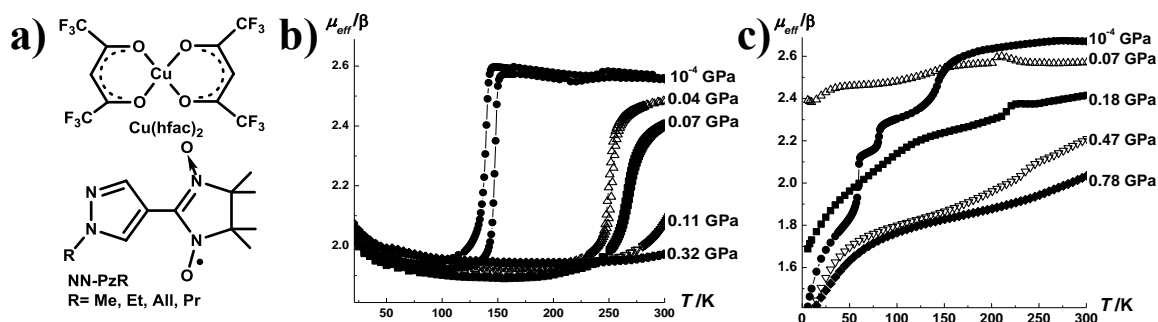


Fig.1 Fragment $\text{Cu}(\text{hfac})_2$ and nitronyl nitroxides NN-PzR (a); experimental dependences of $\mu_{\text{eff}}(T)$ at different pressure for complexes $[\text{Cu}(\text{hfac})_2\text{NN-PzR}]$ showing different type of SCO (b and c).

Artificial Synthesis of Magnetically Anisotropic Materials in Iron Meteorite by Atomic Building Blocks

M. Mizuguchi

Institute for Materials Research, Tohoku University, 2-1-1 Katahira, Aoba-ku, Sendai 980-8577, Japan

Keywords: magnetic anisotropy, $L1_0$, FeNi, iron meteorite

Magnetically anisotropic materials are attracting attention for the application to high-density magnetic storage devices since the thermal stability of magnetization is kept even in a nanometer scale. Particularly, materials with the CuAu crystal lattice structure ($L1_0$) have large uniaxial magnetic anisotropy, thus many studies on $L1_0$ type materials have been reported. However, it is a crucial problem that typical $L1_0$ type materials such as FePt, CoPt, and FePd include noble metals of Pt or Pd. To solve this problem, the development of novel magnetically anisotropic materials without noble metals is now eagerly expected. In this study, we aimed to synthesize an $L1_0$ type FeNi alloy with a large magnetic anisotropy by the vapor deposition using atomic layer deposition[1-12], which exists only in an iron meteorite as a Widmannstätten structure in nature (Fig. 1). $L1_0$ type FeNi films were fabricated by an alternative monatomic deposition of Fe and Ni layers on several underlayers. Uniaxial magnetic anisotropy energy of these films were estimated to be about 7.0×10^6 erg/cm³ from magnetization measurements, and it was confirmed that large magnetic anisotropy was induced by the formation of $L1_0$ type structure. The composition of Fe and Ni was also changed to optimize properties of $L1_0$ type FeNi.

Relation between structural properties and magnetic properties of these FeNi films will be also discussed in detail.

References

1. M. Mizuguchi *et al.*, *J. Appl. Phys.*, **107**, 09A716 (2010).
2. T. Kojima and M. Mizuguchi *et al.*, *J. Phys.: Conf. Series*, **266**, 012119 (2011).
3. M. Mizuguchi *et al.*, *J. Magn. Soc. Jpn.*, **35** 370 (2011).
4. T. Kojima and M. Mizuguchi *et al.*, *Jpn. J. Appl. Phys. (Rapid Communication)*, **51**, 010204 (2012).
5. M. Kotsugi and M. Mizuguchi *et al.*, *J. Magn. Mater.*, **326**, 235 (2013).
6. T. Kojima and M. Mizuguchi *et al.*, *Surface Science*, **619**, 44 (2013).
7. M. Ogiwara and M. Mizuguchi *et al.*, *Appl. Phys. Lett.*, **103**, 242409 (2013).
8. T. Kojima and M. Mizuguchi *et al.*, *J. Phys.: Condensed Matters*, **25**, 064207 (2014).
9. T. Kojima and M. Mizuguchi *et al.*, *J. Phys. D*, **47**, 425001 (2014).
10. T. Tashiro and M. Mizuguchi *et al.*, *J. Appl. Phys.*, **117**, 17E309 (2015).
11. K. Mibu and M. Mizuguchi *et al.*, *J. Phys. D*, **48**, 205002 (2015).
12. T. Kojima and M. Mizuguchi *et al.*, *Thin Solid Films*, **603**, 348 (2016).

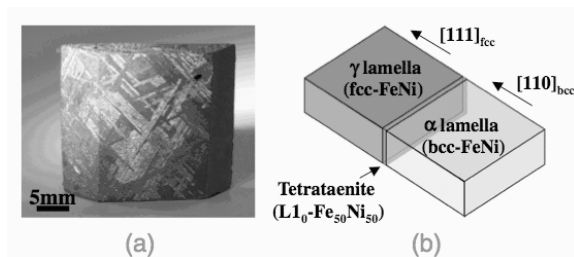


Fig. 1 (a) Widmannstätten structure of iron meteorite and (b) microscopic schematic view of interface structure of the Widmannstätten structure.

Optical Control of Carriers and Spins in Molecular Materials

T. Naito*

* Department of Chemistry and Biology, Graduate School of Science and Engineering, Ehime University, Matsuyama, 790-8577, Japan

Keywords: Metal-dithiolene complexes, electron spin resonance, π -d interaction, molecular crystal

Carrier doping and spin injection to molecular materials have long been the most important subjects in both basic and applied research. Molecular materials are generally non-magnetic insulators, yet some of them drastically vary the conducting and/or magnetic properties in concert with the number of unpaired electrons. Using an appropriate wavelength and strength of light, charge transfer transitions in organic salts could produce a desired number of carriers and/or spins with a sufficiently long relaxation time in a controllable, reproducible, and reversible way. Based on this idea, electrical and magnetic properties in the dark and under irradiated conditions have been examined for a series of simple salts containing redox-active and photo-reactive π -conjugated molecules. In the course of such a study, a nickel-dithiolene complex (Figure 1) has produced paramagnetic [1, 2] or practically non-magnetic conductors [3] under UV radiation, while a copper analogue has enabled reversible control of delocalization of the spin on Cu(II) using UV radiation

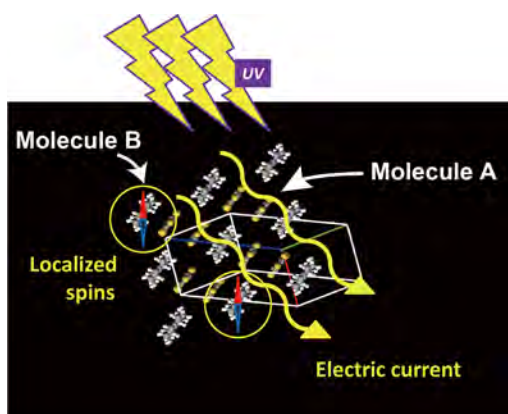


Fig.1 Schematic illustration of simultaneous production of electric current and localized spins during UV-irradiation upon the crystalline solid comprised of Molecule A and Molecule B.

(Figure 2) [4,5]. One can distinguish the contribution of photocarriers from that of thermal carriers by quantitative analysis of relationship between effective activation energy vs. light intensity and that between photocurrent vs. light intensity [6]. These results and a possible photoconduction mechanism will be discussed.

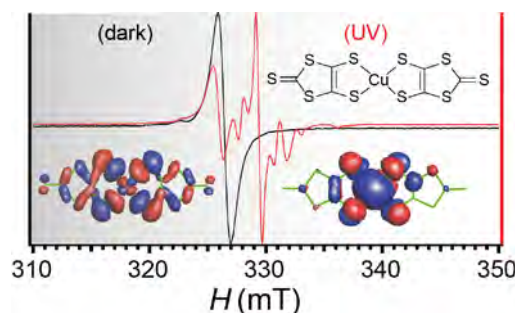


Fig.2 Molecular orbitals and ESR signals on the [Cu(dmit)₂]²⁻ anions under dark (left) and UV-irradiated (right) conditions.

References

1. T. Naito, T. Karasudani, K. Ohara, T. Takano, Y. Takahashi, T. Inabe, K. Furukawa and T. Nakamura, *Adv. Mater.*, **24**, 6153-6157 (2012).
2. T. Naito, T. Karasudani, S. Mori, K. Ohara, K. Konishi, T. Takano, Y. Takahashi, T. Inabe, S. Nishihara and K. Inoue, *J. Am. Chem. Soc.*, **134**, 18656-18666 (2012).
3. T. Naito, T. Karasudani, N. Nagayama, K. Ohara, K. Konishi, S. Mori, T. Takano, Y. Takahashi, T. Inabe, S. Kinose, S. Nishihara, K. Inoue, *Eur. J. Inorg. Chem.*, **2014**, 4000-4009 (2014).
4. H. Noma, K. Ohara, T. Naito, *Chem. Lett.*, **43**, 1230-1232 (2014).
5. H. Noma, K. Ohara, T. Naito, *Inorganics*, **4**(2), 7 (21 pages) (2016).
6. N. Nagayama, T. Yamamoto, T. Naito, *CheM*, **2015**, 74-80 (2015).

Hetero-structures of low-dimensional materials studied by atomic resolution STEM

K. Suenaga*

* National Institute of Advanced Industrial Science and Technology (AIST), Tsukuba 305-8565 Japan

Keywords: low-dimensional material, nano-composite, TEM, hetero-structure

Properties of low-dimensional materials highly depend on the atomic structures and their assembly. The studies of atomic defects and boundaries are of general interest for the fundamental researches and technological applications in any crystalline materials, especially in 1D/2D materials. Hybrid low-dimensional materials with distinct atomic structures recently gather a wide attention. Here I present some new examples for atomic-scale imaging and spectroscopy of various low-dimensional materials with interrupted periodicities studied by (scanning transmission electron microscopy (STEM). Nitrogen defects and their chemical dynamics of graphene are now studied at individual atom basis [1]. Defects and phase transitions of single-layered dichalcogenides (MX_2) are corroborated *in situ* [2]. In plane anisotropy of single-layered group VII dichalcogenides (ReS_2 and ReSe_2) is recently reported [3]. The lateral hetero-structures of MX_2 with different electronic properties have been investigated through the interfaces [4, 5]. Also various new 1D structures inside carbon nanotubes are discovered and investigated [6, 7,

8]. Eventually single atom magnet at graphene atomic defects will be proposed [9].

This work is partially supported by a JST research acceleration programme.

References

1. Y.-C. Lin et al., *Nano Letters*, **15** (2015) pp.7408-7413
2. Y.-C. Lin et al., *Nature Communications*, 6:6736 (2015)
3. Y.-C. Lin, et al., *ACS Nano* (2015) **9** (2015) pp.11249-11257
4. M.-Y. Li et al., *Science*, 349 (2015) pp. 524-528
5. L. Tizei et al., *Phys. Rev. Lett.*, **114** (2015) 107601
6. R. Senga et al., *Nature Materials* 13 (2014) pp. 1050-1054
7. L. Tizei et al., *Phys. Rev. Lett.*, 114 (2015) 197602
8. R. Senga and K. Suenaga, *Nature Communications*, (2015) 6:7943
9. Y.-C. Lin et al., *Phys. Rev. Lett.*, **115** (2015) 206803

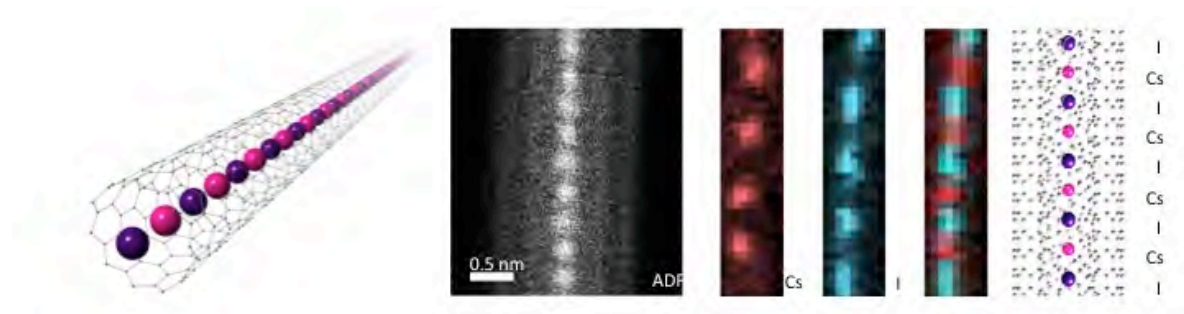


Fig.1 One-dimensional ionic crystal of CsI generated in double-wall carbon nanotube [6]. From left, an atomic model, STEM-ADF image, EELS maps of Cs, I, and composite.

New molecular materials studied by neutron scattering

J. A. Rodríguez-Velamazán*

* *Institut Laue-Langevin, Grenoble, France*

Keywords: Molecular materials, spin-crossover, multiferroics, neutron scattering

(1 blank line)

One of the main features of molecular compounds is the possibility of combining different properties in a synergic way giving a multifunctional material. In this contribution, we will present different examples where this approach produces new materials with interesting properties, and we will show how neutron scattering can give crucial insights in the study of these materials. We will focus mainly in two classes of systems: (i) compounds where the spin-crossover phenomenon is a source of multifunctionality, and (ii) compounds combining electric and magnetic ordering, the so-called molecular multiferroics.

Regarding the first class, we will discuss an example of combination of spin-crossover and long-range magnetic order, and its behaviour under pressure, [1] as well as

the possibility of using spin-crossover as a switch for molecular motion. [2] The second class will be represented by both metal-organic systems combining electric and magnetic order [3] and hybrid systems displaying spin-driven multiferroic behaviour. [4]

References

1. Rodríguez-Velamazán et al., *Chem. Eur. J.*, 20, 7956 (2014)
2. Rodríguez-Velamazán et al., *J. Am. Chem. Soc.*, 134, 5083 (2012)
3. Cañadillas-Delgado et al., *J. Am. Chem. Soc.*, 134, 19772 (2012)
4. Rodríguez-Velamazán et al., *Scientific. Reports.*, 5, 14475 (2015)

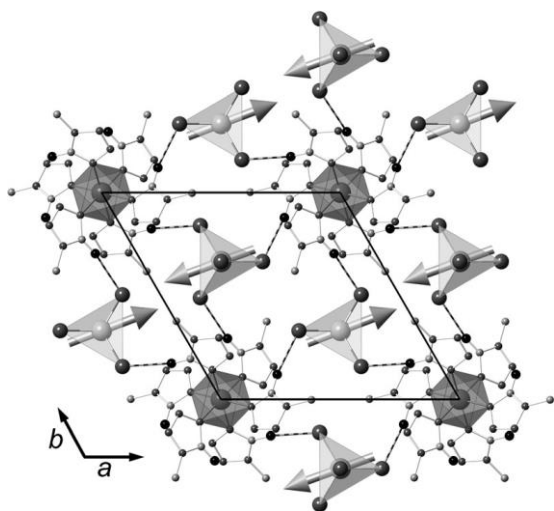


Fig.1 [Fe(Metz)₆](FeBr₄)₂

(Metz=1-methyltetrazole), is a unique and multifunctional magnetic material that combines spin-crossover and long-range magnetic order. The application of pressure modulates both properties. [1]

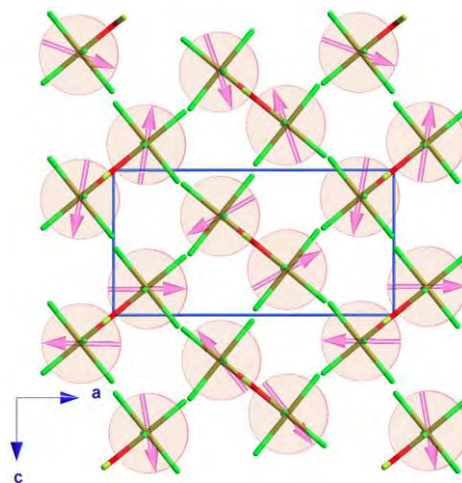


Fig.2 (NH₄)₂[FeCl₅(H₂O)] presents a cycloidal magnetic ordering that is at the origin of its spin-driven multiferroic behaviour.

Exchange-Coupled Heavy-Lanthanoid and Nitroxide Molecular Magnets

Takuya Kanetomo, Takeshi Nakamura, Rina Murakami, and Takayuki Ishida

Department of Engineering Science, The University of Electro-Communications, Chofu, Tokyo 182-8585, Japan

Keywords: single-molecule magnet, exchange interaction, rare earth metal, radical

Toward development of lanthanoid(Ln)-based magnetic materials, reliable prescriptions for molecular/crystal design have long been desired. A spin-only Gd^{3+} ion ($4f^7$) is often chosen as an initial attempt, because of facile comprehension in structure-function relationship.^{1,2} At the second stage, a chemical trend (Ln dependence) in isomorphous series is an important issue for designing various magnets. Single-molecule magnets (SMMs), displaying magnetic hysteresis at their single-molecular level, have attracted much interest, owing to the paradigm shift in science and engineering of magnets and also future application to high-density information storage media and molecular computing devices. We have concentrated attention to $4f-2p$ heterospin systems and utilized persistent nitroxide radicals ($>N-O\cdot$) as a $2p$ (π^*) spin source.

Relatively strong antiferromagnetic coupling was found in $[Gd(hfac)_3(2pyNO)(H_2O)]$, ascribable to the direct radical-Gd coordination,¹ where L is *tert*-butyl 2-pyridyl nitroxide (2pyNO) and hfac stands for 1,1,1,5,5,5-hexafluoropentane-2,4-dionate. A chemical trend was investigated in this motif for novel SMMs.

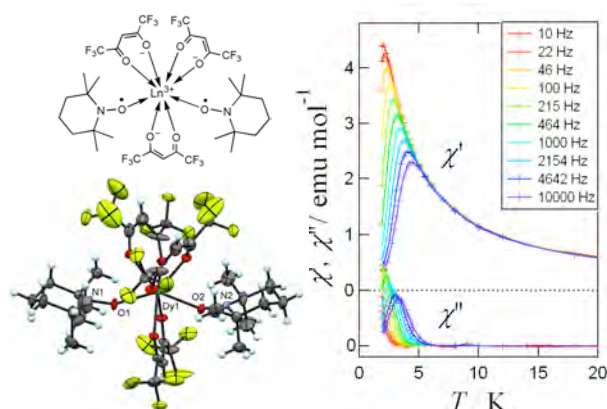


Fig. 1. (Left) Structural formula and X-ray crystal structure of $[Dy(hfac)_3(TEMPO)_2]$. (Right) Ac magnetic susceptibilities of $[Dy(hfac)_3(TEMPO)_2]$ with a dc bias field of 1000 Oe.

The slow magnetization reversal was evaluated with magnetic susceptibility, in particular ac out-of-phase susceptibility (χ_{ac}''). Eventually, the Tb^{3+} ($4f^8$) derivative was characterized as a SMM.³ On the other hand, no χ_{ac}'' was recorded for the Dy^{3+} ($4f^9$) derivative. Similarly, the Ho^{3+} ($4f^{10}$) derivative exhibited appreciable χ_{ac}'' , but the Er^{3+} ($4f^{11}$) derivative did not.

As a series with a Ln/radical ratio of 1/2, $[Ln(hfac)_3(TEMPO)_2]$ complexes have successfully been prepared and characterized (TEMPO is a commercially available nitroxide spin label). Relatively strong exchange coupling was observed for Ln = Gd.⁴ Figure 1 shows the molecular structure and ac susceptibilities of $[Dy(hfac)_3(TEMPO)_2]$. A clear frequency dependence was recorded, being typical of a SMM. The Dy^{3+} ($4f^9$) and Er^{3+} ($4f^{11}$) derivatives showed SMM behavior,⁵ whilst practically no χ_{ac}'' was recorded for the Ho^{3+} ($4f^{10}$) or Tm^{3+} ($4f^{12}$) derivative.

Thus, a distinct spin-parity effect was observed for both series. Ions with half-integer spin are known to be a Kramers ion, which guarantees the ground doublet state as a prerequisite for a SMM. In the strongly exchange-coupled systems having the direct radical-Ln coordination, the total molecular spin may be a useful criterion to predict Kramers doublets and accordingly potential SMM candidates.

References

1. T. Ishida et al. *Polyhedron*, **66**, 183 (2013).
2. T. Kanetomo et al. *Inorg. Chem.* **53**, 10794 (2014); T. Kanetomo et al. *Inorg. Chem.* **55**, 8140 (2016).
3. M. L. Baker et al. *Inorg. Chem.* **54**, 5732 (2015); R. Murakami et al. *Dalton Trans.* **42**, 13968 (2013); T. Kanetomo et al. *Inorg. Chem. Front.* **2**, 860 (2015).
4. R. Murakami et al. *Dalton Trans.* **42**, 5893 (2014).
5. M. Karbowiak et al. *Chem. Phys. Lett.* **662**, 163 (2016).

Solid-state electrochemistry of coordination compounds

H. Yoshikawa*

* *Kwansei Gakuin University, 2-1 Gakuen, Sanda, Hyogo 669-1337, Japan*

Keywords: Rechargeable battery, XAFS, Molecular cluster, Nanocarbon

Solid-state electrochemistry is a wide research area covering various topics from fundamental sciences to applications. At present, one of the most important goals is to develop high-performance rechargeable batteries due to the ever-increasing energy demands and pressing environmental concerns. We have recently proposed a new type of lithium battery, “the molecular cluster battery (MCB)”, in which the cathode active materials are polynuclear metal complexes (molecular clusters) such as Mn₁₂ clusters and polyoxometalates (POMs), in order to achieve both high battery capacity and fast charging/discharging.[1] It is expected that MCBs would show a high capacity and a rapid charging/discharging due to multi-electron redox reactions of the molecular clusters and quick lithium-ion diffusion, respectively (Fig. 1).

By using a Keggin-type POM, [PMo₁₂O₄₀]³⁻ (KPOM) as a cathode-active material, we achieved a higher battery capacity of ca. 270 Ah/kg, which was larger than those of the lithium ion batteries (ca. 148Ah/kg), and a more rapid charging. *Operando* Mo K-edge X-ray absorption fine structure (XAFS) analyses on the KPOM-MCBs demonstrated that

KPOM underwent twenty four electrons reduction in the discharging process, which indicated that all of Mo⁶⁺ ions in KPOM changed into Mo⁴⁺. [2] This means the formation of a super-reduced state, [PMo₁₂O₄₀]²⁷⁻, and the super-reduction electron number of twenty four can explain the large capacity of the KPOM-MCBs. This electron sponge behaviour indicates that molecular clusters are promising cathode active materials for high-performance rechargeable batteries. Furthermore, we prepared nano-hybrid materials between KPOMs and single-walled carbon nanotubes (SWNTs), in which KPOMs are individually adsorbed on the SWNT surfaces, for application to the cathode active materials of MCBs. The charging/discharging measurements for the KPOM-SWNT hybrid MCBs indicated a higher battery capacity and a faster charging/discharging, compared with those of the initial KPOM MCBs.[3]

In this presentation, the performances of the battery including metal organic frameworks (MOFs) as cathode active materials will also be discussed in details.[4]

References

1. H. Yoshikawa et al., *Chem. Commun.*, 3169-3170 (2007)
2. H. Yoshikawa et al., *J. Am. Chem. Soc.*, 134, 4918-4924 (2012)
3. H. Yoshikawa et al., *Angew. Chem. Int. Ed.*, 50, 3471-3474 (2011)
4. H. Yoshikawa et al., *J. Am. Chem. Soc.*, 136, 16112-16115 (2014)

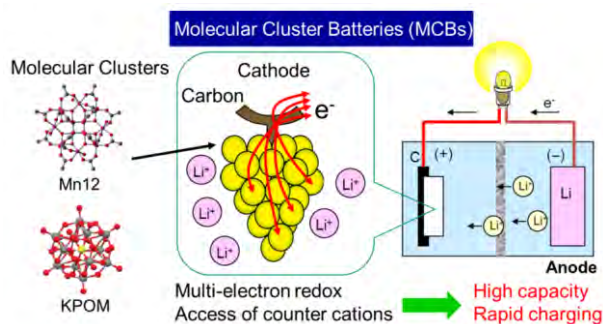


Fig.1 Schematic view of molecular cluster batteries

High-resolution FAIMS for proteomics, lipidomics, and structural elucidation based on isotopologic shifts

Matthew A. Baird, Andrew P. Bowman, Julia L. Kaszycki, Alexandre A. Shvartsburg

Department of Chemistry, Wichita State University, 1845 Fairmount, Wichita, KS 67260, USA

Keywords: Mass Spectrometry, Ion Mobility Separations, Proteomics, Isotopic Analyses

With all the power of modern mass spectrometry (MS), most biological and environmental samples are complex enough to require prior separations. Those were traditionally performed in liquids (electrophoresis) or on solid/liquid boundary (chromatography). These approaches are now complemented or replaced by ion mobility spectrometry (IMS) in gases, which offer faster analyses, unique selectivity, and, in some modes, structural elucidation capability. However, linear IMS separations based on absolute mobility (including drift-tube and traveling-wave implementations) are tightly correlated to the MS dimension, which limits the peak capacity of IMS/MS platforms and ability of IMS to distinguish structural isomers. These constraints are relaxed in the differential or field asymmetric waveform IMS (FAIMS) that separates ions by the difference of mobility in low and high electric fields.

The FAIMS resolving power (R) strongly depends on the field intensity, is sensitive to the gas composition, and (as for other separations in media) scales as the square root of analysis time. We have raised R by over an order of magnitude up to 500 using planar-gap FAIMS units with homogeneous field, helium-rich gas buffers, and extended separation times up to 1 s.¹ Ion losses at the FAIMS/MS junction were mitigated using slit-aperture/electrodynamic ion funnel interfaces comprising a multi-hole slit that maximally overlaps with rectangular ion beams exiting the FAIMS device. Replacing helium in He/N₂ buffers by more insulating H₂ has improved the resolution further (especially for proteins) through greater dispersion fields and/or light gas fractions.² The resolved species are assigned employing the electron transfer dissociation (ETD) for multiply-charged peptides³ and ozone-induced dissociation (OzID) for unsaturated lipids.

The top challenge in proteomics is comprehensive mapping of post-translational modifications (PTMs) that commonly control protein function. Prominently, the complement of various PTMs on histones defines a code underlying the epigenetic mechanism of heredity. Whereas ETD can characterize the PTM localizations on a single protein, mixtures of variants ubiquitous in cells need to be separated first. Unlike condensed-phase methods, FAIMS has broadly resolved the localization variants for methylated, acetylated, and phosphorylated histone tails up to 6 kDa. The acetylation and trimethylation on same sites were also resolved baseline. These results suggest that FAIMS could pull apart such isomers even for intact proteins in top-down strategies.

Similarly in lipidomics, the permutation of trans-acylation, double bond position, and cis/trans variation creates many isomers with distinct activity. While their chromatographic separation is often lengthy and complex, FAIMS has substantially resolved some 3/4 of isomers of all types. The success rate can be increased using metal cationization that yields different ion geometries and OzID to locate the double bonds.

Nearly all compounds form isotopologues that reflect the natural isotopic distribution of constituent elements. Separation of resulting mass envelopes by FAIMS depends on the isotopic label location, enabling the identification of structural isomers based on isotopic shifts in a fundamentally new approach akin to NMR.

References

1. A. A. Shvartsburg et al. J. Am. Soc. Mass Spectrom. 24, 109 (2013).
2. A. A. Shvartsburg. Anal. Chem. 86, 10608 (2014).
3. M. A. Baird, A. A. Shvartsburg. J. Am. Soc. Mass Spectrom. 27, 2064 (2016).

Ionic liquids from metal complexes: physical properties and chemical reactivities

T. Mochida

*Graduate School of Science, Kobe University, Nada, Kobe 657-8501, Japan

Keywords: Metal complex, Ionic liquids

Recently, ionic liquids that show interesting physical properties have been reported. We have designed two groups of metal-containing ionic liquids: organometallic ionic liquids and metal-chelate ionic liquids. These liquids exhibit unconventional physical properties and chemical reactivities.

The structural formulae of the ionic liquids with sandwich-type metallocenium cations are shown in Fig. 1(a) [1]. The ferrocenium ionic liquids (left, $M = \text{Fe}$) are blue or green paramagnetic liquids, whereas the cobaltocenium ionic liquids ($M = \text{Co}$) are orange diamagnetic liquids. The paramagnetic ferrocenium ionic liquids exhibit magnetic susceptibility changes coupled with liquid–solid phase transformation near room temperature. The ruthenium-containing ionic liquids (right, $M = \text{Ru}$) are diamagnetic colorless liquids. Based on the photoreactivity of these liquids, reversible transformation between ionic liquids and coordination polymers by heat and light, was achieved (Fig. 1b).

We also synthesized a series of ionic liquids

containing cationic metal-chelate complexes [2]. These ionic liquids exhibit reversible changes in color, as well as in thermal and magnetic properties in response to organic vapors and gases. Furthermore, by introducing intramolecular coordination sites into the ligand, thermochromic ionic liquids were synthesized.

References

- (a) Y. Funasako, S. Mori, T. Mochida, *Chem. Commun.*, 52, 6277 (2016); (b) T. Inagaki, T. Mochida, M. Takahashi, C. Kanadani, T. Saito, D. Kuwahara, *Chem. Eur. J.*, 18, 6795 (2012); (c) Y. Funasako, T. Mochida, T. Inagaki, T. Sakurai, H. Ohta, K. Furukawa, T. Nakamura, *Chem. Commun.*, 47, 4475 (2011).
- (a) X. Lan, T. Mochida, Y. Funasako, K. Takahashi, T. Sakurai, H. Ohta, *Chem. Eur. J.*, *in press*. (b) X. Lan, H. Hosokawa, Y. Funasako, T. Mochida, *Eur. J. Inorg. Chem.*, 17, 2804 (2016). (c) Y. Funasako, T. Mochida, K. Takahashi, T. Sakurai, H. Ohta, *Chem. Eur. J.*, 18, 11929 (2012).

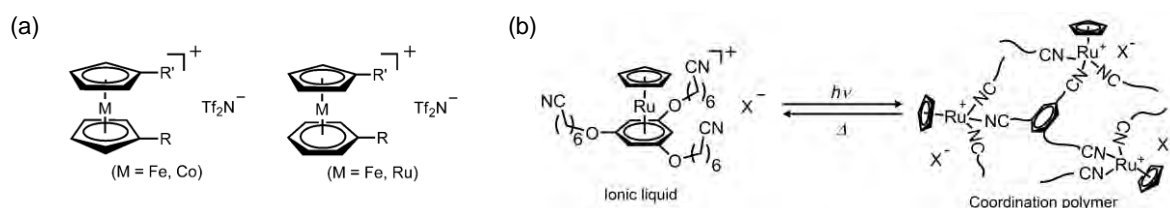


Fig. 1. (a) Structural formulae of the organometallic ionic liquids and (b) transformation between ionic liquids and coordination polymers by heat and light.

New insight into the electronic and magnetic structures of iron porphyrin complexes

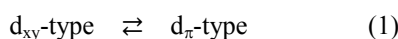
Mikio Nakamura

*Department of Chemistry, Faculty of Science, Toho University
Funabashi, Chiba 274-8510, Japan*

Iron porphyrin, electron configuration, spin crossover, high-valent iron

Elucidation of the electronic and magnetic structures of iron porphyrin complexes are still an issue of great interest not only from the viewpoint of bioinorganic chemistry but also from that of material science. This is because the iron porphyrin complexes adopt a wide variety of electronic and magnetic structures which are converted each other by the external stimuli such as temperature, pressure, photoirradiation, pH, etc.¹⁻³ In this symposium, three topics will be presented, all of which concern the lability of electronic and magnetic structures in iron porphyrin complexes.

Low-spin iron(III) porphyrin complexes exist as an equilibrium mixture of electron configurational isomers having $(d_{xy})^2(d_{xz}, d_{yz})^3$ (d_{π} -type) and $(d_{xz}, d_{yz})^4(d_{xy})^1$ (d_{xy} -type) electronic ground states as shown in Eq (1).



NMR and EPR studies have revealed that the spin distribution on the porphyrin ring changes greatly on going from the d_{π} to the d_{xy} -type complex (Fig. 1).^{1,4}

Six-coordinate iron(III) porphyrins having neutral oxygen ligands usually adopt high-spin state. We have shown for the first time that $[\text{Fe}(\text{Por})(p\text{-X-PyNO})_2]^+$ ($X = (\text{CH}_3)_2\text{N}$) adopt the low-spin state at 100 K and exhibit spin-crossover between $S=1/2$ and $S=5/2$ at higher

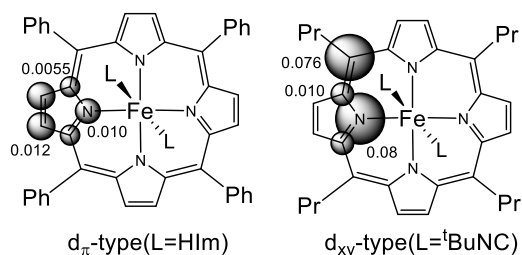
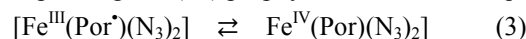


Fig. 1 Spin density and spin distribution on porphyrin ring in d_{π} - and d_{xy} -type complexes.

temperature as shown in Eq (2) and Fig. 2.⁵



One electron oxidation of iron(III) porphyrins followed by the addition of azide produced iron(III) porphyrin radical cations, $[\text{Fe}^{\text{III}}(\text{Por}^{\bullet})(\text{N}_3)_2]$. By manipulating the peripheral substituents, we have succeeded in converting these complexes to the corresponding iron(IV) porphyrins as shown in Eq. (3).⁶



References

- [1] M. Nakamura, *Coord. Chem. Rev.*, **250**, 2271-2294, (2006)
- [2] M. Nakamura et al., *Handbook of Porphyrin Science*, Eds K. M. Kadish, et al., World Scientific, Singapore, Vol. 7, pp. 1-146 (2010)
- [3] A. Ikezaki, M. Takahashi, M. Nakamura, *Angew. Chem. Int. Ed.* **48**, 6300-6304 (2009)
- [4] A. Ikezaki, M. Nakamura and others, *J. Porphyrins and Phthalocyanines*, **18**, 778-791 (2014)
- [5] Y. Ide, T. Ikeue, M. Takahashi, M. Nakamura and others, *Dalton Trans.*, submitted
- [6] A. Ikezaki, M. Takahashi, M. Nakamura, *Chem. Commun.* **49**, 3098-3100 (2013)

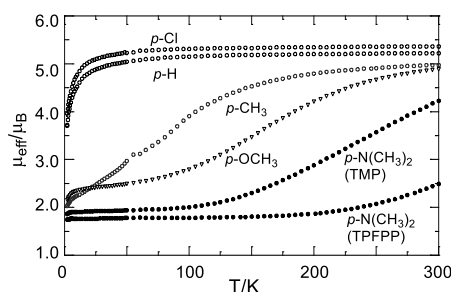


Fig. 2 Temperature dependence of the effective magnetic moments in $[\text{Fe}(\text{Por})(p\text{-X-PyNO})_2]^+$ as determined by SQUID magnetometry.

Contributed Lectures

(20 min. inc. discussion)

Topologically protected spin-wave propagation in magnonic crystals

Jun-ichiro Ohe*

* Department of Physics, Toho University, 2-2-1 Miyama, Funabashi 274-8510, Chiba, Japan

Keywords: Spintronics, Spin wave, Magnonic crystals

Topological phase in condensed matter physics has been attracted because of the robustness of physical properties against the perturbative field. The quantum Hall effect is typical phenomena described by the topological Chern number that indicates the edge mode of the conduction electrons. This Chern number is calculated by the Bloch wave functions of the 2-dimensional electron gas in a high magnetic field. Recent work on the photonic crystal has also clarified that the topological argument can be applied not only for the electron wave but also for the classical light wave.

In this report, we propose the topological magnonic crystal that provides chiral edge mode for spin waves. We theoretically design a couple of periodically-structured ferromagnetic models which supports unidirectional (chiral) propagations of spin

waves along its sample boundaries in their dipolar regime. We present the numerical simulations obtained by solving the Landau-Lifshitz-Gilbert equation that describes the dynamics of magnetic moments. We show the interference of these edge modes provides a new logical circuit using the magnetic materials.

References

1. Y. Kajiwara, K. Harii, S. Takahashi, J. Ohe, K. Uchida, M. Mizuguchi, H. Umezawa, H. Kawai, K. Ando, K. Takanashi, S. Maekawa, and E. Saitoh, Nature 464, 262 (2010)
2. Ryuichi Shindou and Jun-ichiro Ohe, Phys. Rev. B 89, 054412 (2014)
3. Ryuichi Shindou, Jun-ichiro Ohe, Ryo Matsumoto, Shuichi Murakami, and Eiji Saitoh, Phys. Rev. B 87, 174402 (2013)

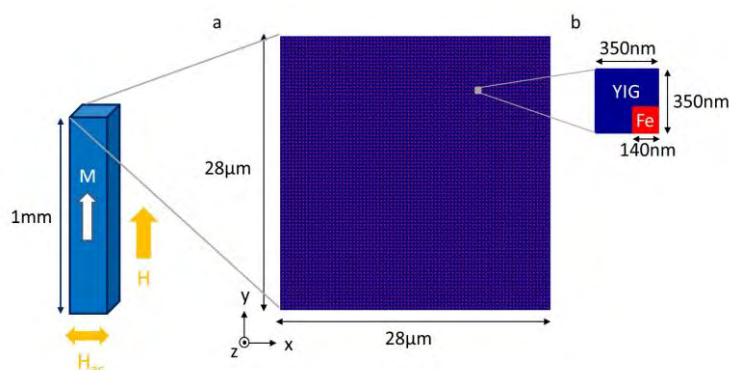


Fig.1 Schematic view of magnonic crystals. YIG is the magnetic insulator that saturation magnetization is small compared with Fe.

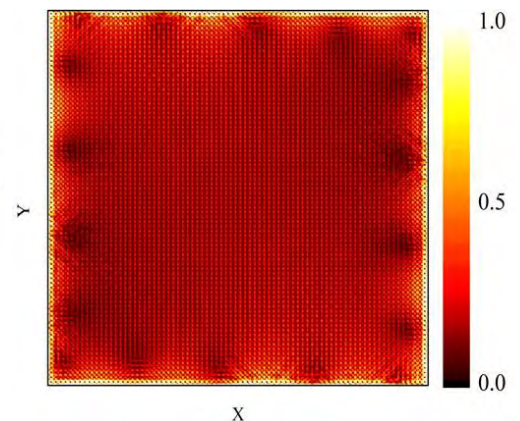


Fig.2. Spatial intensity of the chiral edge mode of spin wave

Interfacial frustration originating from quantum well formation in epitaxial Fe/Ag/Cr trilayers

E. Wada^{*}, K. Yokoyama^{**}, K. Kato^{**}, R. Onodera^{**}, D. Akahoshi^{*,**}, and T. Saito^{*,**}

^{*} Research Center for Materials with Integrated Properties, Toho Univ.

^{**} Dept. Phys., Toho Univ.

Keywords: interfacial frustration, slow dynamics, quantum well, epitaxial film

The interfacial frustration between ferromagnetic Fe layer and antiferromagnetic Cr layer has been actively researched to understand the phenomena in the spintronics systems such as the conventional spin valve devices.

In ref.[1], we observed a long-term relaxation (slow dynamics) of the thermoremanent magnetization (M_{TRM}) over a few hours for the epitaxial Fe/Cr bilayers. From the results, we showed that the slow dynamics arises from the interfacial frustration.

The slow dynamics also occurs for Fe/Au/Cr trilayers despite the separation between Fe and Cr layers by the nonmagnetic Au layer [2]. In order to explain this phenomenon, we proposed a model of novel interfacial frustration between Cr layer and spin polarized Au layer originating from quantum well formation.

In this talk, we report on the interfacial frustration for epitaxial Fe/Ag/Cr trilayers. All Fe/Ag/Cr films were epitaxially grown by MBE (Molecular Beam Epitaxy) method. The sample structures consist of the layer sequence of Ag(25.2 Å)/Fe(35.6 Å)/Ag($z = 0 \sim 30$ Å)/Cr(44.5 Å)/MgO(001) substrate. The relaxation of M_{TRM} was measured by SQUID.

The slow dynamics was observed also in Fe/Ag/Cr. The time (t) dependence of M_{TRM} was fitted into the equation $M_{TRM} = M_0 - S \ln t$, where M_0 is a constant, and S is a degree of slow dynamics (the magnetic viscosity). As seen in

Fig.1, S normalized by the saturation magnetization M_S oscillates as a function of the Ag thickness z with a period of (11.6 Å). This period is very close to that of spin polarization oscillation of Ag layer (11.3 Å) originating from the quantum well formation, which indicates that the slow dynamics of Fe/Ag/Cr trilayer arises from the Ag/Cr interfacial frustration.

References

- [1] M. Nomura, T. Koba, R. Nakamura, C. Kanadani, D. Akahoshi, and T. Saito, J. Phys.: Conf. Ser. 320 (2011) 012042.
[2] E. Wada, K. Fukida, K. Tokoi, D. Akahoshi, and T. Saito, *in preparation*

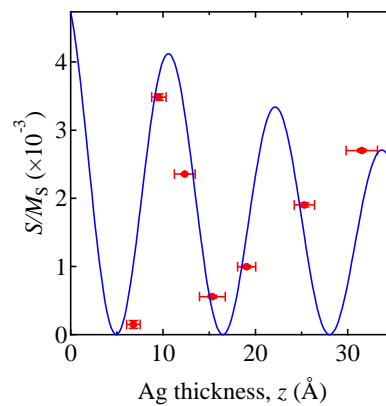


Fig.1 Ag thickness dependence of S/M_S for Fe/Ag/Cr trilayers

Development of multi-stage ion trap ion mobility measurement system.

T. sugai

Department of Chemistry, Toho University, Miyama 2-2-1, Funabashi 274-8510, Japan

Keywords: Ion mobility, ion trap

Ion mobility spectrometry (IMS) have revealed varieties of novel information on nano materials.[1] Furthermore our newly developed ion trap ion mobility measurement system can hold the charged particles for more than 7 hours realizing observations on long term structural changes. However those measurements mainly performed on a single particle and the structural resolution is limited because the system utilizes only two trap units and the transfer length is restricted to 3 mm. To break these limits and to introduce new functions such as separation, here we present the development of multi-stage system.

The system consists of an ionization source, ion trap units, and an optical observation system. To each units, radio frequency field and DC bias were applied to confine and manipulate the particles. The movements of the particles were observed by the semiconductor laser irradiation and recorded by a digital camera with an optical microscope.

Figure 1 shows the observed separation of two particles. The high charge particle ($r=280$ nm and $q=+40e$) stayed in one unit while the low charge particle ($r=350$ nm and $q=+10e$) passed through. Both of them were transferred from the injection point to the trap point achieving the movement of 80 mm, which is 30 times longer than that realized in the previous system. The sizes and charges observed by this system were several orders of magnitude smaller than those observed by the previous system showing the much improved trap capacity and charge sensitivity. We are now trying to separate, hold and characterize many particles simultaneously by the system together with other combined measurement systems.

References

1. T. Sugai et al., J. Am. Chem. Soc. 123, 6427 (2001).

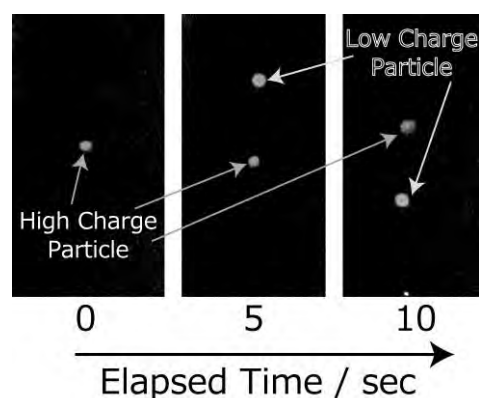


Fig. 1 Particle Separation

Liquid-crystalline Polymers with Benzoxazole Units for Application as Thermally Conductive Films

Masatoshi HASEGAWA, Shunjiro NAGAI, Junichi ISHII

Department of Chemistry, Faculty of Science, Toho University, 2-2-1 Miyama, Funabashi, Chiba 274-8510

Keywords: Thermal conductivity / Polybenzoxazole / Liquid crystal

Heat removal from semiconductor devices is a very important issue. So far, much effort has been devoted to develop electrically insulating and thermally conductive polymeric systems as flexible heat-releasing materials. However, most of electrically non-conductive conventional polymer systems possess a very low level of thermal conductivity ($\lambda = 0.1\text{--}0.2 \text{ W m}^{-1} \text{ K}^{-1}$). Among organic polymer systems, polybenzoxazole (PBO) fiber is known to possess much higher thermal conductivity along its fiber direction than other organic fiber systems [1]. However, it is difficult to directly apply the PBO fiber as thermal conductive layers (films) because of the absence of processability (insolubility and infusibility).

We have previously developed a thermotropic liquid-crystalline (LC) PBO and revealed that the magnetically oriented PBO film at an LC state along the thickness (Z) direction displayed a very high Z-direction λ of $1.79 \text{ W m}^{-1} \text{ K}^{-1}$ even without any fillers [2]. However, this main chain-type (M-type) liquid crystalline PBO required a complicated manufacturing process and possessed some undesirable properties, e.g., a rather high LC transition temperature with a high melt viscosity. In the present work, we report a novel thermotropic liquid-crystalline methacrylate polymer incorporating a benzoxazole mesogenic unit (BO-M) as side group, and we attempted to obtain excellent thermal conductivity even without magnetic/electric

fields for significantly simplifying the fabrication process of thermally conductive films.

A side chain-type (S-type) BO-pendant polymer was prepared by radical polymerization of the corresponding methacrylate using AIBN in toluene as shown in **Fig. 1(a)**, where X and Y denote connecting groups and R is a long alkyl chain. This BO-pendant polymer film showed a clear liquid crystal-like optically anisotropic phase in the ranges of $193.5\text{--}223.2 \text{ }^\circ\text{C}$ (heating) and $184.6\text{--}205.8 \text{ }^\circ\text{C}$ (cooling) on a polarizing microscope (POM) as shown in **Fig. 1(b)**. A frozen LC structure of this polymer was fixed by quenching from the LC temperature range to room temperature. **Fig. 2** shows the comparison of the Z-direction λ values; conventional polymers possessed a low level of λ ranging 0.08 to $0.17 \text{ W m}^{-1} \text{ K}^{-1}$. On the other hand, the BO-pendant polymer with the frozen LC structure developed in this work achieved an enhanced λ value of $0.60 \text{ W m}^{-1} \text{ K}^{-1}$, whereas the completely optically isotropic counterpart had a common level of λ . The results suggest that the enhanced λ value observed here is attributed to the combined effect between the incorporation of the BO-M unit and the ordered structure involving the frozen LC state.

References

1. X. Wang *et al.*, *Macromolecules*, **46**, 4937 (2013).
2. M. Hasegawa *et al.*, *Polym. Int.*, **60**, 1240 (2011).

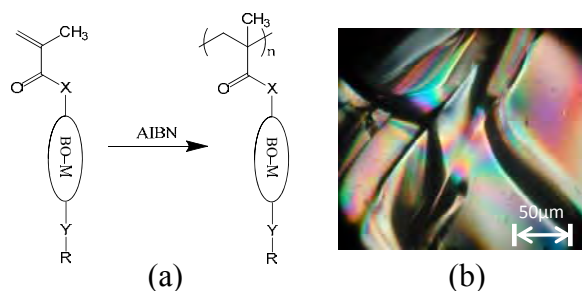


Fig. 1. Radical polymerization scheme of BO-pendant methacrylate (a) and POM photograph of the resultant polymer film at $204 \text{ }^\circ\text{C}$ (b).

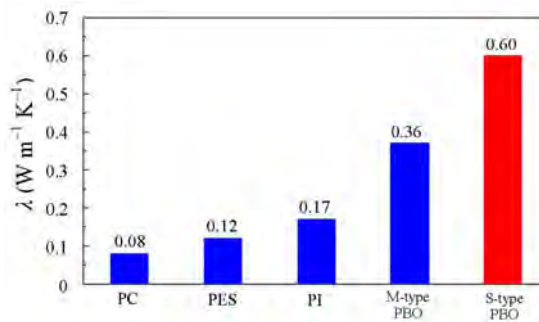


Fig. 2. Comparison of thermal conductivity for main chain-type (M-type) and side chain-type (S-type) PBO films and other conventional polymer films (PC: polycarbonate, PES: poly(ether sulfone), and PI: polyimide (Upilex-S)).

Poster Session

Calix[4]arene-based Metal-Organic Frameworks (CalixMOFs) & Metallopolycapsular Networks

Eunji Lee, Huiyeong Ju, Suk-Hee Moon,[†] and Ki-Min Park*

Research Institute of Natural Science and Department of Chemistry, Gyeongsang National University,
Jinju 52828, Republic of Korea.

[†]Department of Food and Nutrition, Kyungnam College of Information and Technology,
Busan 47011, Republic of Korea.

Keywords: Calix[4]arene, Metal-organic Framework, Metallopolycapsular Network, Tubular Structure

1,3-Alternate calix[4]arene derivative (H₄CTA) with four acetic acid arms at the low rim was synthesized for the development of fascinating metal-organic frameworks involving calixarene moiety. The metallation of H₄CTA has allowed the creation of 1-D and higher-order metal organic frameworks (calixMOFs) including metallopolycapsular networks. Assembly of calix[4]arene tetraacetate (CTA) with AgClO₄ afforded a two-metal-mediated tube-type calixMOF of the formula {[Ag₂(Ag₂@CTA)]·4H₂O}_n (Fig. 1a).¹ The use of H₄CTA with Pb(NO₃)₂ gave a three-dimensional calixMOF of the formula {[Pb₂@CTA]·2DMF}_n (Fig. 1b), which underwent single-crystal to single-crystal transformation induced by the desolvation process.²

Additionally, the reaction of H₄CTA with Zn(NO₃)₂ in the presence of α,ω -diaminoalkanes resulted in the formation of two-dimensional metallopolycapsular network (Fig. 1c).³ This metallopolycapsular network is built up of metallocapsules that consist of two CTA and two Zn(II)

ions. Short alkanediyldiammonium (⁺NH₃-(CH₂)_n-NH₃⁺, n = 2, 3, 4) guest ions are accommodated in each capsule of the metallopolycapsular network through a variety of supramolecular interactions. When *trans*-1,4-cyclohexanediamine with central bulky group instead of α,ω -diaminoalkanes used under the same condition, 1-D metallopolycapsular chain accommodating cyclohexyldiammonium (⁺NH₃-(C₆H₁₀)-NH₃⁺) guest ions was obtained (Fig. 1d). Herein, we present the structures and the physical properties of calixMOFs and metallopolycapsular networks

References

1. Reference1, Journal, Volume, pages (year) Park, K.-M.; Lee, E.; Park, C. S.; Lee, S. S. *Inorg. Chem.*, *50*, 12085 (2011).
2. Lee, E.; Kim, Y.; Heo, J.; Park, K.-M. *Cryst. Growth Des.*, *15*, 3556 (2015).
3. Lee, J.; Ju, H.; Kang, Y.; Lee, S. S.; Park, K.-M. *Chem. Eur. J.*, *21*, 6052 (2015).

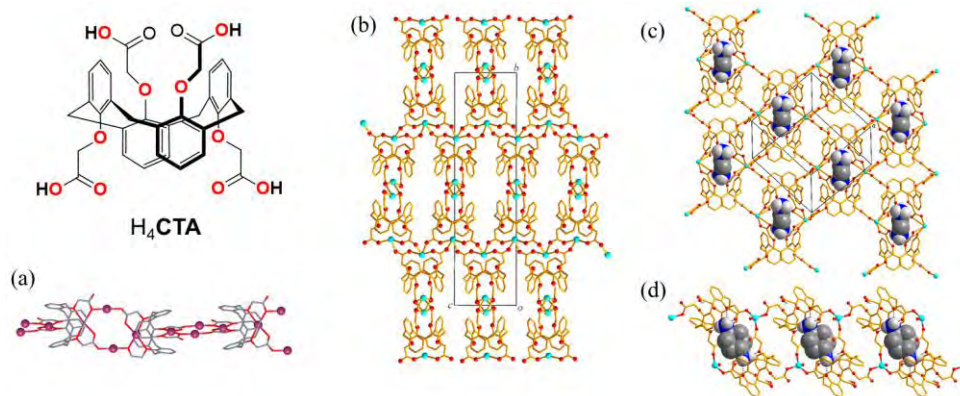


Fig. 1. (a) 1-D and (b) 3-D calixMOFs, and (c) 2-D and (d) 1-D metallopolycapsular networks.

Cation-Selective and Anion-Controlled Fluorogenic Behaviors of a Benzothiazole-Attached Macrocyclic That Correlate with Structural Coordination Modes

Huiyeong Ju,^a Duk Jin Chang,^{a,b} Seulgi Kim,^a Hyunsoo Ryu,^a Eunji Lee,^a In-Hyeok Park,^a Mari Ikeda,^c Yoichi Habata,^{*,d} and Shim Sung Lee^{*,a}

^aDepartment of Chemistry, Gyeongsang National University, Jinju 52828, S. Korea

^bBongilcheon High School, Paju 10938, S. Korea

^cEducation Center, Faculty of Engineering, Chiba Institute of Technology, Japan

^dDepartment of Chemistry, Faculty of Science, Toho University, Japan

Keywords: Dual-probe chemosensor, Anion-controlled Hg(II)-sensing, Structure-function relationship

Previously we have reported an *N*-azo-coupled chromogenic macrocycle whose mercury(II) selectivity is controlled by anions.¹ In this work, we propose a benzothiazole-attached NO₂S₂-macrocyclic **L** and undertaken a structure-function relationship as an extension of the anion dependency on the mercury(II) sensing, with emphasis on the fluorescence-modulation because no examples of the fluorescence sensor showing the cation-selective and anion-controlled behaviors have been reported so far.² Among metals, mercury(II)-selectivity as a dual-probe channel (UV-vis and fluorescence) chemosensor was observed. In the mercury(II) sensing with different anions, ClO₄⁻ and NO₃⁻ only showed the largest blue shift and the fluorescence turn-off behavior. A crystallographic approach for the endocyclic mercury(II) perchlorate complex [Hg(L)(ClO₄)₂] (**1**) and the exocyclic

mercury(II) iodide complex [Hg(L)I₂]_n (**2**) revealed that the observed anion-controlled mercury(II) sensing in the fluorescence mainly stems from the endo- and exo-coordination modes, depending on the anion coordinating ability which induces either the Hg-N_{tert} bond formation or not. The detailed complexation process with mercury(II) perchlorate associated with the cation sensing was also monitored with the titration methods by UV-vis, fluorescence spectroscopy, and cold-spray ionization mass spectrometry.

References

1. S. J. Lee, J. H. Jung, J. Seo, I. Yoon, K.-M. Park, L. F. Lindoy, S. S. Lee, *Org. Lett.*, **8**, 1641 (2006).
2. H. Ju, D. J. Chang, S. Kim, H. Ryu, E. Lee, I.-H. Park, J. H. Jung, M. Ikeda, Y. Habata, S. S. Lee, *Inorg. Chem.*, **55**, 7448 (2016).

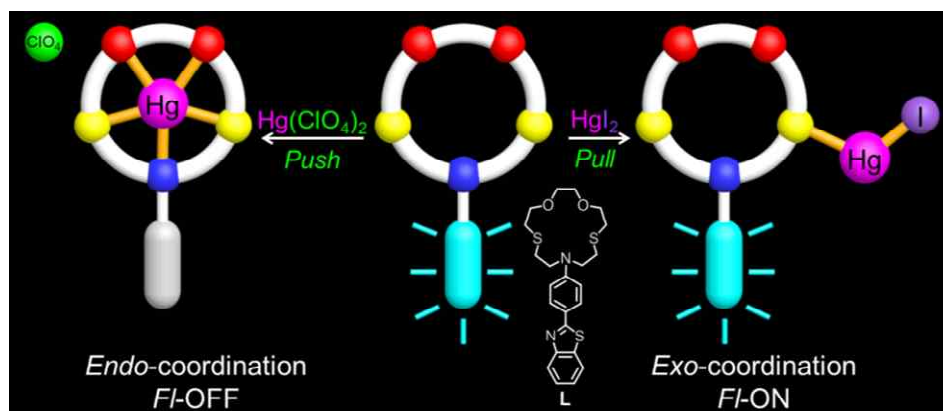


Fig.1 Anion-controlled cation selectivity of fluorescent macrocycle **L** via endo- or exocoordination

Metallation-Mediated Adaptive Guest Binding: Formation of Cascade Complexes with Pillar[5]-bis-thiacrown as a New Fused Macrocycle

Eunji Lee and Shim Sung Lee*

Department of Chemistry, Gyeongsang National University, S. Korea

Keywords: Pillar[5]-bis-thiacrown, Adaptive Guest Binding, Cascade Complex

In biomolecular recognition such as enzyme-substrate or protein-RNA, some host systems change their shapes in order to bind selectively to a suitable guest molecule. One of hot issues in the supramolecular chemistry as well as mimetic chemistry comes from how the selective binding of guest molecule in artificial host might be controlled and how such phenomena might be applied.^{1,2} In this presentation, pillar[5]-bis-thiacrown (**L**) was synthesized as a new fused macrocycle and was employed to examine the organic guest recognition on the coordination assembly with the metal ion. In the assembly reaction with the organic guests, **L** shows a non-selective binding behavior toward a series of dicyanoalkanes $[\text{CN}(\text{CH}_2)_n\text{CN}, n = 2-6]$. In the NMR studies, **L** shows a selective affinity to dicyanoethane $[\text{CN}(\text{CH}_2)_2\text{CN}$, shortly C2] in the presence of silver(I)

ion. In the solid state, **L** forms a cascade complex with C2 in which two silver(I) atoms in the crown rings are linked by one C2, exhibiting a shape-changing of the host (*see Fig. 1*). In another word, the observed results both in solution and the solid state suggest that the selective binding is strongly associated with the coordination-induced conformation change of the proposed host. We suggest that the present host system might be a model case for the adaptive guest binding system found in the biosystem.

References

1. T. Sawada, H. Hisada, M. Fujita, *J. Am. Chem. Soc.* 136, 4449 (2014).
2. D. E. Koshland Jr., *Angew. Chem. Int. Ed.* 33, 2375 (1994).

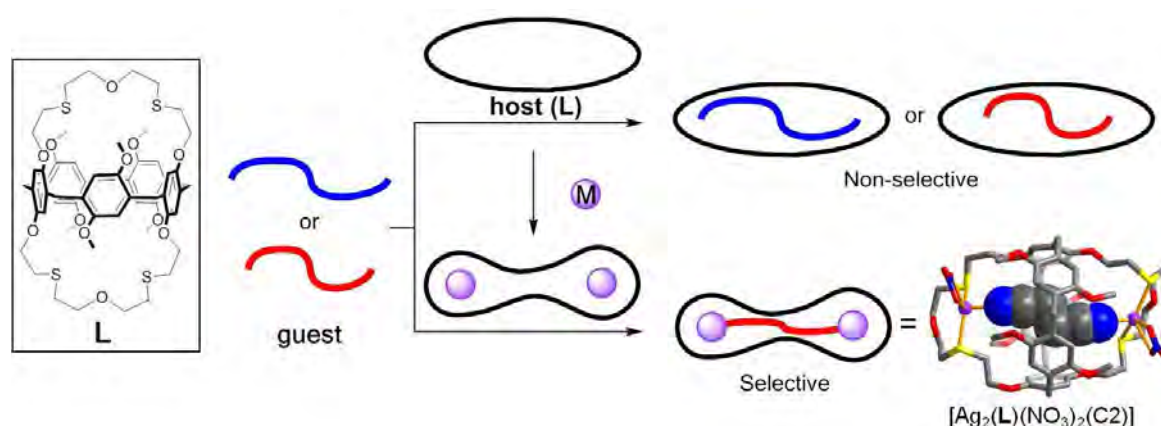


Fig.1 Schematic presentation of metallation-mediated adaptive guest binding with pillar[5]-bis-thiacrown (**L**).

Aggregation and disaggregation of highly water-soluble phthalocyanines

H. Isago and H. Fujita

National Institute for Materials Science (NIMS), 1-2-1, Sengen, Tsukuba, Ibaraki, 305-0047, Japan

Keywords: water-soluble phthalocyanines, aggregation

Phthalocyanines (Pcs) have attracted much attention from the view point of their potential applications to photodynamic therapy and/or photodynamic diagnosis of tumors owing to their intense optical absorption and emission in a bioimaging window (650 – 900 nm) [1]. It is known that Pcs are generally prone to strong molecular aggregation in aqueous media even though they are highly soluble therein. This might be a serious problem because aggregation, in particular in a face-to-face fashion (H-aggregation), significantly shortens lifetimes of the photo-excited molecules and allows them to rapidly relax back to their ground state through nonradiative transitions. Therefore, it is quite important to elucidate what dominates aggregation phenomena of dye molecules.

We have investigated highly water-soluble Pcs with four hydrophilic groups on the periphery (Fig. 1), [2]. The copper(II) complex (Fig. 1b) and its metal-free analog strongly H-aggregate in water (Fig. 2) while the antimony(V) derivative is free-from aggregation even

without cosolvent or surfactant. On the other hand, the copper complex stacks in a slipped cofacial manner (J-aggregation) in ethanol although the metal-free Pc H-aggregates as is the case in water. In this work, we report effects of solvent on their aggregation behaviour, as well as those of the central element in the cavity of the macrocyclic ligand, on the basis of spectral (optical absorption and magnetic circular dichroism) studies, which are powerful tools to monitor aggregation phenomena of dye molecules that have degenerate electronic transitions [1].

References

1. H. Isago, "Optical Spectra of Phthalocyanines and Related compounds", Springer (Tokyo), 2015.
2. H. Isago, H. Fujita, and T. Sugimori, *J. Inorg. Biochem.*, 117, 111 (2012).

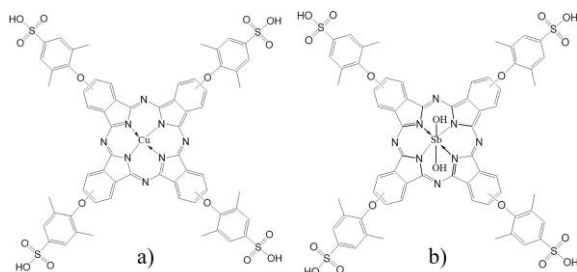


Fig.1 a) The antimony(V) complex of the highly water-soluble Pc and b) its copper(II) analog.

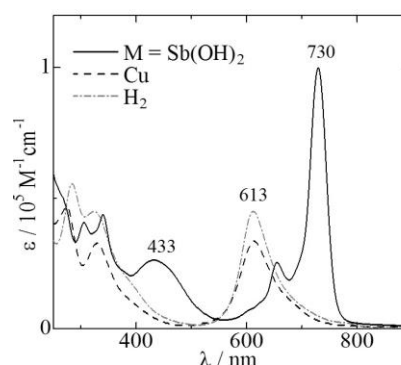


Fig.2 Optical absorption spectra of antimony(V) (solid), copper (dashed), and metal-free (dotted gray) Pcs in water.

Structure and Thermodynamics of Bis(tetra-armed cyclen)/Ag⁺ Complex

M. Iwase*, C. Kachi-Terajima***, M. Ikeda***, S. Kuwahara***, and Y. Habata***

*Department of Chemistry, Faculty of Science, Toho University

**Research Center for Materials with Integrated Properties, Toho University

***Department of Chemistry, Education Centre, Faculty of Engineering, Chiba Institute of Technology

Keywords: Cyclen; Silver; Argentivorous Molecules; Silver- π Interaction; Complex

Weak interactions such as metal-cation- π and CH- π interactions have attracted much attention from researchers because the shapes of compounds are controlled by these weak interactions. Recently, we reported that quadruple-, triple-, and double-armed cyclens with aromatic side arms behave like insectivorous plants (Venus flytrap) in organic solvents and water when they form complexes with Ag⁺. On the other hand, when other metal cations are added, no conformational changes are observed. We, therefore, refer to these armed-cyclens as “argentivorous molecules”. It is important to note that “argentivorous” is different from “argentophilic.” “Argentophilic” is used to describe Ag⁺-Ag⁺ interactions.

In a continuation of our previous work, we also found that the structures of the Ag⁺ complexes in the solid state are the racemic form (a mixture of Δ - and Λ -forms). These results prompted us to make a new armed-cyclen connected by aromatic rings such as *p*-xylyl group (**1**). There are three possible conformations ($\Delta\Delta$, $\Lambda\Lambda$, and $\Delta\Lambda$ forms) in the Ag⁺

complex. Our interests for the bis(tetra-armed cyclen) are as follows; (i) when the aromatic side-arms cover the Ag⁺ ions or not, and (ii) which is the most stable conformer? Here we report the synthesis, complexing property towards Ag⁺ ions, and X-ray structures of the 1/Ag⁺ complexes.

References

- Habata, Y.; Ikeda, M.; Yamada, S.; Takahashi, H.; Ueno, S.; Suzuki, T.; Kuwahara, S. *Org. Lett.* **14**, 4576-4579 (2012); Habata, Y.; Taniguchi, A.; Ikeda, M.; Hiraoka, T.; Matsuyama, N.; Otsuka, S.; Kuwahara, S. *Inorg. Chem.* **52**, 2542-2549 (2013); Habata, Y.; Oyama, Y.; Ikeda, M.; Kuwahara, S. *Dalton Trans.* **42**, 8212-8217 (2013); Habata, Y.; Okeda, Y.; Ikeda, M.; Kuwahara, S. *Org. Biomol. Chem.* **11**, 4265-4270 (2013); Habata, Y.; Kizaki, J.; Hosoi, Y.; Ikeda, M.; Kuwahara, S. *Dalton Trans.* **44**, 1170-1177 (2015); Ikeda, M.; Sah, A. K.; Iwase, M.; Murashige, R.; Kuwahara, S.; Habata, Y. *Supramolecular Chem.* DOI: Org/10.1080/106103278.2016.1239829.

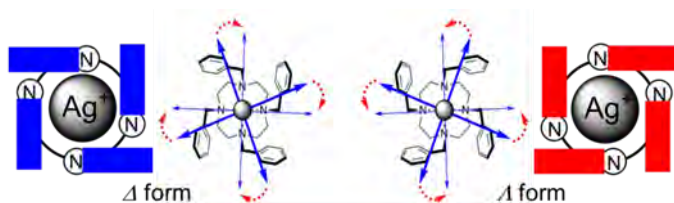


Fig. 1. Λ - and Δ -forms of tetra-armed cyclen/Ag⁺ complexes.

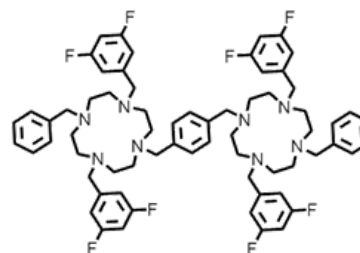


Fig. 2. Bis(armed-cyclen)s

Synthesis of Cylindrical Cyclen-Based Cryptands and Allosteric Property of their Ag⁺ Complexes

S. Kamo^{*}, Y. Nihei^{*}, M. Ikeda^{**}, S. Kuwahara^{*,***}, and Y. Habata^{*,***}

^{*} Department of Chemistry, Faculty of Science, Toho University

^{**} Education Centre, Faculty of Engineering, Chiba Institute of Technology

^{***} Research Centre for Materials with Integrated Properties, Toho University

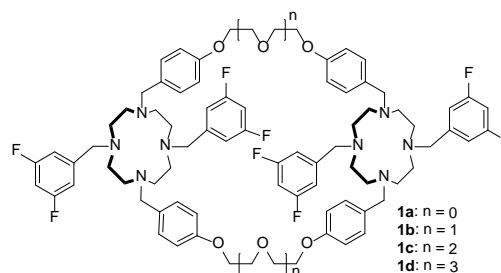
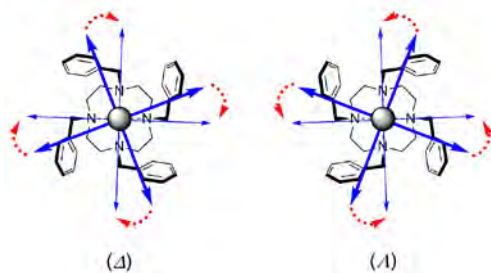
Keywords: Cyclen, Ag⁺- π Interactions, Allosteric Effect

We have reported⁽¹⁾ that tetra-armed, triple-armed, and double-armed cyclens are having aromatic rings act as an *insectivorous plant (Venus flytrap)* when they form complexes with Ag⁺ ion. The aromatic side-arms in these armed-cyclens cover the Ag⁺ incorporated into the cyclen cavities by Ag⁺- π interactions between Ag⁺ and side-arms, and CH- π interactions between the nearest neighbors side-arms. We named them *argentivorous* (silver-eating) molecules. “*Argentivorous*” is a coined word that was made by a combination of *argentum* (silver) and *vorous* (eating) in the *Latin*. It is important to note that *argentivorous* is different from *argentophilic*. “*Argentophilic*” is used in the sense of Ag⁺-Ag⁺ interactions.⁽²⁾ X-ray structures of Ag⁺ complexes with the *argentivorous* molecules showed that both Δ and Λ stereoisomers exist as a racemic form in the solid state. This result prompted us to prepare a new type of cylindrical cryptand. The new cylindrical cryptands are based on tetra-armed cyclens, and the two aromatic side-arms of the cyclens are bridged with mono, di, tri, or tetra ethylene glycol units (**1a–1d**). Our interest in the new molecules is as follows. (i) When these cylindrical cryptands bind Ag⁺ ions in the cyclen rings, the aromatic

rings cover the Ag⁺ ions incorporated in the cryptand units? (ii) Three stereoisomers can be formed in the Ag⁺ complexes with **1a–1d**, that is, $\Delta\Delta$, $\Lambda\Lambda$, and $\Delta\Lambda$ ($=\Lambda\Delta$). Which diastereomer is the most stable? (iii) Allosteric effect between the stereoisomers of aromatic side-arms in two cyclens is observed or not? We prepared cylindrical cryptands *via* six steps from dioxocyclen. Here we report the synthesis of the new cylindrical cryptands and structures with Ag⁺ complexes in the solid state and solution.

References

- 1) Habata, Y.; Ikeda, M.; Yamada, S.; Takahashi, H.; Ueno, S.; Suzuki, T.; Kuwahara, S. *Org. Lett.* **2012**, *14*, 4576-4579; Habata, Y.; Taniguchi, A.; Ikeda, M.; Hiraoka, T.; Matsuyama, N.; Otsuka, S.; Kuwahara, S. *Inorg. Chem.* **2013**, *52*, 2542-2549; Habata, Y.; Oyama, Y.; Ikeda, M.; Kuwahara, S. *Dalton Trans.* **2013**, *42*, 8212-8217; Habata, Y.; Okeda, Y.; Ikeda, M.; Kuwahara, S. *Org. and Biomol. Chem.* **2013**, *11*, 4265-4270; Habata, Y.; Kizaki, J.; Hosoi, Y.; Ikeda, M.; Kuwahara, S. *Dalton Trans.* **2015**, *44*, 1170-1177.
- 2) Schmidbaur, H.; Schier, H. *Angew. Chem. Int. Ed.* **2015**, *54*, 746-784.



Synthesis of Dendrimer-type Penta Cyclen

F. Nemoto*, M. Iwase*, M. Ikeda***, S. Kuwahara***, and Y. Habata***

*Department of Chemistry, Faculty of Science, Toho University

**Research Center for Materials with Integrated Properties, Toho University

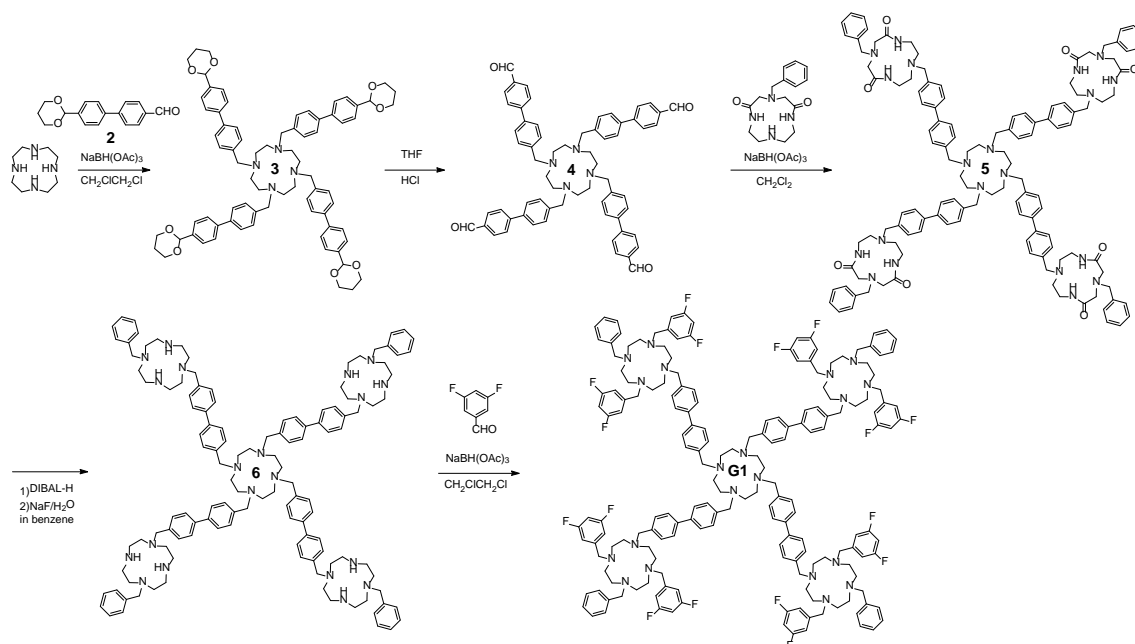
***Department of Chemistry, Education Centre, Faculty of Engineering, Chiba Institute of Technology

Keywords: Cyclen; Dendrimer; Argentivorous Molecules; Silver- π Interaction

Cyclen is a 12-membered cyclic tetra-amine that forms stable complexes with typical and transition metal cations. It is easy to construct branched structures such as a dendrimer because of four the nitrogen atoms in the cyclic structure.

Recently, we have reported that cyclens with aromatic rings as side-arms behave like an insectivorous plant (*Venus flytrap*) when they form complexes with Ag^+ . The aromatic side-arms in these molecules cover the Ag^+ incorporated into the cyclen cavities by Ag^+ - π interactions between Ag^+ and the aromatic rings and CH- π interactions between the nearest neighbors aromatic rings. We named these molecules “argentivorous (silver-eating) molecules.” The “Argentivorous” is a coined word made by a combination of argentum (silver) and vorous (eating) in the Latin. We also found that the Ag^+ complexes

with the armed cyclens exist as racemic mixtures of enantiomers (*A*- and *A*-forms) in the solid state and solution. These results led us to design dendrimer-type argentivorous molecule (**G1**). **G1** was prepared from cyclen via five steps. Cyclen was reacted with acetal-protected biphenyl aldehyde (**2**) in the presence of $\text{NaBH}(\text{OAc})_3$ in 1,2-dichloroethane to afford **3**. The protecting groups in **3** were removed under acidic condition (**4**). *N*-Benzylidioxocyclen was connected in the presence of $\text{NaBH}(\text{OAc})_3$ in dichloromethane to give **5**. A precursor (**6**) of **G1** was obtained by the reduction of **5** with DIBAL-H. Finally, **G1** was prepared by the reductive amination of **6** with 3,5-difluorobenzaldehyde in the presence of $\text{NaBH}(\text{OAc})_3$ in 1,2-dichloroethane. Now, structure and property of Ag^+ complex with **G1** are now in progress.



Ionic liquid chelate extraction of trivalent metals using 2-mercaptopyridine N-oxide

Ayano Eguchi*, Kotaro Morita*, and Naoki Hirayama*.,**

* Department of Chemistry, Faculty of Science, Toho University, Funabashi 274-8510, Japan

** Research Center for Materials with Integrated Properties, Toho University, Funabashi 274-8510, Japan

Keywords: ionic liquid, chelate extraction, trivalent metal ion, 2-mercaptopyridine N-oxide

Introduction

2-Mercaptopyridine N-oxide (HSPyO, Fig. 1a) is a bidentate ligand with a soft S-donor. HSPyO has preferable solubility into ionic liquids (ILs), and it can be used as an extractant for IL chelate extraction. Actually, Cu(II), Ni(II) and Zn(II) were extracted successfully as uncharged complexes ($M(\text{SPyO})_2$) in IL chelate extraction of divalent metal ions.¹⁾ In this study, IL chelate extraction behavior of four trivalent metal ions, Fe(III), Al(III), Ga(III) and In(III), was revealed using HSPyO as an extractant.

Experimental

Three ILs having different hydrophobicity, 1-alkyl-3-methylimidazolium bis(trifluoromethanesulfonyl)imides ($[\text{C}_n\text{mim}][\text{Tf}_2\text{N}]$, $n = 2, 4, 8$, Fig. 1b), were used as extraction solvents. In a centrifuge tube, an aliquot (1 mL) of an extraction phase ($[\text{C}_n\text{mim}][\text{Tf}_2\text{N}]$ or chloroform) containing $1.0 \times 10^{-4} - 1.0 \times 10^{-2}$ M HSPyO and 5 mL of an aqueous phase containing $0.32 - 2.0 \text{ mg L}^{-1}$ of M^{3+} ($M = \text{Fe, Al, Ga or In}$), 1.0×10^{-1} M KNO_3 and 1.0×10^{-2} M of a buffer were mechanically shaken at 25°C . After phase separation by centrifugation, the pH in the aqueous phase was measured. The metal concentration in the aqueous

phase was determined using FAAS or ICP-OES, and that in the extraction phase was determined similarly after back-extraction into $1.0 - 3.0 \text{ M HNO}_3$.

Results and Discussion

Extraction behavior of Fe(III), In(III), and Ga(III) into $[\text{C}_4\text{mim}][\text{Tf}_2\text{N}]$ and chloroform is shown in Fig. 2 as example. The extraction selectivity order for M^{3+} was $\text{Fe(III)} \geq \text{In(III)} > \text{Ga(III)}$, whereas Al(III) was not extracted into all of the solvents. In comparison between solvents, the extractability order is $[\text{C}_2\text{mim}][\text{Tf}_2\text{N}] > [\text{C}_4\text{mim}][\text{Tf}_2\text{N}] \approx [\text{C}_8\text{mim}][\text{Tf}_2\text{N}] > \text{chloroform}$ for Fe(III), $[\text{C}_2\text{mim}][\text{Tf}_2\text{N}] \approx [\text{C}_4\text{mim}][\text{Tf}_2\text{N}] \approx [\text{C}_8\text{mim}][\text{Tf}_2\text{N}] \approx \text{chloroform}$ for In(III), and $[\text{C}_2\text{mim}][\text{Tf}_2\text{N}] \approx [\text{C}_4\text{mim}][\text{Tf}_2\text{N}] \approx [\text{C}_8\text{mim}][\text{Tf}_2\text{N}] > \text{chloroform}$ for Ga(III).

In the extraction of Fe(III), increase in aqueous phase acidity resulted in drastic drop in the extractability at ca. 1 M HNO_3 . On making the shaking time longer, similar drop was observed also in the extraction of In(III) into $[\text{C}_4\text{mim}][\text{Tf}_2\text{N}]$. These results seemed to be due to the decomposition of HSPyO.

Reference

1) S. Kimura *et al.*, *Solvent Extr. Res. Dev. Jpn.*, **23**, 145 (2016).

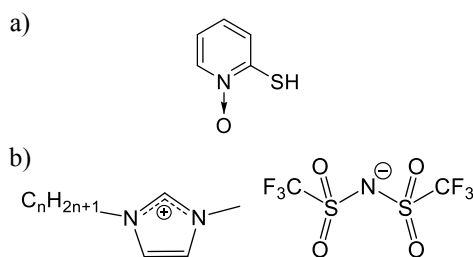


Fig. 1 Structural formulas of chemicals

- a) 2-Mercaptopyridine N-oxide
 b) $[\text{C}_n\text{mim}][\text{Tf}_2\text{N}]$ ($n = 2, 4, 8$)

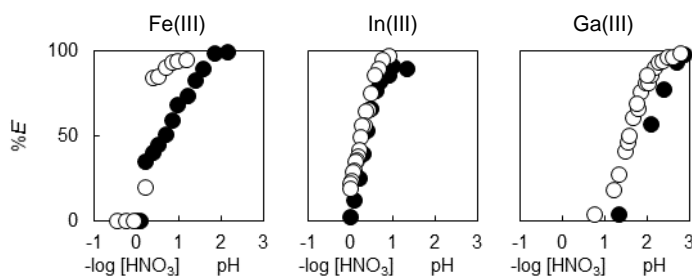


Fig. 2 The extraction behavior of M^{3+}

Extraction phase, \circ ; $[\text{C}_4\text{mim}][\text{Tf}_2\text{N}]$, \bullet ; chloroform

Anion-exchange transport behavior of zinc(II) as its thiocyanato complex through ionic liquid supported liquid membrane

Aika Suda*, Kotaro Morita*, and Naoki Hirayama*.**

* Department of Chemistry, Faculty of Science, Toho University, Funabashi 274-8510, Japan

** Research Center for Materials with Integrated Properties, Toho University, Funabashi 274-8510, Japan

Keywords: supported liquid membrane, ionic liquid, thiocyanato complex, zinc(II)

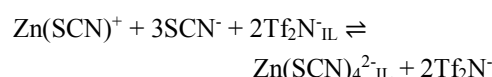
[Introduction]

Supported liquid membrane (SLM) technique, as an advanced solvent extraction technique, provides an effective and simple separation method for metal ions. In the SLM system, extraction and stripping processes are combined in a single step and tiny amounts of the extraction solvent is required. However, ion-exchange transport mechanism in ionic liquid SLM system can be different from that in batch extraction system. In this study, SLM transport behavior of Zn(II) as its thiocyanato complex through an ionic liquid ([Omim][Tf₂N]) was evaluated in terms of comparison with its batch extraction.

[Batch extraction]

Extraction study was performed as follows. Aqueous phase (5.0 mL) containing 2.0 mg L⁻¹ Zn(II), 0.1 M KSCN and 0.01 M buffer was shaken for 30 min with the extract phase ([Omim][Tf₂N], 1.0 mL). After phase separation, back extraction was performed with using 0.1 M HNO₃. The Zn(II) concentration in the aqueous phase was determined using FAAS. From logarithmic distribution ratio (log *D*) vs. log [Tf₂N⁻] and

log *D* vs. log [SCN⁻] plots, this extraction reaction was found to be as:



In addition, the extracted Zn(II) was able to be back-extracted not only into 0.1 M HNO₃ but also into pure water.

[SLM transport]

The SLM transport experiments were carried out in a diffusion cell consisting of two compartments separated by membrane (Fig. 1). In use of pure water as the receiving phase, Zn(II) was transported up to ca. 250 mg L⁻¹, that is, 0.21 mmol (Fig. 2). The transported Zn(II) is extraordinarily large compared to the [Omim][Tf₂N] amount supported in the membrane (0.078 mmol). Namely, it was suggested that different extraction mechanism contributed to the transport. In addition, use of more hydrophobic acid as the receiving phase resulted in further enhancement of transported Zn(II) amount (Fig. 2). It suggests that the anion in the receiving phase may contribute in the transport.

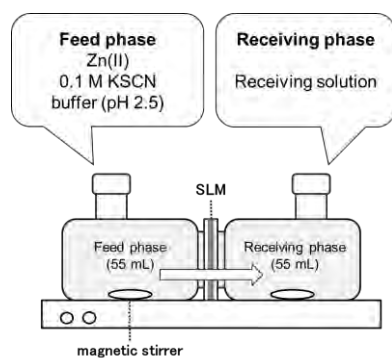


Fig. 1 Apparatus of SLM transport

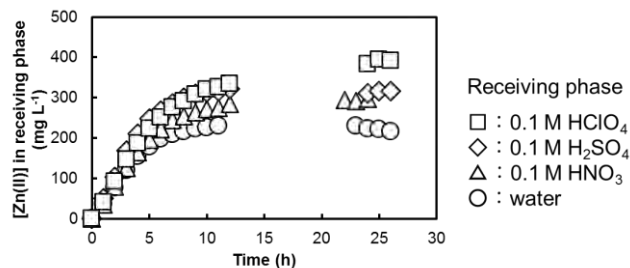


Fig. 2 Effect of receiving phase component on transport of Zn(II) through the SLM Initial feed phase concentration: 500 mg L⁻¹ Zn(II), 0.1 M SCN⁻

Extraction behavior of Fe(II) and Fe(III) in ionic liquid triphasic extraction system using 2,2'-bipyridine and TOPO

Mizuki Toita*, Kotaro Morita*, and Naoki Hirayama****

* Department of Chemistry, Faculty of Science, Toho University, Funabashi 274-8510, Japan

** Research Center for Materials with Integrated Properties, Toho University, Funabashi 274-8510, Japan

Keywords: ionic liquid, triphasic extraction, iron

Iron (Fe) exists generally as different oxidation states such as Fe(II) and Fe(III), and their mutual separation is very important for the speciation of Fe. From this viewpoint, we have investigated on a novel cyclohexane/water/ionic-liquid (IL) triphasic extraction system. In this system, Fe(II) can be extracted into the IL phase as its 2,2'-bipyridine (bpy) complex based on cation-exchange mechanism, whereas Fe(III) can be extracted into the cyclohexane phase as its trioctylphosphine oxide (TOPO) complex based on ion-pair extraction. In this presentation, we report on these extraction behaviors in detail.

Extraction behavior of Fe(II) was investigated with using water/IL biphasic extraction system. In the extraction of Fe(II) into the IL phase, preparation process for the aqueous phase affected the extraction

behavior. Concretely, adding bpy into the aqueous phase initially resulted in higher extractability than adding it finally (Fig. 1). In addition, the extracted Fe(II) was hardly stripped with HNO₃. These facts suggested that the formation and the dissociation of Fe(II)-bpy complex were relatively slow under acidic condition.

In the extraction of Fe(III) into the cyclohexane phase, the triphasic system showed lower extractability than the cyclohexane/water biphasic system. In the triphasic system, however, longer shaking time resulted in enhancement of %*E* (Fig. 2). These results suggested that the extraction rate of Fe(III) in the triphasic system was lower than that in the biphasic system for some reason.

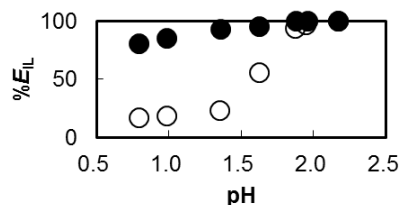


Fig. 1 Extraction behavior of Fe(II) in water/IL biphasic system
● Adding bpy initially, ○ Adding bpy finally

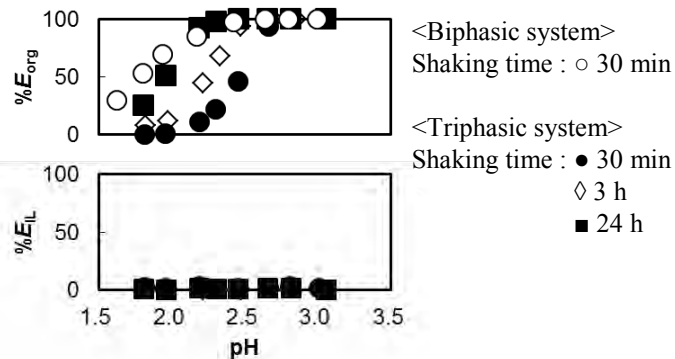


Fig. 2 Extraction behavior of Fe(III)

Ionic liquid chelate extraction of divalent metals using 1-(2-pyridylazo)-2-naphthol

Wataru Tsuzaki*, Kotaro Morita*, and Naoki Hirayama***

* Department of Chemistry, Faculty of Science, Toho University, Funabashi 274-8510, Japan

** Research Center for Materials with Integrated Properties, Toho University, Funabashi 274-8510, Japan

Keywords: ionic liquid, chelate extraction, divalent metals, 1-(2-pyridylazo)-2-naphthol

In chelate extraction of metals into an ionic liquid (IL), coordination state in the extracted complexes is very important. In the extraction of divalent metals with bidentate ligands, for example, ILs showed higher extraction ability than organic solvents¹⁾. However, the extraction of divalent metals into ILs using tridentate ligands has not been researched in detail. In this study, we investigated the extraction behavior and mechanism with using three ILs, 1-alkyl-3-methylimidazolium bis-(trifluoromethanesulfonyl)imides ($[\text{C}_n\text{mim}][\text{Tf}_2\text{N}]$, $n = 2, 4, 8$ Fig. 1), as extraction solvents, and 1-(2-pyridylazo)-2-naphthol (HPAN) as a tridentate ligand.

Extraction study was performed as follows. An aliquot (1 mL) of extraction phase ($[\text{C}_n\text{mim}][\text{Tf}_2\text{N}]$ or CHCl_3) containing 1.0×10^{-2} M HPAN and 5 mL of aqueous phase containing $2 \mu\text{g mL}^{-1}$ M^{2+} ($\text{M} = \text{Cd}, \text{Zn}, \text{Cu}$), 1.0×10^{-1} M KNO_3 and 1.0×10^{-1} M buffer was mechanically shaken for 0.5–2 h. After phase separation by centrifugation, the pH in the aqueous phase was measured. The metal concentration in the aqueous phase was determined

using FAAS, and that in the extraction phase was determined similarly after back-extraction into 1.0 M HNO_3 .

Fig. 2 shows extraction behavior of the metals (Cd(II), Zn(II), Cu(II)) into $[\text{C}_4\text{mim}][\text{Tf}_2\text{N}]$ and CHCl_3 . For Cd(II) and Zn(II), the ILs showed slightly higher extraction efficiency than CHCl_3 , and similar efficiency was showed between the ILs. For Cu(II), moreover, extraction curve for ILs shifted to ca. 1 lower pH compared with that for CHCl_3 . Namely, in the extraction system, ILs are more effective extraction solvent than CHCl_3 .

For Cd(II) and Zn(II), both of logarithmic distribution ratio ($\log D$) vs pH plot (Fig. 3) and $\log D$ vs $\log [\text{HPAN}]_{\text{IL}}$ showed straight lines with slope of ca. 2. Therefore, the extracted chemical species were determined as $\text{Cd}(\text{PAN})_2$ and $\text{Zn}(\text{PAN})_2$.

Reference

1) N. Hirayama, *Bunseki Kagaku*, 57, 949-959 (2008).

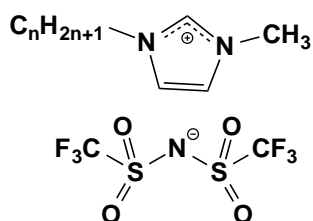


Fig. 1 Structural formula of $[\text{C}_n\text{mim}][\text{Tf}_2\text{N}]$ ($n=2,4,8$)

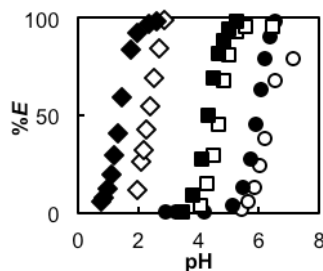


Fig. 2 Extraction behavior of metals

Metals ○● : Cd(II) □■ : Zn(II)
◇◆ : Cu(II)
Solvents ○□◇ : CHCl_3
●■◆ : $[\text{C}_4\text{mim}][\text{Tf}_2\text{N}]$

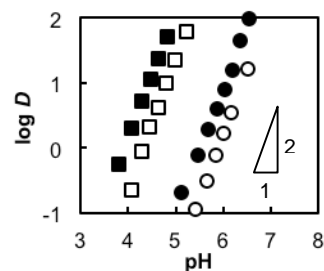


Fig. 3 $\log D$ vs pH plot

Metals ○● : Cd(II) □■ : Zn(II)
Solvents ○□◇ : CHCl_3
●■◆ : $[\text{C}_4\text{mim}][\text{Tf}_2\text{N}]$

Cadmium(II) cyanide complexes containing 2-alkoxyethanol

Takeshi Kawasaki* and Takafumi Kitazawa*[#]

* Department of Chemistry, Faculty of Science, Toho University,

2-2-1, Miyama, Funabashi, Chiba 274-8510, Japan.

[#] Research Centre for Materials with Integrated Properties, Toho University,

2-2-1 Miyama, Funabashi, Chiba 274-8510, Japan.

Keywords: Coordination polymer, Cadmium(II) cyanide, Host-guest, 2-alkoxyethanol

Cadmium(II) cyanide host frameworks with the formula $\text{Cd}(\text{CN})_2$ include various guest molecules (ex. CCl_4) by van der Waals interaction in the cavity [1]. In $\text{Cd}(\text{CN})_2$ framework, Cd^{II} ion is normally coordinated by only the four bridging cyanides and the Cd^{II} ion is tetrahedral 4-coordination geometry. But, the Cd^{II} ion might be also trigonal-bipyramidal 5-coordination or octahedral 6-coordination geometry according to other ligand (ex. H_2O). At $\text{Cd}(\text{CN})_2$ clathrates with lipophilic guest, Cd^{II} ion were only tetragonal geometry. On the other hand, at the clathrates with alcohol or short alkyl-ether guests, there were also trigonal-bipyramidal or octahedral Cd^{II} ions [2].

In this work, three novel cadmium(II) cyanide coordination polymers containing 2-alkoxyethanol, $[\text{Cd}(\text{CN})_2(\text{Etel})]_n$ (**II**, Etel = 2-ethoxyethanol), $[\{\text{Cd}(\text{CN})_2(\text{Bucel})\}_3\{\text{Cd}(\text{CN})_2\}]_n$ (**IV**, Bucel = 2-butoxyethanol) and $[\{\text{Cd}(\text{CN})_2(\text{H}_2\text{O})_2\}\{\text{Cd}(\text{CN})_2\}_3 \cdot 2(\text{Hexcel})]_n$ (**VI**, Hexcel = 2-hexyloxyethanol), were synthesized and structural determination [3]. Three complexes have 3D $\text{Cd}(\text{CN})_2$ frameworks; complex **II** has distorted tridymite-like structure (Fig. 1), and complexes **IV** and **VI** have zeolite-like structures (Figs.

2 and 3). In complex **II**, hydroxyl oxygen atoms of Etel molecules coordinate to the all Cd^{II} ions, and the Cd^{II} ions exhibit slightly distort trigonal-bipyramidal coordination geometry. Complex **IV** has both of the slightly distort trigonal-bipyramidal Cd^{II} ions and tetrahedral Cd^{II} ion. The framework in complex **IV** contains trigonal-bipyramidal Cd^{II} and tetrahedral Cd^{II} in a 3 : 1 ratio. In complexes **II** and **IV**, the hydroxyl oxygen atoms of 2-alkoxyethanol connects etheric oxygen atoms of the neighboring 2-alkoxyethanol by hydrogen bond. In complex **VI**, Hexcel molecules do not coordinate to the Cd^{II} ions, and two water molecules are located in the *cis*-positions of the octahedral Cd^{II} ion. The Hexcel molecules connect with the water molecules by hydrogen bonds. The framework in complex **VI** contains octahedral Cd^{II} and tetrahedral Cd^{II} in a 1 : 3 ratio.

References

1. T. Kitazawa, J. Mater. Chem., 8, 671, (1998).
2. T. Kitazawa, T. Kikuyama, M. Takahashi, M. Takeda, J. Chem. Soc., Dalton Trans., 2933, (1994).
3. T. Kawasaki, T. Kitazawa, Crystals, 6, 103, (2016).

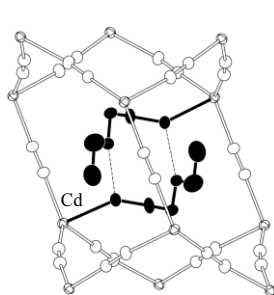


Fig. 1 Crystal structure for complex **II**

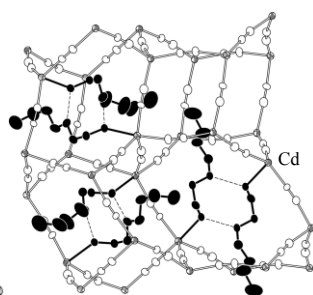


Fig. 2 Crystal structure for complex **IV**

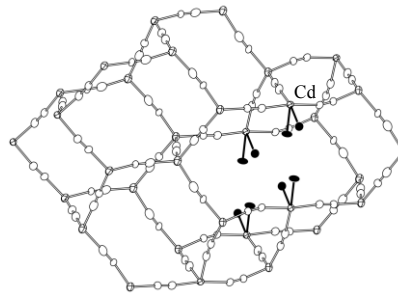


Fig. 3 Host framework for complex **VI**

Multistep Spin-Crossover Complex

Fe(4-methylpyrimidine)₂[Au(CN)₂]₂

Kosuke Kitase¹, Jun Okabayashi², and Takafumi Kitazawa*^{1,3}

¹ Department of Chemistry, Toho University, 2-2-1 Miyama, Funabashi, 274-8510, Japan

² Research Center for Spectrochemistry, The University of Tokyo, Bunkyo-ku, 113-0033, Japan

³ Research Centre for Materials with Integrated Properties, Toho University, 2-2-1 Miyama, Funabashi, 274-8510, Japan

Keywords: spin-crossover complex, Fe–Au, Hofmann-type structure, multistep transition

Spin-crossover (SCO) phenomena in magnetic complexes are important for molecular materials. Hofmann-type complexes, octahedral M^{II} (M = Mn, Fe, Co) central metal ion is coordinated equatorially by bridging ligand [M'(CN)₂]⁻ (M' = Cu, Ag, Au) or [M'(CN)₄]²⁻ (M' = Ni, Pd, Pt) and axially by pyridine-like ligand, are one of these complexes. Especially, SCO complexes with d⁶ metal ion such as Fe^{II} are very important because this low spin (LS) state is diamagnetic whereas high spin (HS) state is paramagnetic, so these complexes have the potentiality of use for on-off devices. Many SCO complexes have been reported, and some of these show multistep transition. For example, Hofmann-type 2D network complex Fe(4-methylpyridine)₂[Au(CN)₂]₂ shows three-step transition [1].

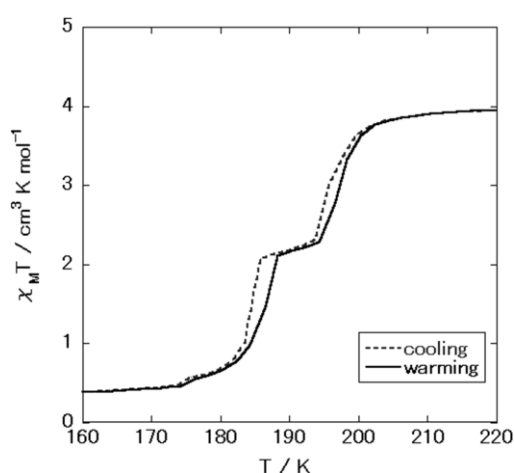


Fig.1 Magnetic susceptibility data of complex **1**. (Dashed curve: cooling, solid curve: warming.)

We have synthesized Fe-Au novel Hofmann-type 2D network complex Fe(4-methylpyrimidine)₂[Au(CN)₂]₂ (**1**). Complex **1** was synthesized using Mohr's salt, L-ascorbic acid, K[Au(CN)₂] and 4-methylpyrimidine. CHN elemental analysis for C₁₄H₁₂N₈FeAu₂, found (calcd) (%): C, 22.55 (22.66); H, 1.66 (1.63); N, 15.07 (15.10). IR spectrum of complex **1** shows C≡N stretch bands at 2171 cm⁻¹ and pyrimidine ring stretch band at 1598 cm⁻¹. Magnetic susceptibility of complex **1** shows three-step spin transition but third step came out to be very small (**Fig.1**). However, complex **1** was previously synthesized in our laboratory, and result of magnetic susceptibility was different from result in this time. In one case, it showed incomplete two-step spin transition. In other case, it showed four-step spin transition. These results may be attributed by mechanochemical effect. This effect has been reported on SCO complex [Fe^{III}(3-MeO-salenEt)₂PF₆] [2], this complex shows spin transition at 162 K, however, this spin-crossover was became incomplete by grind. This phenomenon may be occurred on complex **1**. We will measure magnetic susceptibility on single crystal and X-ray Absorption Fine Structure (XAFS).

References

- [1] T. Kosone, I. Tomori, C. Kanadani, T. Saito, T. Mochida, T. Kitazawa, Dalton Trans., 39, 1719 (2010).
- [2] M. Sorai, R. Burriel, E. F. Westrum, Jr., D. N. Hendrickson, J. Phys. Chem. B, 112, 39, 4344 (2008).

The designing of spin crossover behavior by controlling cooperativity by using Hoffman-like structural system

T. Kosone*, T. Kawasaki**, J. Okabayashi and T. Kitazawa***

* Department of Creative Technology Engineering, National Institute of Technology, Anan College, 265 Aoki, Minobayashi, Anan, Tokushima, 774-0017, Japan. Tel: +81-884-23-7195; E-mail: kosone@anan-nct.ac.jp

** Department of Chemistry, Faculty of Science, Toho University, 2-2-1 Miyama, Funabashi, Chiba 274-8510, Japan. Fax: 047 472 5077; Tel: 047 472 5077; E-mail: kitazawa@chem.sci.toho-u.ac.jp

*** Research Center for Spectrochemistry, University of Tokyo, Bunkyo-ku, Tokyo 113-0033, Japan; E-mail: jun@chem.s.u-tokyo.ac.jp

Keywords: Coordination polymer, Spin crossover, Crystal engineering

The important relationship between an intermolecular interaction and spin crossover system has been studied for the new Hoffman-like coordination polymer. The synthesis, crystal structures and magnetic properties of $\{\text{Fe}^{\text{II}}(3\text{-Fluoro-4-Methyl-pyridine})_2[\text{Au}^{\text{I}}(\text{CN})_2]_2\}$ (**1**) is described. The crystal structures of **1** at 90 K and 300 K have been determined. An octahedral Fe^{II} ion of **1** is coordinated to nitrogen atoms of $[\text{Au}^{\text{I}}(\text{CN})_2]$ linear units at equatorial positions and monodentate Alkyl-py ligands at axial positions (Fig. 1), which give rise to an infinite mesh-layer. The layers interact by pairs defining bilayers, in which aurophilic interactions hold them together. Same bilayer structures have been already reported.¹ This series has different bulky substituents of py rings. Although the bilayer structures of these compounds are completely same, py rings array between interlayer spaces are dramatically different strictly according to the substituent size, which cause

different 3-D network cooperativity. The rings form almost face-to-face superposition. The parallel stacking of the rings seems to play a significant role in the enhancing cooperativity. Interestingly, in the series of halo substituents, the complex of **1** ($L = 3\text{-F-4-Methyl-py}$) and $\{\text{Fe}^{\text{II}}(3\text{-F-py})_2[\text{Au}^{\text{I}}(\text{CN})_2]_2\}$ (**2**)^{1b} has the same dihedral angles but there are quite different cooperativity because there are different hysteresis loop and thermal quenching. It is worth noting that there is strong F-F interaction for **2**. On the other hand, **1** cause breaking F-F contact between the rings. We have already found the first (Au-Au) and second (py stacking) interaction based on the bilayer series. In addition, there seems to be third important interaction. This template structure is easy to modulate local structural design, which will achieve the control of a cooperativity. In this presentation, we will show the detail structural information and spin transition properties.

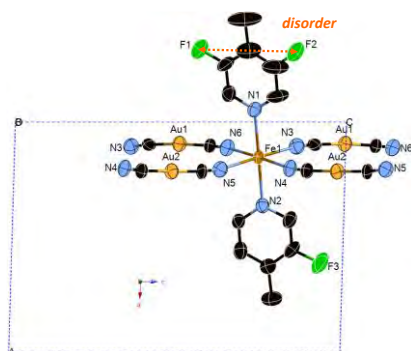


Fig.1 Coordination structure around Fe(II) of **1** at 293 K.

References

- (a) Agustí, G.; Muñoz, M. C.; Galet, A.; Real, J. A. *Inorg. Chem.* **2008**, *47*, 2552. (b) Kosone, T.; Kachi-Terajima, C.; Kanadani, C.; Saito, T.; Kitazawa, T. *Chem. Lett.* **2008**, *37*, 422. (c) Kosone, T.; Kanadani, C.; Saito, T.; Kitazawa, T. *Polyhedron* **2009**, *28*, 1991. (d) Kosone, T.; Tomori, I.; Kanadani, C.; Saito, T.; Mochida, T.; Kitazawa, T. *Dalton Trans.* **2010**, *39*, 1719.1. Reference1, Journal, Volume, pages (year)

Spin Crossover Coordination Polymer based $[\text{Au(III)(CN)}_4]^-$ unit

Kouhei Mitani¹, and Takafumi Kitazawa^{1,2}

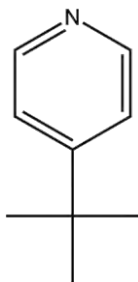
¹*Department of Chemistry, Toho University, 2-2-1 Miyama, 274-8510, Japan*

²*Research Centre for Materials with Integrated Properties, Toho University, 2-2-1 Miyama, Funabashi, 274-8510, Japan*

Keywords: spin crossover, 4-*tert*-butylpyridine, Fe(II), Au(III)

Spin crossover (SCO) phenomena are well-known as bistability magnetic conversion phenomena occurred by complexes containing iron(II) ions. It is a phenomenon that the state of the complex reversibly converts between high-spin (HS) state and low-spin (LS) states. At a Fe(II) centre, the paramagnetic HS states are stable at high temperature ranges and the diamagnetic LS states are stable at low temperature ranges [1].

In this context, we report here a novel Fe(II)-Au(III) SCO complex. Synthesis: $\text{Fe(II)(SO}_4)_2(\text{NH}_4)_2 \cdot 6\text{H}_2\text{O}$, L-ascorbic acid, and $\text{K[Au(III)(CN)}_4]$ were dissolved in water. 4-*tert*-butylpyridine (Scheme.1) was added and allowed to stand, and then white powder crystals were obtained as the new compound with the formula $\text{Fe(II)[4-}i-butylpyridine]₂ $[\text{Au(III)(CN)}_4]_2 \cdot 2\text{H}_2\text{O}$ [4-*tert*-butylpyridine]₂} (**1**). In **1**, four 4-*tert*-butylpyridine molecules act both ligand coordinating to the Fe(II) atoms and guest molecules accommodated with host structures (Fig.1). The color of **1** is colorless at RT and that at 78K is red. In order to identify the complex **1**, infrared (IR) spectra, CHN elemental analysis and thermogravimetry (TG) were measured.$



4-*tert*-Butylpyridine

Scheme.1 Ligand structure.

IR (cm^{-1} selected peaks): 3157 (C-H), 2210 ($\text{C}\equiv\text{N}$). The CHN elemental analysis confirmed the formula (found: C, 43.49; H, 4.12; N, 13.65 %. Calcd for **1** C, 42.80; H, 4.57; N,

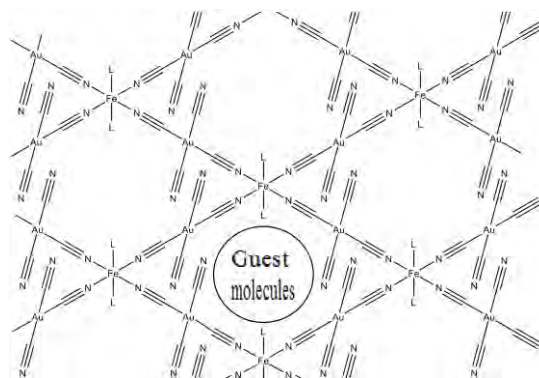


Fig.1 Proposal structure of the coordination polymer **1**.

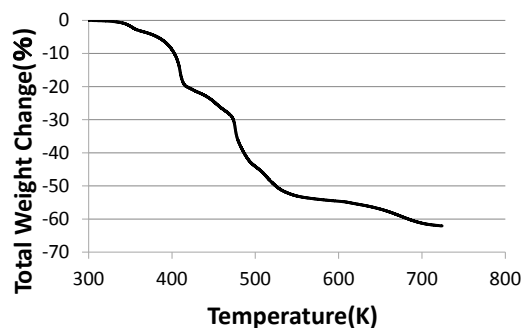


Fig.2 TG Date of **1**

13.61 %). As shown in Fig.2, the TG Date indicate the coordination polymer **1** releases two water molecules and four 4-*tert*-butylpyridine molecules step by step.

Our future work is to synthesise single crystal and determine the crystal structure by using single crystal X-ray diffraction and SQUID measurements.

References

1. T. Kosone, I. Tomori, C. Kanadani, T. Mochida, T. Kitazawa, Dalton Trans, 39, 1719 (2010)

Spin Crossover in Fe^{II} compounds based on the [M(CN)₄]²⁻ (M = Ni, Pd, Pt) units

Suzue Saito¹, Takafumi Kitazawa^{1,2}

¹Department of Chemistry, Toho University, 2-2-1 Miyama, 274-8510, Japan

²Research Centre for Materials with Integrated Properties, Toho University, 2-2-1 Miyama, Funabashi, 274-8510, Japan

Keywords: Spin crossover, Ni, Pd, Pt, coordination polymer, Hofman-like structure.

Spin crossover (SCO), spin-switching phenomena which usually take place in octahedrally coordinated d⁴-d⁷ metal ions, have been extensively explored in the field of molecular magnetism. Under an appropriate ligand field strength, their electron configurations can be reversibly switched between the low spin and the high spin states by external stimuli such as temperature, pressure, light irradiation, and guest molecule absorption/desorption. Such processes are usually accompanied by changes in physical properties such as magnetism, color, fluorescence, and dielectric constant. Hence, SCO coordination polymer materials are great potential for the applications in sensing, data storage, information processing and display devices [1].

The three types of the spin crossover materials using the 3,5-Lutidine molecules were reported in the formula Fe(3,5-Lutidine)₂Ni(CN)₄ · n(H₂O) · m3,5-Lutidine, in

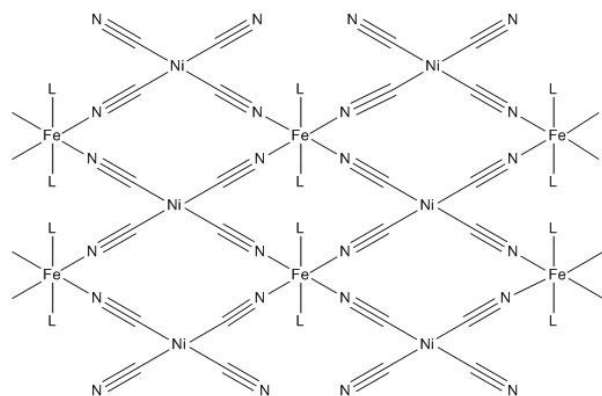


Fig.1 Proposal structure of 2D Fe(3,5-Lutidine)₂Ni(CN)₄ coordination polymer. (L = 3,5-Lutidine)

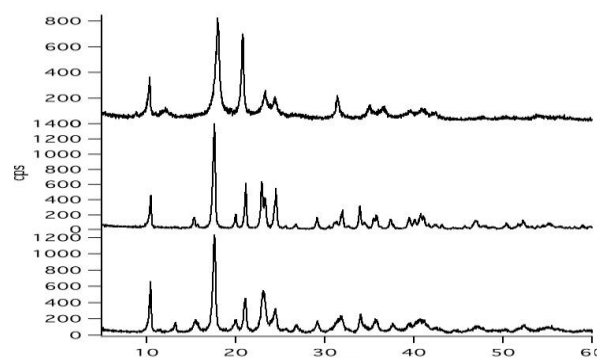


Fig.2 Powder X-ray diffraction (XRD) of Fe(3,5-Lutidine)₂M(CN)₄ (top: M = Ni, middle: M = Pd, bottom: M = Pt)

where 3,5-Lutidine molecular act as ligands and guest molecules[2,3]. Herein, we report new SCO complexes of Fe(Ligand)₂M(CN)₄ (M = Ni, Pd, Pt; L = 3,5-Lutidine). The CHN elemental analysis, infrared (IR) spectrum, thermogravimetry (TG) and powder X-ray diffraction (XRD) were performed. Fig.1 shows the proposal structure of Fe(3,5-Lutidine)₂Ni(CN)₄. Each Fe^{II} ion is coordinated by two nitrogen atoms from two ligands and four nitrogen atoms from [Ni(CN)₄]²⁻ species in a arrangement. As shown in Fig.2, the powder XRD patterns of the coordination polymers Fe(3,5-Lutidine)₂M(CN)₄ (M = Ni, Pd, Pt) are similar, indicating the three compounds are the same structures shown in Fig.1.

References

- [1]. S. L. Zhang, X. H. Zhao, Y. M. Wang, D. Shao, X. Y. Wang, Dalton Trans., 44, 9682 (2015)
- [2]. T. Kitazawa, M. Takahashi, Hyperfine Interact., 226, 27 (2014)
- [3]. T. Kitazawa, M. Takahashi, T. Kawasaki, Hyperfine Interact., 218, 133 (2013)

Spin crossover behavior in 2 dimensional MOF; Fe(Ethyl Isonicotinate)₂M(CN)₄ (M = Ni, Pd, Pt)

Hitomi Shiina¹, Jun Okabayashi², Masashi Takahashi^{1,3}, and Takafumi Kitazawa^{1,3}

¹ Department of Chemistry, Faculty of Science, Toho University, 2-2-1 Miyama, 274-8510, Japan

² Research Center for Spectrochemistry, The University of Tokyo, Bunkyo-ku, Tokyo 113-0033, Japan

³ Research Center for Materials with Integrated Properties Toho University, 2-2-1 Miyama, 274-8510, Japan

Keywords: Spin crossover (SCO), Hofmann-type structure, planar tetracoordination, Ethyl Isonicotinate

Spin crossover (SCO) phenomena are found in d⁴-d⁷ configuration, and a massive number of examples can be found in octahedral Fe²⁺ (d⁶). These specific electron configurations can be switched between high spin (HS) and low spin (LS) states by external stimuli, such as temperature, pressure, or light irradiation. By changing its spin states, size and volume of the complex changes, and also color and magnetic change appears. In addition, Hofmann-type SCO complexes, having the bidentate cyanometalate-bridged ligands [M^I(CN)₂]⁻ (M^I= Ag or Au) and planar tetracoordination cyanometalate-bridged ligands [M^{II}(CN)₄]²⁻ (M^{II}= Ni, Pd, or Pt), have been the subjects in many researchers because they can lead to additional functionalities in SCO properties. In past, many planar tetracoordination Hofmann-type SCO complexes has been reported[1,2].

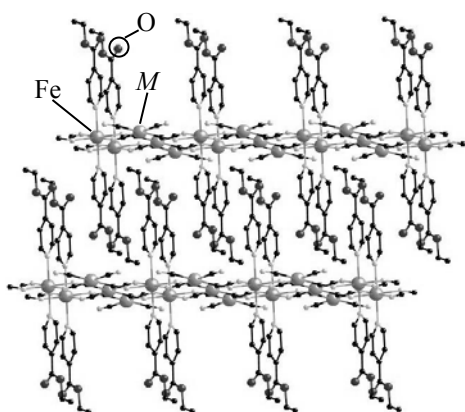


Fig.1 Crystal structure of Fe(Ethyl Isonicotinate)₂M(CN)₄ (M = Pd or Pt) determined from single crystal XRD.

In this context, we report here the novel cyano (CN)-bridged Fe-M (M=Ni, Pd, Pt) complexes using Ethyl Isonicotinate; Fe(Ethyl Isonicotinate)₂M(CN)₄. The crystal structures of Fe(Ethyl Isonicotinate)₂M(CN)₄ (M=Pd or Pt) were determined from the single-crystal X-ray diffraction (XRD) (Fig.1). The crystal structure of Fe-Ni complex was similar to that of Fe-Pd and Fe-Pt one from the powder XRD analysis. The magnetic properties reveal the abrupt SCO with relatively wide hysteresis temperature width. We also measured a temperature dependence X-ray Absorption Fine Structure (XAFS) for Fe, Ni, and Pt, and ⁵⁷Fe Mössbauer spectra for Fe-Pd complex. We will discuss much more information about each results on the presentation day.

References

- [1] T. Kitazawa, Y. Gomi, M. Takahashi, M. Takeda, M. Enomoto, A. Miyazaki, and T. Enoki, *J. Mater. Chem.*, **6**, 119 (1996)
- [2] O. Kucheriv, S. Shylin, V. Ksenofotov, S. Dechert, M. Haukka, I. Fritsky, and I. Gural'skiy, *Inorg. Chem.*, **55**, 4906 (2016)

Spin Crossover MOF Materials with 4-(5-Nonyl)pyridine

Tomoyuki Shimoide¹, Takafumi Kitazawa^{1, 2}

¹ Department of Chemistry, Toho University 2-2-1 Miyama 274-8510, Japan

^{1, 2} Research Centre for Materials with Integrated Properties, Toho University 2-2-1 Miyama 274-8510, Japan

Keywords: Spin-crossover, Fe, Au, 4-(5-Nonyl)pyridine

Spin-crossover (SCO) complexes using Fe(II) are a promising source for new functional molecular switches because they can alternate between high-spin (HS) and low-spin (LS) states depending on the circumstances and show variations in chemical magnetism, color and structural properties[1]. We focus on Hofmann type complexes containing a iron(II) ion as a central metal ion and a linear type of $[\text{Au}(\text{CN})_2]^-$ as bridging ligand. We have planned to synthesize a novel Fe-Au Hofmann type SCO complex by using a new ligand 4-(5-Nonyl)pyridine (Scheme 1), because 4-(5-Nonyl)pyridine has similar structures to 4-(3-Pentyl)pyridine which have been reported [2].

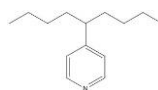
Synthesis was performed in the direct method, using Mohr's salt, L-ascorbic acid, $\text{K}[\text{Au}(\text{CN})_2]_2$ and 4-(5-Nonyl)pyridine. We were able to obtain the powder crystal of $\text{Fe}[4-(5\text{-Nonyl})\text{pyridine}]_2[\text{Au}(\text{CN})_2]_2 \cdot 4-(5\text{-Nonyl})\text{pyridine}$ (**1**) and $\text{Fe}[4-(5\text{-Nonyl})\text{pyridine}]_2[\text{Au}(\text{CN})_2]_2$ (**2**) depending on the ratio of the Fe(II) ions to the pyridine ligands. These materials were found to be SCO coordination polymers. The color of the complex **1** changes from colorless (white) to red under liquid nitrogen, while **2** does from colorless to red probably

due to the SCO behaviours. **1** and **2** have different SCO behaviours, being associated with host-guest interactions. We have identified the complex **1** and **2** by using CHN elemental analysis, IR measurement, and thermogravimetric measurement (TG) analysis. CHN elemental analysis for **1**, Calcd for $\text{C}_{46}\text{H}_{69}\text{Au}_2\text{FeN}_7$ (FW:1169.43) C, 47.23; H, 5.95; N, 8.38 %, Found: C, 47.24; H, 5.69; N, 8.44 %. For **2**, Calcd for $\text{C}_{32}\text{H}_{46}\text{Au}_2\text{FeN}_6$ (FW:964.55) C, 39.85; H, 4.81; N, 8.71 %, Found: C, 39.82; H, 4.66; N, 8.73 %. As shown in Fig.1, the TG data indicate that the coordinate polymer **1** decomposes in three stages.

Our future works are to determine the crystal structure by using single crystal X-ray diffraction and SQUID measurement.

References

- [1] K. Hosoya, S. Nishikiori, M. Takahashi, T. Kitazawa, *Magnetochemistry*, 2, 1 (2016)
- [2] T. Kosone, T. Kitazawa *Inorg. Chimi. Acta*, 439, 159 (2016)



Scheme 1. Structure of 4-(5-Nonyl)pyridine.

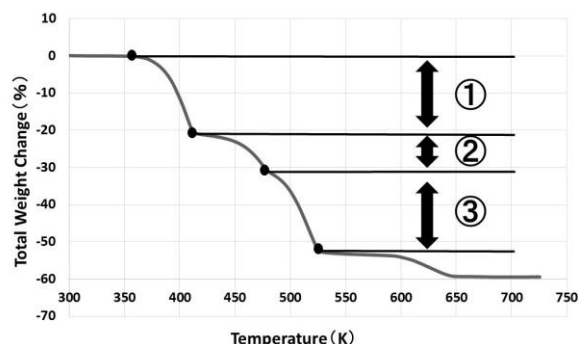
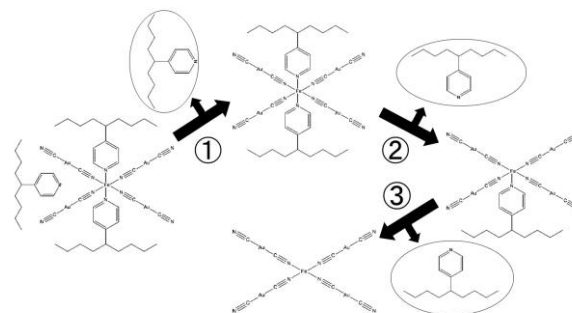


Fig.1 The TG measurement analysis of $\text{Fe}[4-(5\text{-Nonyl})\text{pyridine}]_2[\text{Au}(\text{CN})_2]_2 \cdot 4-(5\text{-Nonyl})\text{pyridine}$ (**1**).



Synthesis of Fe(II)-Au(I) 2D Hofmann-type spin crossover compounds using n-Ethynylpyridine

Shiho Suzuki¹, Takafumi Kitazawa^{1,2}

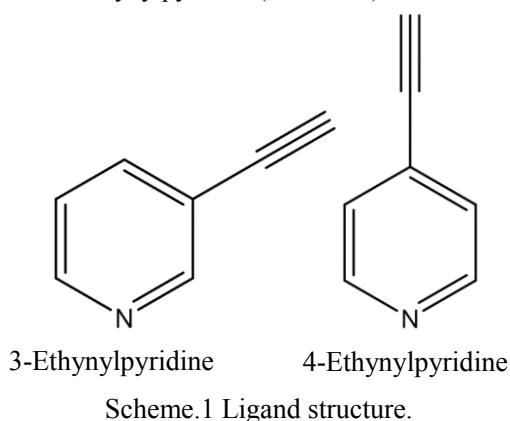
¹ Department of Chemistry, Toho University, 2-2-1 Miyama, 274-8510, Japan

² Research Centre for Materials with Integrated Properties, Toho University, 2-2-1 Miyama, Funabashi, 274-8510, Japan

Keywords: spin crossover, 4-Ethynylpyridine, 3-Ethynylpyridine, powder X-ray diffraction

The Fe^{II} spin crossover (SCO) complexes have been investigated by various research groups for their applications, in which a change in the configuration at a Fe^{II} ion center, the paramagnetic high-spin (HS) state is stable at high temperature and the diamagnetic low spin (LS) state is stable at low temperature [1]. Among the synthetic strategies for SCO coordination 2D Hofmann-type, cyanometalates [M^I(CN)₂]⁻ (M^I = Cu, Ag, or Au) and [M^{II}(CN)₄]²⁻ (M^{II} = Ni, Pd, or Pt) are useful as building blocks, because they can link coordination SCO metal centers, through the N atom of the bidentate CN⁻ substituent. Therefore, in recent years, many researchers have studied cyanometalate-bridged SCO compounds with monodentate pyridine derivatives (L), Fe^{II}(L)₂[M^{II}(CN)₄] and Fe^{II}(L)₂[M^I(CN)₂]₂ called Hofmann-type structure.

We report here on the synthesis, CHN elemental analysis, IR data, thermogravimetry (TG), and powder X-ray diffraction (XRD) of new bimetallic cyano (CN)-bridged SCO compounds with 3-Ethynylpyridine and 4-Ethynylpyridine (Scheme.1).



We have obtained the new compounds, Fe^{II}(L)₂[Au^I(CN)₂]₂ · [L]_{0.5} (**1**) (L = 3-Ethynylpyridine) and Fe^{II}(L)₂[Au^I(CN)₂]₂ (**2**) (L = 4-Ethynylpyridine).

The CHN elemental analysis confirmed the organic content of **1** (found: C, 31.54; H, 1.64; N, 11.19 %. Calcd for FeAu₂N_{6.5}C_{21.5}H_{12.5}: C, 31.81; H, 1.55; N, 11.22 %). CHN elemental analysis for **2** (found: C, 28.33; H, 1.44; N, 11.04 %. Calcd for FeAu₂N₆C₁₈H₁₀: C, 28.44; H, 1.33; N, 11.06 %). IR (cm⁻¹) of **1** : 2174 (νCN), **2** : 2172(νCN). Thermogravimetry of **1** (Fig.1) shows decrease of 2.5 ligands, and **2** shows decrease of 2 ligands.

These data also show that **1** contains the guest molecules, but **2** doesn't contain the guest molecules. Details will be report on the presentation day.

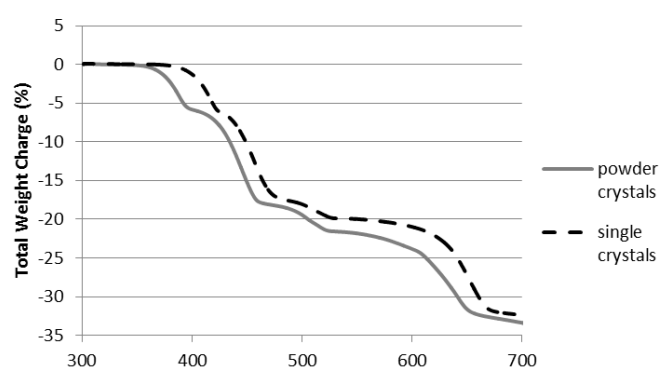


Fig.1 Thermogravimetry of **1**.

References

- [1] S. Ueno, T. Kawasaki, J. Okabayashi, T. Kitazawa, Bull. Chem. Soc. Jpn., 89, 581 (2016)

Correlation between Guest molecules and 2D Hofmann-type Spin crossover complexes

Yusuke Ueki¹, Jun Okabayashi², and Takafumi Kitazawa^{1,3}

¹ Department of Chemistry, Toho University, 2-2-1 Miyama, 274-8510, Japan

² Research Center for Spectrochemistry, The University of Tokyo, Bunkyo-ku, Tokyo 113-0033, Japan

³ Research Center for Materials with Integrated Properties, Toho University, 2-2-1 Miyama, 274-8510, Japan

Keywords: Spin crossover (SCO), microporous framework, coordination polymer, Host-Guest clathrate

Spin crossover (SCO) complexes with bistability between high-spin (HS) and low-spin (LS) states have been interested as switchable molecular device fabrications. SCO phenomena are derived from the specific electronic configurations in the 3d⁴ to 3d⁷ transition metal complexes by external stimuli such as temperature, light, pressure, and guest molecule insertion, resulting in the changes of color, unit-cell volume, and magnetic susceptibility. The two-dimensional Hofmann-type SCO complexes using the cyanide bridges of $[M^I(\text{CN})_2]^-$ ($M^I = \text{Cu}, \text{Ag}, \text{or Au}$): $\text{Fe}(\text{butyl nicotinate})_2[\text{Au}(\text{CN})_2]_2$ [1] have been investigated from the view point of structural and magnetic properties.

Recently, the spin transition depending on the guest molecules in $\text{Fe}[4-(3\text{-Pentyl})\text{pyridine}]_2[\text{Au}(\text{CN})_2]_2 \cdot n$

Guest, where the Guest is 4-(3-Pentyl)pyridine, was reported [2]. Microporous frameworks with SCO have led to additional functionality. In this presentation, we introduce that inserted guest molecules *o*-, *m*-, *p*-dichlorobenzene and chlorobenzene into the host $\text{Fe}[4-(3\text{-Pentyl})\text{pyridine}]_2[\text{Au}(\text{CN})_2]_2$, which clathrates are detected by the host magnetic properties. The values of $\chi_M T$ are 3.46 to 3.78 cm³ K mol⁻¹ at 300 K, which are in the range of the values expected for an iron (II) ion in the HS states. The SCO behaviour of clathrates was observed as the rapid spin transition around 200 K (Fig. 1), where it drops down to the complete LS states. In the case of *p*-dichlorobenzene guest, spin transition temperature becomes higher than those other guests. We found that the guest molecules are accommodated into the interstitial sites in the two-dimensional cyanide-bridged coordination polymer host frameworks. We focused on the interlayer distances of clathrates and the spin transition temperature. The important finding here is that the shapes of captured guest molecules into the host frameworks are related to the increase of the spin transition temperature through the cooperative effects between the host-guest molecules.

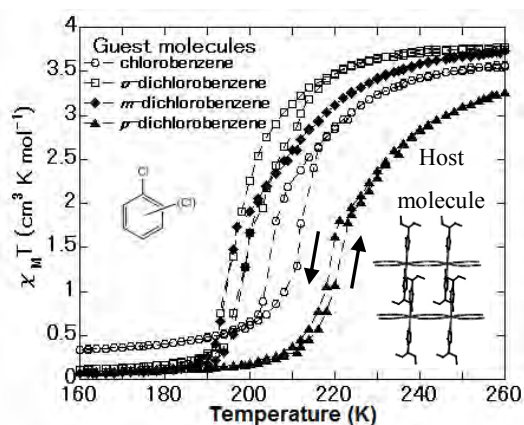


Fig.1 The magnetic properties of clathrates with guest molecules of Cl substituents. Insets show the schematic views of host and guest molecules.

References

- [1]. S. Ueno, T. Kawasaki, J. Okabayashi, T. Kitazawa, Bull. Chem. Soc. Jpn., 88, 551 (2015)
- [2]. T. Kosone and T. Kitazawa, Inorg. Chim. Acta, 439, 159 (2016)

Numerical study of irrational charges in fermion vortex systems

R.Itagaki, Y.Hatsugai *, H.Aoki**, T.Kawarabayashi

Toho University Funabashi 274-8510

*Institute of physics, University of Tsukuba, Tsukuba 305-8071

** Department of Physics, University of Tokyo, Tokyo 113-0033,
and Advanced Industrial Science and Technology(AIST), Tsukuba 305-8568

Keywords: Irrational charge, fermion-vortex system

Irrational charges in fermion-vortex systems, in particular with higher winding numbers, are investigated numerically by the kernel polynomial method [1]. We carry out large-scale numerical calculations for honeycomb lattice models having 10^6 atomic sites and a vortex structure shown in Fig.1. We then demonstrate clearly that the irrational charges are proportional to the winding number

of vortex and robust against the bond disorder respecting the chiral symmetry (Fig.2). Estimated value of irrational charges are consistent with the effective theory [2].

References

1. A.Weiß et al, Rev. Mod. Phys. **78**, 275 (2006).
2. C.Chamon et al, Phys. Rev. B **77**, 235431 (2008).

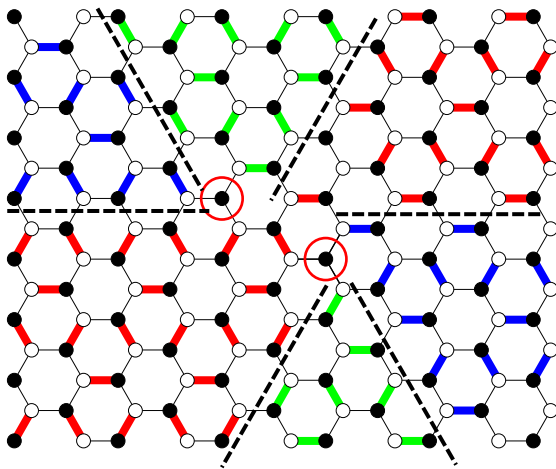


Fig1. Fermion-vortex system with the winding number $n=2$ realized in a honeycomb lattice model

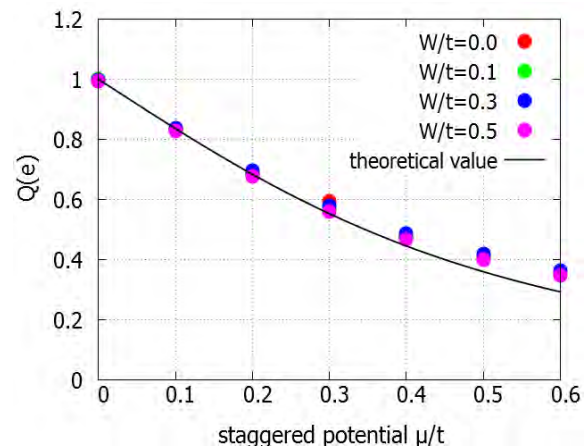


Fig2. Numerical values of irrational charge in fermion-vortex systems with the winding number $n=2$ in the presence of a bond disorder W/t .

The effect of spin-orbit interaction on the spin current in helimagnets

Koujiro Hoshi, Jun-ichiro Ohe

Department of Physics, Toho University, 2-2-1 Miyama, Funabashi, Chiba, Japan

Key words: spin-orbit interaction, helimagnet, spin current

In recent years, a magnetic structure that has geometric order chirality such as helimagnet and skrmion lattice originated from Dzyaloshinskii-Moriya (DM) interaction was reported. Especially, one-dimensional Spiral magnetic structure has been reported by using the Lorentz TEM [1]. Watanabe et al., have shown that the electric current through the helimagnet has a non-trivial spin polarization that direction is perpendicular to the magnetization [2]. On the other hand, the spin precession during the propagation is also obtained in the presence of the spin-orbit interaction.

In this study, we investigate theoretically the effect of spin-orbit interaction on the spin current through helimagnets. We calculate the time evolution of the wave packet of the conduction electron by using Chebyshev propagator [3]. We consider the two type of helimagnet, the Néel (Bloch) type has the spiral magnetization structure in which the magnetization

rotates in the plane perpendicular (parallel) to the current direction. We use the Rashba spin-orbit interaction (RSOI) and the Dresselhaus spin-orbit interaction (DSOI) as SOI. We confirm the additional spin polarization due to the propagating current. When SOI exists, we found that the additional spin polarization can be controlled by choosing the proper combination of helical magnet and SOI.

References

1. Y. Togawa, et. al., Phys.Rev.Lett **108**, 107202(2012)
2. H. Watanabe, K. Hoshi, J. Ohe, Phys. Rev. B **94**, 125143 (2016)
3. R. Chen and H. Guo, J. Comp. Phys. Commun. **119**, 19(1999)

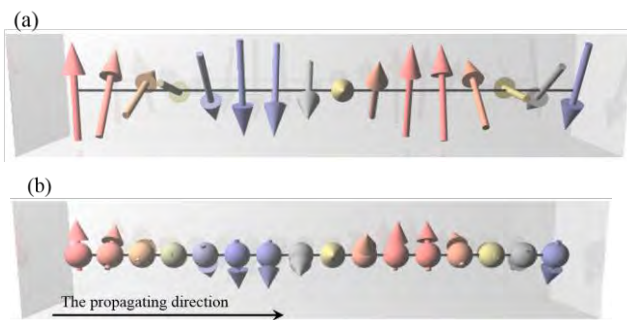


Fig.1 Schematic view of the helimagnet (the local magnet) and the spin precession (the conduction electron).
 (a) The helimagnet of Bloch type.
 (b) The spin precession by the DSOI.

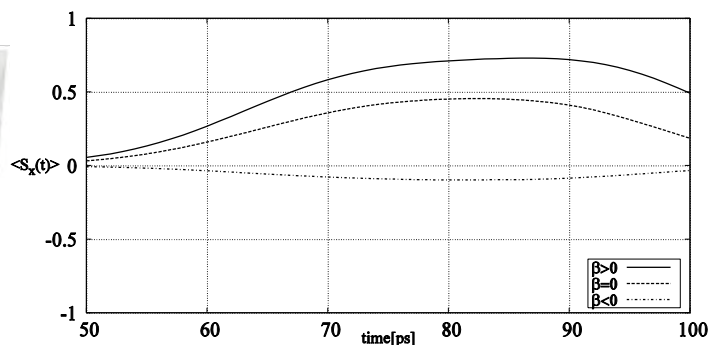


Fig.2 Time dependent spin polarization in the x direction in the combination of Bloch and DSOI. Solid (dashed) line is the case that the strength of SOI is positive(negative). Dotted line is the case that the strength of SOI is zero.

Internal deformation of magnetic skyrmion due to excitation of exchange spin-wave mode

Yuhki Shimada and Jun-ichiro Ohe

Department of Physics, Toho University, Miyama 2-2-1, Funabashi, Chiba 274-8510, Japan

Keywords: Numerical simulation, Magnetization dynamics, Collective excitation, Spin-wave resonance

Magnetic skyrmion, shown as Fig.1 (a), is one of the nano-scale magnetic structure which is appeared in a non-centrosymmetric magnetic crystal such as MnSi, FeGe, $\text{Fe}_x\text{Co}_{1-x}\text{Si}$, Cu_2OSeO_3 , etc. On the spintronics application field, the potential of this structure is most attracted as a next generation information carrier because of the nature of a quantized topological quantity and the ultra-low threshold of driven charge current density. In 2010, the skyrmion lattice (SkL) is first observed in MnSi by Yu *et al.* using Lorentz transmission electron microscopy.¹ Theoretically, this texture is stabilised as cycloidal (Néel-type) or helical (Bloch-type) magnetization configuration by competition of interactions between magnetizations and external magnetic field; spin exchange interaction, Dzyaloshinskii-Moriya interaction due to broken the symmetry, and Zeeman coupling.

Mochizuki numerically revealed that SkL has three collective exciting mode, e.g. counter-clockwise(CCW)-, clockwise(CW)-rotation motion, and expand/shrink motion, caused by spin-wave excitation.² These modes

have already confirmed other aspects from theoretical,³ and experimental^{4,5} researches. Especially in theoretical approach, the collective mode of SkL is deal with *rigid* skyrmion scheme in which the skyrmion structure is fixed during the resonant motion. In the present work, we numerically show that the each skyrmion of SkL is deformed during the resonant motion by analysing the magnetization dynamics in Fourier space. As shown in Fig.1 (b), each excited spin-wave has non-centrosymmetric amplitude. This result evidence of that the skyrmion structure is modulated non-monotonically by the linearly polarized light.

References

1. X. Z. Yu *et al.*, Nature **465**, 901 (2010)
2. M. Mochizuki, Phys. Rev. Lett. **108**, 017601 (2010)
3. G. Tatara and H. Fukuyama, J. Phys. Soc. Jpn. **83**, 104711 (2014)
4. Y. Onose *et al.*, Phys. Rev. Lett. **109**, 037603 (2012)
5. F. Buttner *et al.*, Nature Phys. **11**, 225 (2015)

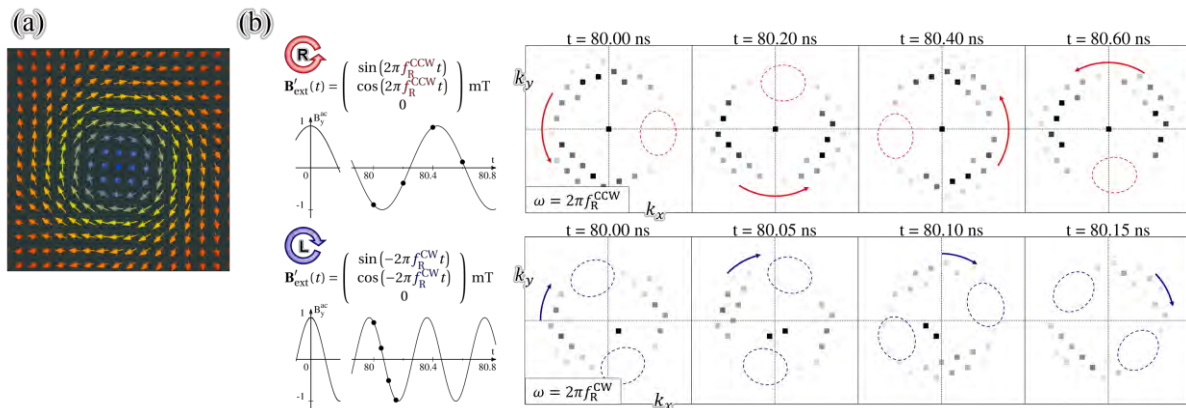


Fig.1 (a) Individual two-dimensional magnetic skyrmion in real-space under uniform static magnetic field normal to in-plane. Each vector represents normalized magnetization direction. (b) Snapshots of excited spin-wave on SkL in reciprocal-space under uniform in-plane magnetic AC field with resonant frequencies.

Acceleration of micromagnetics simulation using GPU

Takumi. Sugiura, Junichiro. Ohe

Department of physics, Toho University

Keywords: GPGPU, CUDA, Micromagnetics

The designing of spintronics devices requires the micromagnetic simulation which computes the magnetization dynamics in micro-scale. The calculated system size is often limited by the computer resources. Calculation time is proportional to the system size N when the system includes short-range exchange interaction (EXI) and Dzyaloshinskii-Moriya interaction (DMI). When one includes long-range Dipole-Dipole interaction, the calculation time is proportional to $N \log_2 N$ even the Fast Fourier Transformation (FFT) is employed. In the case of the

system including DDI, the system size is limited to $N \approx 10^4$.

In this work, we accelerate simulation using GPGPU which is specialized to parallel processing. We use CUDA as a development environment for GPU. Because CUDA is equipped with various libraries including cuBLAS and cuFFT. We show a result of acceleration to the micromagnetic simulation and technique of parallelizing method with CUDA-Fortran.

The micromagnetic simulation becomes 10 times faster than the non-parallel program.

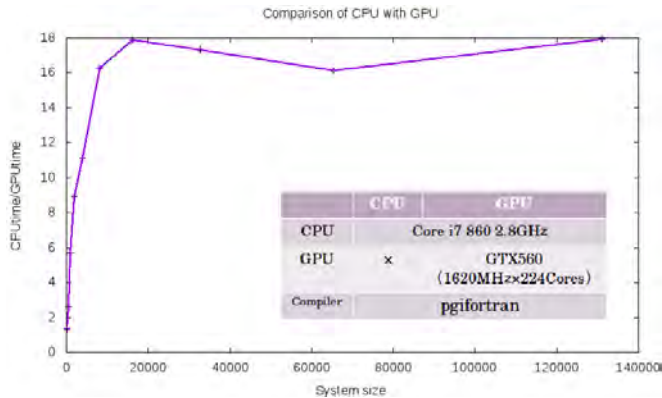


Fig.1 Comparison between CPU time and GPU time for calculating LLG equation. GPU is about 16 times faster than CPU when system size is larger than 10^4 .

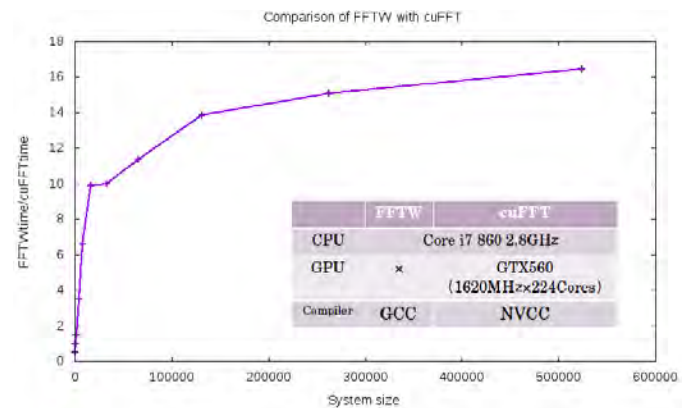


Fig.2 Comparison of computing speed for different FFT libraries. cuFFT (calculate by GPU) is 10 times faster than FFTW (calculate by CPU) when system size is larger than 10^4 .

α -Methylphenacyl thioesters as convenient thioacid precursors

T. Hatanaka*, R. Yuki*, R. Saito*** and K. Sasaki*

* Department of Chemistry, Toho University, 2-2-1 Miyama, Funabashi 274-8510 Japan

** Research Center for Materials with Integrated Properties, Toho University, 2-2-1 Miyama, Funabashi 274-8510 Japan

Keywords: Thioacids, thioesters, peptides

The thioacid functional group, due to its unique reactivity, can be an expedient handle by which to convergently and chemoselectively install modification modules, particularly in peptides.¹ For example, thioacid-based amide ligation reactions relying on electron-deficient arylsulfonamides² and isocyanates³ have been reported. Furthermore, condensation reactions between thioacids and amines have also been described recently, employing the Sanger and Mukaiyama reagents.⁴

A promising approach to preparing peptide thioacids is to carry thioesters through the peptide elongation sequence and then release the thioacids by reliable and simple reactions. Currently, several thioesters are available as thioacid precursors, including 2,4,6-trimethoxybenzyl (Tmob), 9-fluorenylmethyl (Fm), trityl (Trt), and 2-cyanoethyl, which release thioacids under either basic or acidic conditions. We were interested in a different type of precursor that would permit a wider range of applications for thioacid chemistry, and herein, report a novel thioacid precursor that has, notably, reactivity orthogonal to the Boc group. As thioesters are not generally stable to nucleophilic amines such as piperidine, Boc- based elongation would be the first choice for preparing thioacid-bearing peptides. Therefore, thioacid precursors with reactivity orthogonal to the Boc group could be useful for the preparation of peptide thioacids. In this context, we focused on phenacyl groups.

α -Methylphenacyl (Mpa) thioesters are accessible via the condensation of carboxylic acids and phenacyl thiol, which is easily prepared without column chromatography. Mpa thioesters can be converted to the corresponding thioacids by reduction with zinc dust (Figure 1), even in the presence of conventional

thioacid protecting groups, which facilitates the preparation of peptides bearing a thioacid either at the C-terminus or on the side chain. The orthogonal reactivity to the Boc-group and chemoselectivity over Tmob- and Fm-thioesters are expected to enable the preparation of complex thioacids such as peptide thioacids.⁵

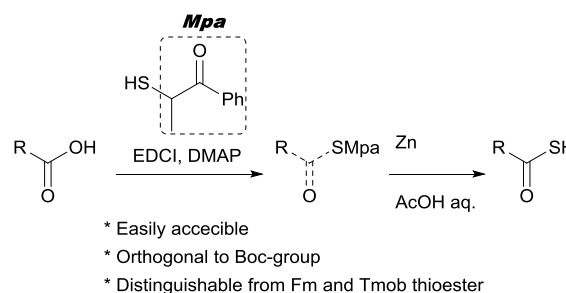


Figure 1. α -Methylphenacyl (Mpa) thioesters were developed as precursors for thioacids. MpaSH, which is easily accessible from commercially available, low-cost materials, is readily introduced to carboxylic acids. Mpa thioesters can be converted to the corresponding thioacids by gentle reduction with zinc dust.

References

- (1) Sasaki, K.; Aubry, S.; Crich, D. *Phosphorus, Sulfur Silicon Relat. Elem.* **2011**, *186*, 1005-1018.
- (2) Crich, D.; Sasaki, K.; Rahaman, M. Y.; Bowers, A. *J. Org. Chem.* **2009**, *74*, 3886-3893.
- (3) Crich, D.; Sasaki, K. *Org. Lett.* **2009**, *11*, 3514-3517.
- (4) Sasaki, K.; Crich, D. *Org. Lett.* **2010**, *12*, 3254-3257.
- (5) Hatanaka, T.; Yuki, R.; Saito, R.; Sasaki, K. *Org. Biomol. Chem.* **2016**, *14*, 10589-10592.

Structure-activity relationship study on the inhibition of aldose reductase by botryllazine B analogues having bicyclic heterocycles on the C6 position

A. Kato*, K. Sasaki**, and R. Saito***, ****

* Grad. School of Toho University

** Dept. of Chemistry, Toho University

*** Research Center for Materials with Integrated Properties, Toho University

Keywords: Aldose reductase inhibitor, botryllazine B, Structure-activity relationship

Aldose reductase (AR) is an enzyme that catalyzes reduction of glucose into sorbitol in the polyol pathway in many tissues, and believed to be strongly concerned with diabetic complications. Aldose reductase inhibitors (ARIs), therefore, have attracted much attention of medicinal chemists as therapeutics for the diabetic complications. In the previous study, we have demonstrated *in vitro* inhibitory activities of botryllazine B, isolated from *Botryllus leachi*, and its analogues of diverse substitution patterns against recombinant human aldose reductase (h-AR). It was found that introducing 2-naphthyl and 3-quinolyl groups at the C6 position as well as an additional hydroxyl group on the 2-benzoyl moiety improved the inhibitory activity. This implies that introducing a bicyclic or heterobicyclic ring at the C6 position leads to more potent ARIs, but the detailed structure-activity relationship study about the C6 substituents has not been performed yet. Thus, in the present study, we have synthesized botryllazine B analogues possessing various bicyclic heterocycles at the C6 position and evaluated their *in vitro* AR inhibitory activity against glyceraldehyde reduction by h-AR in the presence of NADPH to understand structural requirements implicated in the AR inhibitory activity of botryllazine B analogues.

The results are summarized in Table 1. All of the present botryllazine B analogs exhibited high AR inhibitory activity with IC_{50} values less than 1 μ M, indicating that the introduction of bicyclic heterocycles on the C6 position led to high AR inhibitory activity. Among the compounds tested, 6-quinoln-2-yl analogue (**1b**) showed the best inhibitory activity, which is

comparable to that of epalrestat, the only drug available commercially for the diabetic complications.

To obtain better insights into the interaction of **1b** with the active site of AR, docking simulations were conducted, and revealed that the quinolone moiety was incorporated into the specificity pocket of AR and made a hydrogen-bonding with Leu300. Since these moieties of AR are important for manifesting enzyme selectivity against other AR relating enzymes to suppress the toxicity of the inhibitors, these observations indicates **1b** is a potential candidate as a less toxic chemotherapeutic for diabetes complications.

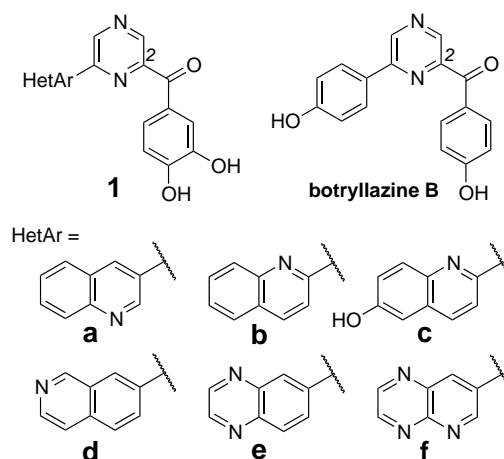


Table 1. *In vitro* inhibitory activity of **1a–f** against h-AR

Compound	IC_{50} (nM)
1a	100
1b	58
1c	92
1d	430
1e	570
1f	460
Botryllazine B	2,000
epalrestat	31

Synthesis of acetamidopyrazine dendrimer as fluorescent chemosensor

R. Saito*, **

* Dept. of Chemistry, Toho University

** Research Center for Materials with Integrated Properties, Toho University

Keywords: Fluorescent chemosensor, Acetamidopyrazine, Dendrimer

N-Acylaminopyrazines are widely distributed as light emitters of luminous marine organisms such as a jellyfish *Aequorea Victoria* and a cypridinid *Vargula hilgendorffii*. Although numerous derivatives of the acetamidopyrazines have been synthesized to investigate their fluorescent character, no attempt that involves application of these compounds as fluorescent chemosensors. Thus, we have designed and synthesized an *N*-acylaminopyrazine-based fluorescent chemosensor (**1**) composed of pyridine-2,6-dicarboxamide core and two *N*-acylaminopyrazines modified with polybenzyl-ether dendrons to improve the solubility and to reduce the intermolecular interaction between the adjacent chromophores for the purpose of suppressing the fluorescence energy deactivation with collision between the chromophores.

The synthesis of compound **1** was achieved as shown in Scheme 1.

The binding affinity of the sensor **1** toward metal ions was evaluated in benzene. The results, shown in Figure 1, indicate that compound **1** is a selective sensor for Ga(III) ion. The binding affinity of **1** toward Ga³⁺ was

evaluated by photometric titration and the association constant (K_S) for this system was estimated to be $1.67 \times 10^5 \text{ M}^{-1}$. The effect of the counter anion on the Ga³⁺ detection with **1** was also investigated to find that Ga(ClO₄)₃ gave the best fluorescent signal than GaX₃ (X = Cl, I), implying that the host **1** seems to recognized Ga³⁺ and perchlorate anion (ClO₄⁻) simultaneously by cooperative binding these ions at the appropriate sites.

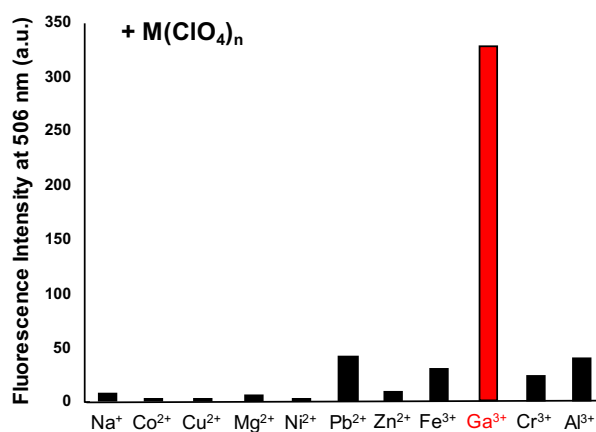
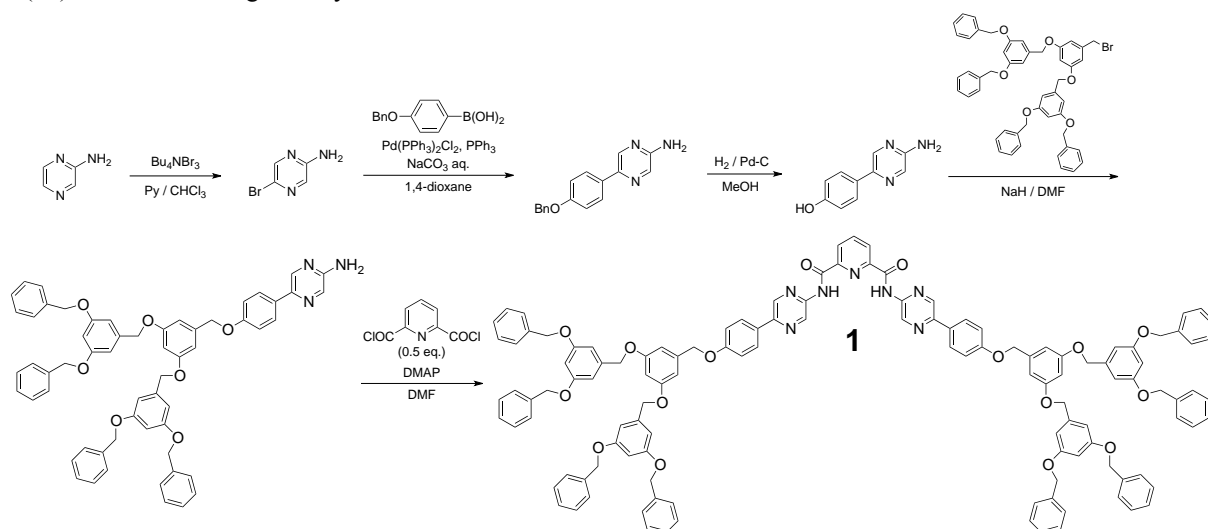


Figure 1. Fluorescence response of **1** on adding metal ions in benzene at 25°C.



Scheme 1. Synthesis of the acetamidopyrazine dendrimer **1**.

Structure-activity relationship study of (Z)-4-arylmethylidene-1H-imidazol-5(4H)-ones as aldose reductase inhibitors

A. Kato* and R. Saito**·***

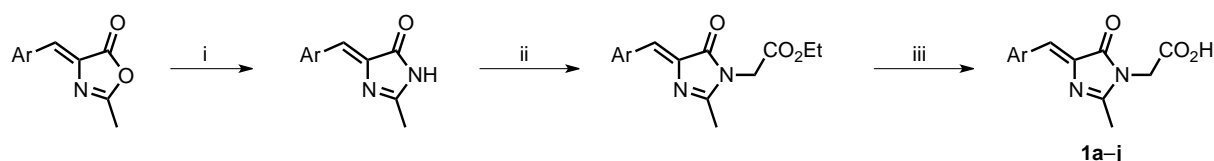
* Grad. School of Toho University

** Dept. of Chemistry, Toho University

*** Research Center for Materials with Integrated Properties, Toho University

Keywords: Aldose reductase inhibitor, (Z)-4-Arylmethylidene-1H-imidazol-5(4H)-ones, Structure-activity relationship

Aldose reductase (AR) is an enzyme that is believed to be strongly concerned with diabetic complications. Aldose reductase inhibitors (ARIs), therefore, have attracted much attention of medicinal chemists as therapeutics for the diabetic complications. In the present study, a number of (Z)-4-arylmethylidene-1H-imidazol-5(4H)-ones, which are related to the fluorescent chromophore of the *Aequorea* green fluorescent protein (GFP), have been synthesized (Scheme 1) and evaluated their *in vitro* inhibitory activity against recombinant human AR for the first time. The GFP chromophore model **1a**, with a *p*-hydroxy group on the 4-benzylidene and a carboxy-methyl group on the N1 position, exhibited strong bioactivity with an IC₅₀ value of 0.36 μM (Table 1). This efficacy is higher than that of sorbinil, a known highly potent aldose reductase inhibitor. Compound **1h**, the 2-naphthylmethylidene analogue of **1a**, exhibited the best inhibitory effect among the tested compounds with an IC₅₀ value of 0.10 μM. Structure-activity relationship studies combined with docking simulations revealed the interaction mode of the newly synthesized inhibitors toward the target protein as well as the structural features required to gain a high inhibitory activity. In conclusion, the GFP chromophore model compounds synthesized in this study have proved to be potential drugs for diabetic complications.



Scheme 1. Reagents and conditions: (i) 28% NH₄OH, K₂CO₃, EtOH, reflux; (ii) ethyl bromoacetate, K₂CO₃, acetone, reflux; (iii) NaOH, EtOH, then H₃O⁺.

Table 1. *In vitro* inhibitory activity of **1a–j** against recombinant human AR

Compound	Ar	R	IC ₅₀ (μM)	
	1a	4-OH-C ₆ H ₄	CH ₂ CO ₂ H	0.36
	1b	3-OH-C ₆ H ₄	CH ₂ CO ₂ H	3.20
	1c	C ₆ H ₅	CH ₂ CO ₂ H	0.58
	1d	4-OMe-C ₆ H ₄	CH ₂ CO ₂ H	0.51
	1e	4-F-C ₆ H ₄	CH ₂ CO ₂ H	0.65
	1f	4-Cl-C ₆ H ₄	CH ₂ CO ₂ H	0.27
	1g	4-Br-C ₆ H ₄	CH ₂ CO ₂ H	0.24
	1h	2-naphthyl	CH ₂ CO ₂ H	0.10
	1i	1-naphthyl	CH ₂ CO ₂ H	0.54
	1j	3,5-diCH ₃ -4-OH-C ₆ H ₄	CH ₂ CO ₂ H	0.13
epalrestat			0.085	

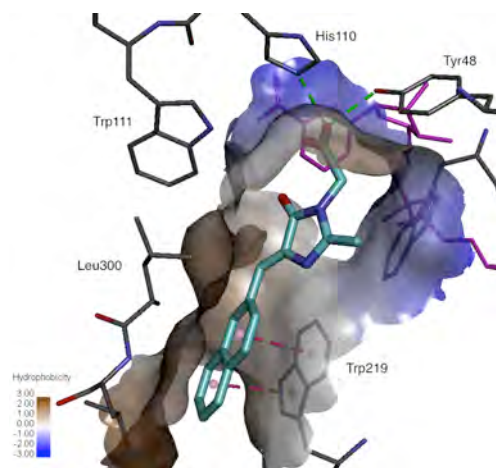


Figure 1. The contour map of aromatic interaction surfaces of the binding-site residues in human AR superposed with the predicted docking pose for compound **1h**.

Synthesis of fluorescent dendrimer having 2,5-bis(benzimidazol-2-yl)pyrazine core

Y. Suzuki*, K. Sasaki**, and R. Saito***, ****

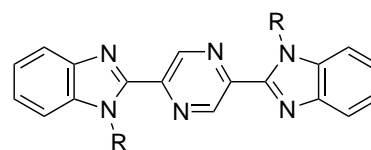
* Grad. School of Toho University

** Dept. of Chemistry, Toho University

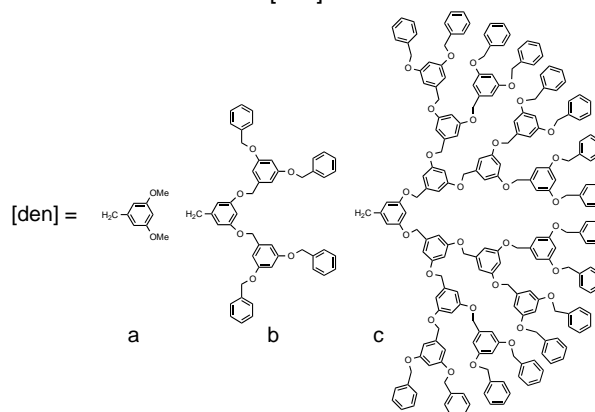
***Research Center for Materials with Integrated Properties, Toho University

Keywords: Fluorescent compound, Dendrimer, 2,5-Bis(benzimidazol-2-yl)pyrazine

The design and synthesis of intensely fluorescent organic molecules has been an attractive field because of the increasing demand for developing effective light emitting devices and bioimaging probes. We have previously reported that 2,5-bis(benzimidazol-2-yl)pyrazine (BBIP, **1**) exhibited strong fluorescence with maximum emission at 444 nm and a fluorescence quantum yield (Φ_F) of 0.90 in dimethyl sulfoxide (DMSO).¹ Despite this fascinating property as a blue fluorescent dye, **1** has the fatal drawback of poor solubility in most conventional solvents except for DMSO and *N,N*-dimethyl formamide (DMF). To apply **1** to organic luminescent device field, the solubility of **1** should be improved. For this purpose, we have previously synthesized BBIP derivatives possessing two alkyl chains at the N-1 and N-1' positions of the two benzimidazole moieties (**2**) and investigated its fluorescent properties in various organic solvents to find that they exhibited high fluorescence intensity even in protic solvents. The best fluorescence intensity was observed in benzene with Φ_F being almost unity, while the intensity decreased with increasing the solvent polarity.² Based on these findings, we came up with an idea of introducing benzene-based dendrons to BBIP in order to develop solubility-improved as well as still strongly fluorescent BBIP derivatives. Thus, in the present study, the BBIP derivatives modified with polybenzylether dendrons (**3a-c**) have been designed and their synthesis has been studied.



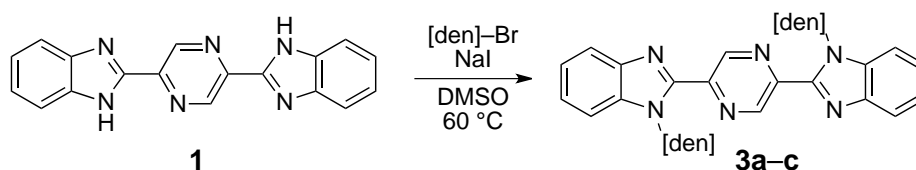
- 1:** R = H (BBIP)
2: R = (CH₂)₃NHBoc
3: R = [den]



Scheme 1 shows the synthetic strategy for gaining compounds **3ac**. The synthesis of **3a** and **3b** have achieved successfully. Fluorescent property of these compounds will be also discussed.

References

- (1) Saito, R.; Machida, S.; Suzuki, S.; Katoh, A. *Heterocycles* **2008**, 75, 531.
 (2) Saito, R.; Matsumura, Y.; Suzuki, S.; Okazaki, N. *Tetrahedron* **2010**, 66, 8273.



Scheme 1

Synthesis of glycosyl donors bearing the 2,6-lactam moiety

M. Tatsuta*, Y. Hashimoto*, R. Saito*^{**,**} and K. Sasaki*

* Department of Chemistry, Toho University, 2-2-1 Miyama, Funabashi 274-8510 Japan

** Research Center for Materials with Integrated Properties, Toho University, 2-2-1 Miyama, Funabashi 274-8510 Japan

Keywords: Mannosamine, 2,6-lactam, glycosyl donors

Gram-negative *Enterobacteriaceae* family, such as bacteria that cause dysentery, plague and salmonella poisonings, expresses a common antigenic polysaccharide known as enterobacterial common antigen, ECA. ECA contains numerous trisaccharide repeats, which are composed of $\rightarrow 3$ - α -D-Fucp4Nac-(1 \rightarrow 4)- β -D-ManpNacA-(1 \rightarrow 4)- α -D-GlcpNac-(1 \rightarrow) as shown in **Figure 1**. We believe that with well-defined ECA in hand, the development of immunotherapeutics would be enhanced, and have studied on precise chemical synthesis of ECA.

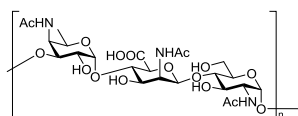


Figure 1. The structure of enterobacterial common antigen, ECA. All the *Enterobacteriaceae* express ECA, which could be an immunotherapeutics motif.

All the sugar components in ECA bears 1,2-*cis*-glycosidic bonds, to which neighbouring group participation is not applicable in construction. Recently, we have reported that 1,2-*cis*- β -glycosylation using donors with 2,6-hydroxy groups tethered by lactone moiety (**Figure 2**).¹ The reaction proceeded with high stereoselectivities *via* S_N2-like stereoinversion from α -trichloroacetimidate donors. Further, the lactone glycosides obtained could be converted either to mannosides by gentle reduction with NaBH₄, or to mannuronates by solvolysis. We plan to extend this methodology to the reactions using 2,6-lactams, which could presumably be cleaved into amino carboxylic acids as found in β -D-ManpNacA.

We have managed to prepare a 2,6-lactam from the corresponding amino acid via dehydrative ring-closure

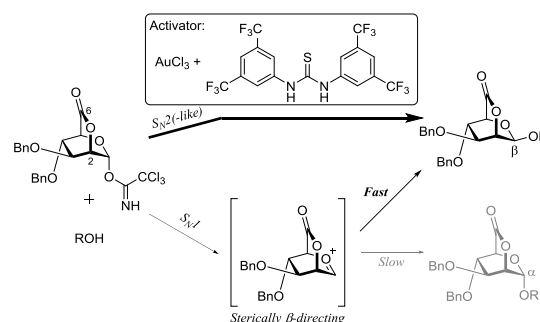
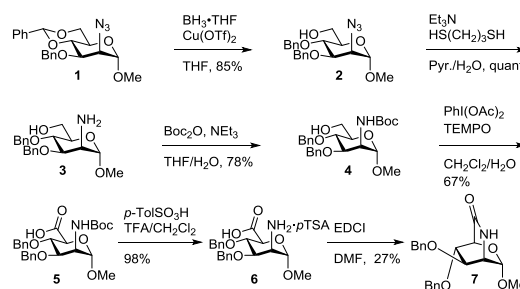


Figure 2. Stereoselective 1,2-*cis*- β -glycosylations using donors bearing 2,6-lactone moiety.¹ The reaction proceeds dominantly *via* S_N2-like pathway.

so far, as shown in **Scheme 1**. We are now working on saving steps and manipulation of the leaving group at C-1 position.



Scheme 1. Preparation of 2,6-lactam **7** from known azidoglycoside **1**.²

References

- (1) Hashimoto, Y.; Tanikawa, S.; Saito, R.; Sasaki, K. *J. Am. Chem. Soc.* **2016**, *138*, 14840-14843.
- (2) Walvoort, M. T. C.; Lodder, G.; Overkleeft, H. S.; Codée, J. D. C.; van der Marel, G. A. *J. Org. Chem.* **2010**, *75*, 7990-8002.

Control of fluorescence color of 2,5-bis(benzimidazol-2-yl)pyrazines with substituent effects

T. Yanagiba*, K. Sasaki**, and R. Saito***, ****

* Grad. School of Toho University

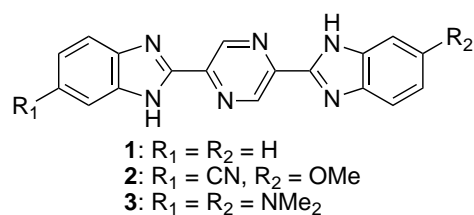
** Dept. of Chemistry, Toho University

***Research Center for Materials with Integrated Properties, Toho University

Keywords: Fluorescent compound, 2,5-bis(benzimidazol-2-yl)pyrazine, Wavelength control

Fluorescent organic molecules continue to arouse strong interest because of their fascinating applications such as electroluminescent materials, molecular probes for clinical uses, and molecular sensors for chemical and biochemical analytes. Recently, we have reported new luminescent chromophores (**1**: BBIP) based on the pyrazine nucleus, which possesses two imidazole-2-yl substituents on the central pyrazine ring and exhibited intense fluorescence with maximum emission at 444 nm and a fluorescence quantum yield (Φ_F) of 0.90 in dimethyl sulfoxide (DMSO).¹ Despite the fascinating properties as a blue fluorescent dye, **1** has a drawback as a bioimaging tool because the blue emission is not good for sensitive bioimaging in the presence of biomaterials that are capable of absorbing the blue light. To overcome this problem, we have designed two types of 2,5-bis(benzimidazol-2-yl)pyridines, a push-pull-type BBIP derivative (**2**) and a BBIP derivative having electron-donating dimethylamino group symmetrically on the benzimidazole moiety (**3**) for the purpose of gaining red-shifted fluorescence.

Fluorescence spectra of **2** and **3** were measured in various solvents and the results are shown in Figure 1. It was found that **2** exhibited solvatochromic fluorescence and its maximum wavelength was shifted bathochromically with increasing the solvent polarity. For compound **3**, a similar solvatochromism was observed and, moreover, the fluorescence maxima in polar solvents were longer than those for the push-pull one in the same solvents. The best red-shifted fluorescence was observed with **3** in ethanol at 546 nm, which is 100-nm longer than the original BBIP (**1**).



References

- Saito, R.; Machida, S.; Suzuki, S.; Katoh, A. *Heterocycles* **2008**, *75*, 531.

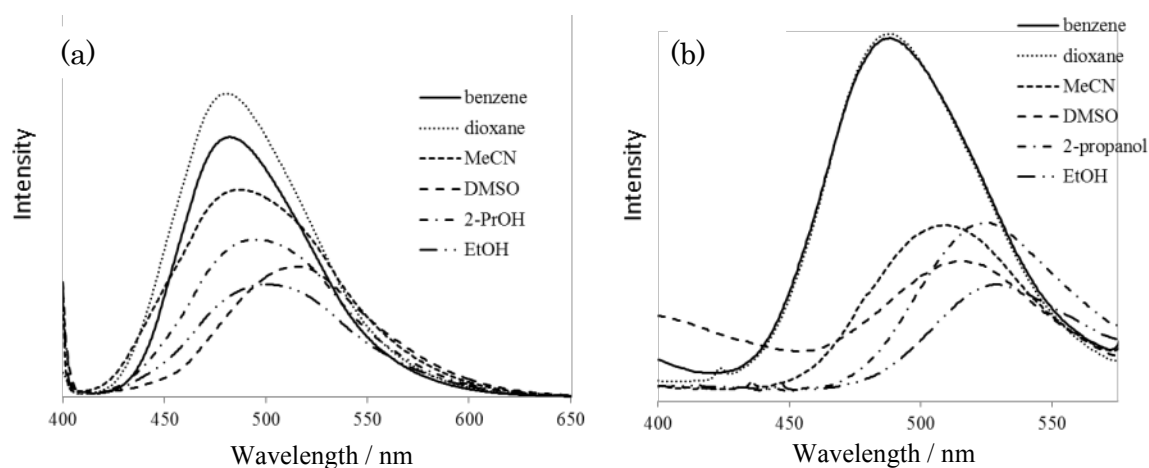


Figure 1. Fluorescence spectra of **2** (a) and **3** (b) in various solvents at 25 °C.

Improved gram-scale synthesis of shikonin derivatives

M. Ono*, K. Sasaki**, and R. Saito**·***

* Grad. School of Toho University

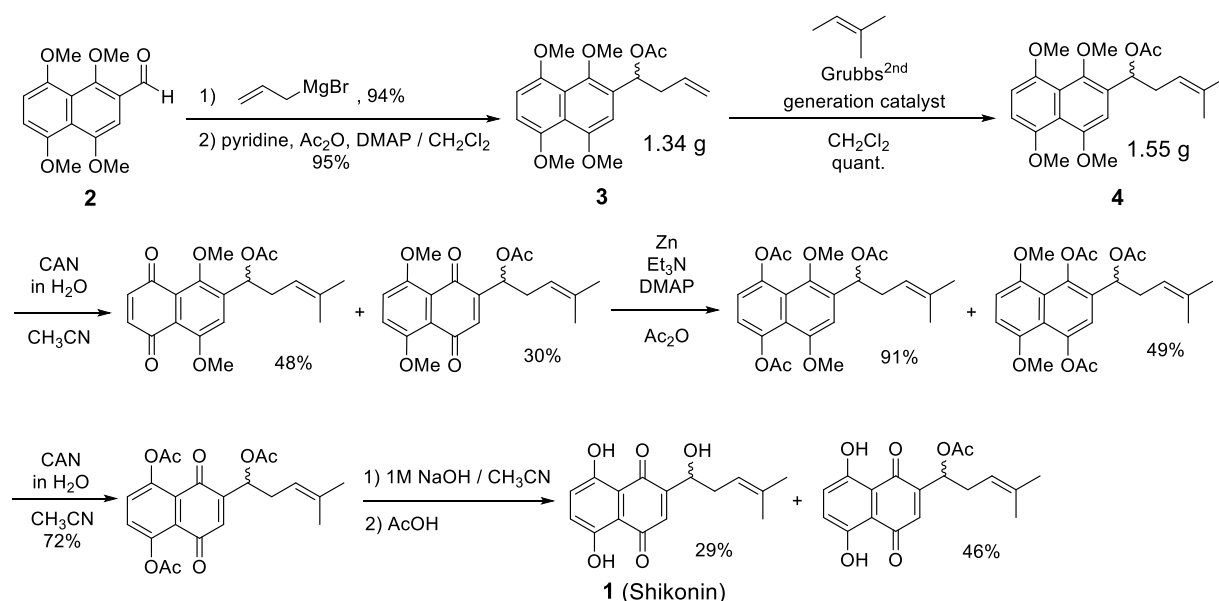
** Dept. of Chemistry, Toho University

***Research Center for Materials with Integrated Properties, Toho University

Keywords: Shikonin, Olefin metathesis

Shikonin is isolated from the roots of the traditional oriental herb Murasaki. Shikonin and Alkannin are a pair of enantiomers. Shikonin has been used as natural red dyes and has a long history in treating burns, bacterial infection, wound and inflammation. Over the past few decades, it has collected wide attentions due to its potency as a drug candidate for cancer treatment. Some shikonin derivatives having substituent on its sidechain have proved to exhibit higher anticancer activity. Especially, the *O*-acyl derivatives showed 100-times higher inhibitory activity against A875 and HeLa cells than shikonin as well as no cytotoxicity on normal cells. Despite these fascinating features, providing a large number of shikonin samples have still been challenging because most of synthetic studies so far have been conducted with mg-scales and no report

that deals a gram-scale synthesis of shikonin has been published. In the present study, we have developed an alternative synthetic route that makes it possible to prepare shikonin and its *O*-acyl derivatives over gram-scales. The overview of the synthetic strategy is shown in Scheme 1. Naphthazarin aldehyde (**2**), which was prepared with a literature method, was reacted with allylmagnesium bromide followed by *O*-acetylation to give **3**, which was then converted into a key synthetic intermediate **4** by utilizing the olefin metathesis. The noteworthy thing is that this protocol enables us to provide **4** on a gram-scale. Subsequent treatments of **4** with known procedures successfully gave the desired shikonin in a satisfactory yield. Further modification of shikonin to its *O*-acyl derivatives will be also reported.



Scheme 1. Synthesis of shikonin by utilizing olefin metathesis as a key reaction

Synthesis of propeller shaped triple[5]helicene derivatives

Hiroaki Hiyama,¹ Tomoya Matsushima,^{1,2} Soichiro Watanabe^{1,2}

¹ Department of Biomolecular Science, Faculty of Science, Toho University, 2-2-1 Miyama, Funabashi, Chiba 274-8510, Japan

² Research Center for Materials with Integrated Properties, Toho University, 2-2-1 Miyama, Funabashi, Chiba 274-8510, Japan

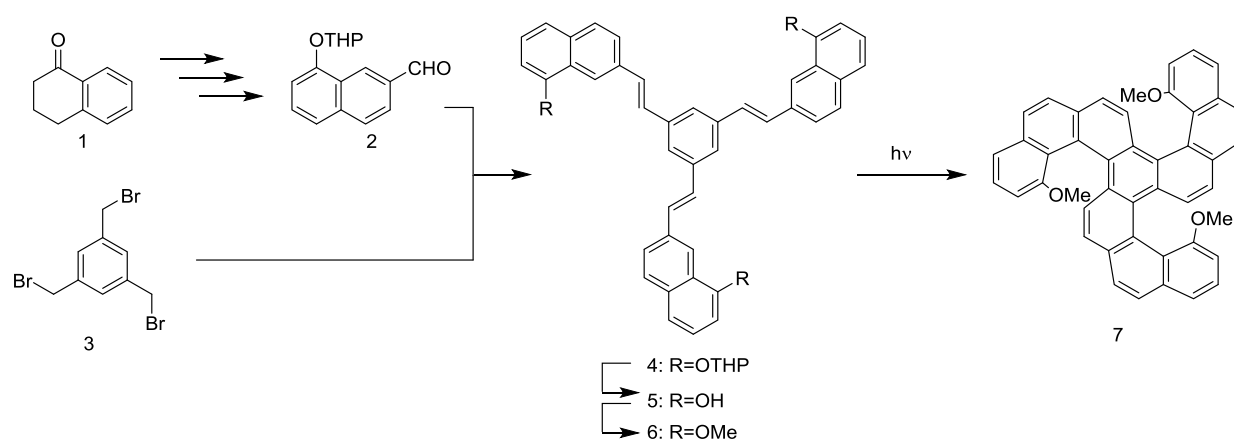
Keywords: Helicene, Polycyclic aromatic compound, host-guest chemistry

Although many compounds have been reported to interact with metal ions, a few of them can recognize specific metal ions. Representative examples that can selectively capture metal ions are crown ethers and Calixarenes. Calixarene derivatives have rigid three dimensional structure with multiple hydroxy groups in the close vicinity and hydrophobic concave regions that can interact with metal ions and small organic molecules, respectively.

We are trying to develop new host molecules taking advantage of propeller shaped triple[5]helicene which we have synthesized recently. In this paper, we will report our attempt to synthesize triple[5]helicene

derivatives with three phenolic hydroxy group at their periphery.

Scheme 1 shows the synthesis of a triple[5]helicene derivative with three methoxy groups. Compound **2** was prepared by four step reactions from 1-tetralon as a starting material. This compound was reacted with tribromide **3** to give a compound **4**. After THP ether was converted to methyl ether, an oxidative photocyclization of the compound **6** afforded triply cyclized compound **7** with three methoxy groups in low yield. We are currently trying to optimize the reaction conditions to improve the yield.



Scheme 1. Synthesis of the triple[5]helicene derivative **7**.

Synthesis of Triple Helicene Cage

Tomoya Matsushima, Soichiro Watanabe

*Department of Biomolecular Science, Faculty of Science, Toho University
Research Center for Materials with Integrated Properties, Toho University
Miyama 2-2-1, Funabashi, Chiba, 274-8510 Japan*

Keywords: oxidative photocyclization, helicene, π -conjugation, polycyclic aromatic hydrocarbons

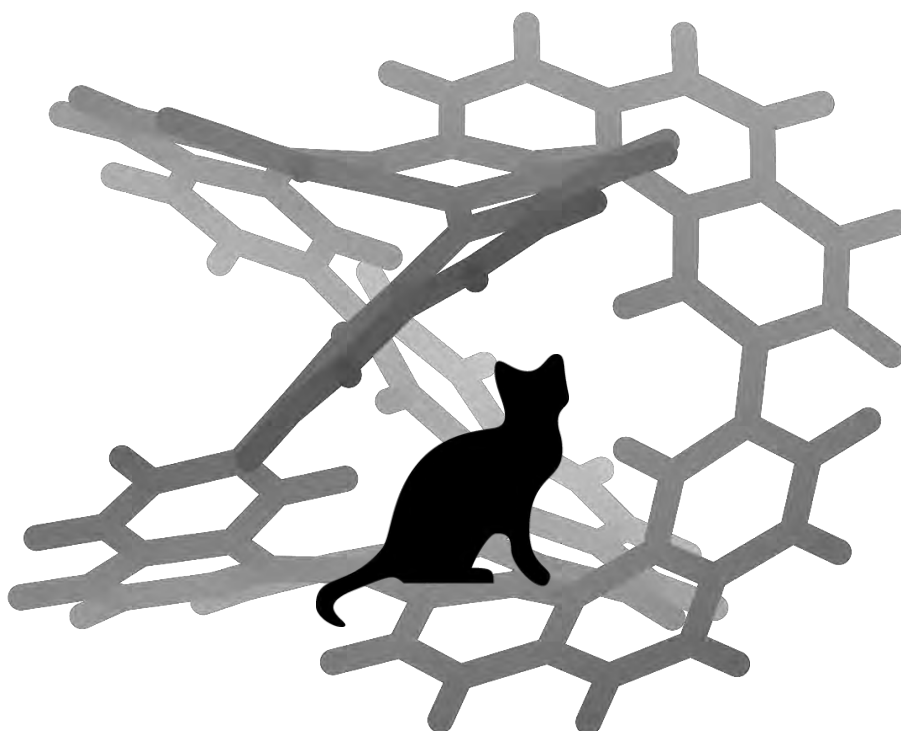
Much attention has been paid to structurally definite nanocarbons consisting of benzene rings such as fullerene, nanographenes and nanotube segments, because they exhibit various interesting properties. Therefore many researchers are studying on the application of these compounds in the field of carbon materials.

We have reported a synthesis of a triple [5]helicene with three [5]helicene moieties in the same molecule, using oxidative photocyclization as a key reaction. In order to construct π -conjugated three-dimensional structure using this claw-shaped helical motif, we synthesized a triple helicene cage having a chiral interior cavity. Synthesis of this molecule was achieved by dimerization of a triple [5]helicene derivative having a trifluoromethanesulfonyl group at

the tip of each helicene moiety by Ni catalyzed coupling reaction.

Although triple helicene cage is composed of twenty aromatic rings, their π stacking is efficiently suppressed by the helical distortion of the helicene moiety. Therefore, they have enough solubility to be purified and identified using NMR spectra even without introduction of any substituents. Since it has a cavity surrounded by aromatic rings, this compound is expected to work as an acceptor molecule taking advantage of cation- π and/or CH - anion interactions. Furthermore, this cavity can be used to chiral applications such as chiral recognition and asymmetric synthesis.

In this presentation, we report the synthetic method and physical properties of the triple helicene cage.



Dissociative Ionization Processes of Molecules by Scattered Electron–Ion Coincidence Measurements

T. Hasegawa, K. Takahashi, K. Homma, S. Oomori, N. Miyauchi, and Y. Sakai

Dep. of Physics, Toho Univ. Miyama, Funabashi, Chiba, 2748510, Japan

Keywords: doubly excited state, dissociative ionization, generalized oscillator strength, isotope effect

Scattered electron-ion coincidence measurements were performed on some simple molecules to study dissociative ionization processes. The dissociative ionization is a relaxation process of doubly excited states. Doubly excited states are typically so unstable that they result in either auto-ionization or a neutral dissociation. With auto-ionization, ionization and dissociation typically occur together. To study the dissociative ionization in detail, determination of the generalized oscillator strength distributions (GOSDs) is indispensable. In our scattered electron-ion coincidence (SEICO) measurements^{1,2}, the GOSDs can be determined as the absolute values by combining the coincidence ion signals, which revealed some doubly excited states of molecules and using a mixed-gas method^{1,2}. In this symposium, we introduce the results of molecular hydrogen, and deuterium.

The total GOSDs of H₂ and D₂ determined for a 200 eV incident electron energy and a scattering angle of 6 degrees are shown in Fig.1(a). Although the GOSD of D₂ around $(1s\sigma_g)^{-1}$ ionization threshold was slightly smaller than that of H₂, the behaviour against the electron energy-loss was almost similar. The partial ionic GOSDs of H₂⁺ and D₂⁺ are shown in Fig.1(b). Both GOSDs increased from the first ionization threshold $(1s\sigma_g)^{-1}$ at 15.4 eV, which has a maximum value at about 18 eV. After the energy-loss value exceeded the peak, both the ionic GOSD decreased gradually with further increase in the energy-loss values. There was little difference in their ionic GOSDs. However, the D⁺ formation by dissociative ionization was completely different from that of H⁺, as can be seen from Fig.1(c). The partial ionic GOSD of D⁺ was almost half of the H⁺ one in magnitude. In particular, the GOSD of D⁺ was very small in the energy-loss

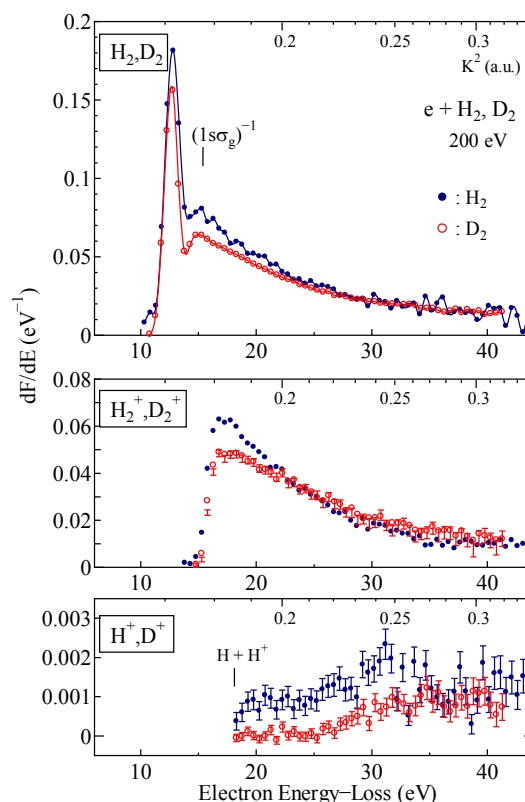


Fig.1 (a) The absolute total generalized oscillator strength distributions(GOSDs) of H₂ and D₂, (b) the partial ionic GOSDs of H₂⁺ and D₂⁺, (c) the partial ionic GOSDs of H⁺ and D⁺, respectively.

region of 18 to 22e V. Besides, we estimated the ratio of the dissociative ionization to neutral dissociation. When doubly excited molecules were decayed by dissociation from the $Q_1^1\Sigma_g^+(1)$ state, the ratio in the case of H₂ was 3:7, while that of D₂ was 1:9.

References

1. K. Yamamoto and Y. Sakai, 2012 *J. Phys. B*, **45**, 055201.
2. K. Takahashi et al., 2014 *Eur. Phys. J. D*, **68**, 83.

Development of a Time-of-Flight Mass Spectrometer Combined with an Ion Attachment Method

Y. Motegi*, K. Takeuchi*, C. Mori*, K. Takahashi*, and Y. Sakai***

*Dep. of Physics, Toho Univ. Funabashi, Chiba, 274-8510, Japan

**Research Center for Materials with Integrated Properties, Toho Univ., Funabashi, Chiba, 274-8510, Japan

Keywords: time-of-flight mass spectrometer, ion attachment method, fragment free, mass resolution

We developed a new mass spectrometer that can analyze multicomponent gases without fragmentation¹. This is essentially a time-of-flight (TOF) mass analyzer in which the ion attachment method is used for ionization. The method using this new device is referred to as “time-of-flight analysis in combination with ion-attachment” (TOFIA).

The ion-attachment (IA) method developed by Fujii² is similar to chemical ionization, in which a cation is attached to the sample molecule (M). We used an alkali metal ion, Li⁺, as the cation. Li⁺ ions collide with sample molecules in a rarefied nitrogen (N₂) gas atmosphere at a pressure of about 100 Pa. The N₂ gas works as a nonreactive collision partner and decelerates Li⁺ ions. Furthermore, the N₂ gas deactivates the internal energy of adduct ions [M+Li]⁺. As a result, the excess energy during ion attachment is lower than the binding energy of the sample molecules; thus, the adduct ions [M+Li]⁺ survive without dissociating. Consequently, a single peak corresponding to one component appears in the mass spectrum, and fragment-free ionization is attained.

Now, TOFIA has the capability to analyze breath gas in about 600 s using the radio-frequency (RF) ion guiding method and a multichannel scaler (MCS)¹. Figure 1 shows a typical TOF spectrum obtained by TOFIA. The target gas was hexane. Other experimental conditions are shown in the figure. Two notable peaks appeared in the short-flight-time region are ⁶Li⁺ and ⁷Li⁺, respectively. These are primary ions that remained as atomic species without attaching to other molecules. Among the four peaks that appeared in the TOF spectrum, only one peak (42 μs) remained in hexane (C₆H₁₄): the (C₆H₁₄)⁷Li⁺ adduct ion of the parent

molecule with a mass number of 93. The small peak at a mass number of 35 corresponds to (N₂)⁷Li⁺. Thus, we have already confirmed the absence of fragment peaks in the TOF spectra obtained by TOFIA for any sample, i.e., alcohol, ketone, alkene, and alkane hydrocarbons.

However, the mass resolution of our trial device was unsatisfactory. Therefore, we began to improve the TOFIA device from linear type to vertical one to enhance the mass resolution. Besides, the reflection type named “Reflectron” will be also developed in this project. We expect that the TOFIA will contribute significantly to the development of new multicomponent gas analysis techniques.

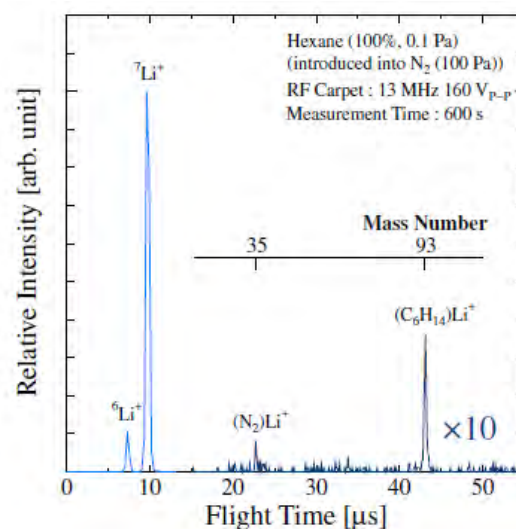


Fig.1 Typical TOF spectrum obtained by TOFIA¹.

References

1. K.Takaya et.al., *Jpn. J. Appl. Phys.*, **53**, 106602(2014).
2. T. Fujii, *Mass Spectrom. Rev.* **19**, 111 (2000).

Production and characterization of fluorescent gold nanoclusters

Y. Hamano, and T. sugai

Department of Chemistry, Toho University, Miyama 2-2-1, Funabashi 274-8510, Japan

Keywords: Fluorescent gold nanoclusters, Size effect

Gold Nanoclusters (AuNCs) have been considered as remarkable nanomaterials, which consist of several tens of Au atoms and show distinct size effect on various properties.[1] One of promising their properties is fluorescence. Size-tunable emission wavelength of fluorescent AuNCs, which is absent from organic fluorescent materials, have gained much attention.[2] Furthermore, the emission can be controlled by the surrounding molecules. Here we present the production and characterization of fluorescent AuNCs.

AuNCs were produced by Brust method[3]. The obtained sample solution showed blue fluorescence with 365 nm excitation. The produced AuNCs covered with the thiol was characterized by transmission electron microscopy (TEM) with FEI tecnai G2 20 and fluorescence with HORIBA Fluorolog-3.

Fig. 1 shows the observed TEM images of the produced AuNCs. Spherical structures were observed and most of the diameters were from 1 to 3 nm. The minimum size of 1 nm corresponding to Au₁₃ is

determined by the image contrast, which is degraded by the supporting micro grid. So there should exist much smaller ones. Fig. 2 shows the fluorescence with excitation from 350 to 380 nm. Excitation peaks were observed at 410, 430, 460, and 500 nm. Au₁₃ is reported to have emission at 500 nm [4], which confirms the production of much smaller AuNCs in this sample, such as Au₅ and Au₈. The peak positions are independent of excitation. The results are understood as molecular like fluorescence suggesting stable and uniform magic number AuNCs.[4]

References

1. R. Kubo, J. Phys. Soc. Jap., 17, 975-986, (1962)
2. J. Yu, S. Choi, and R. M. Dickson, Angew. Chem. Int. Ed., 48, 318-320, (2009)
3. M. Brust et al. Chem.Soc., Chem.Commun. , 801-802, (1994)
4. J Zheng et al. Phys. Rev. Lett., 93, 077402, (2004)

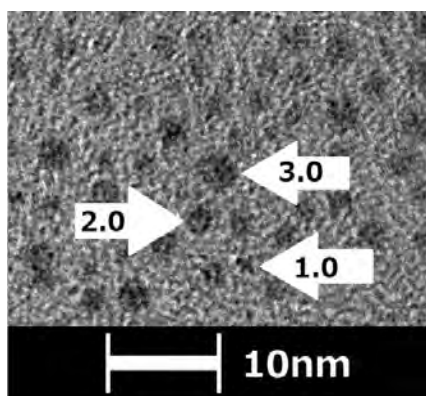


Fig.1 Images of gold nano clusters observed by transmission electron microscopy. The size are less than 3 nm.

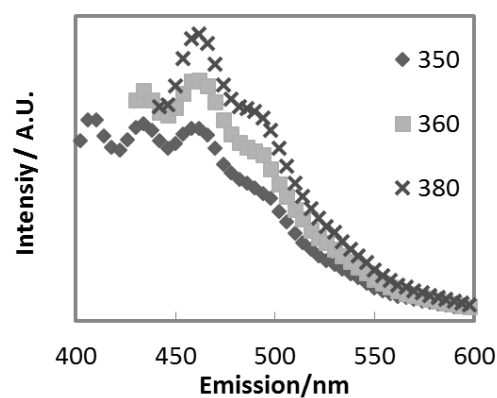


Fig.2 Emission spectra of gold nano clusters. The peak positions of 410-510 nm are independent of excitation wavelength of 350-380 nm

Flow rate dependence of production of double-wall carbon nanotubes by high-temperature pulsed-arc discharge

Yuto Hikichi, Toshiki Sugai

Department of Chemistry, Toho University, Miyama 2-2-1, Funabashi 274-8510, Japan

Keywords: High-temperature pulsed-arc discharge, Double-wall carbon nanotube, Flow rate

A high-temperature pulsed-arc discharge (HTPAD) has been developed to produce nanocarbon materials. The system utilizes width controlled pulsed arc discharge for the vaporization of electrode in temperature controlled ambient (~ 760 Torr) Ar. With this width and temperature control, novel materials have been produced by the system such as high-quality double wall carbon nanotubes (DWNW) with outer diameter of around 1.8 ± 0.2 nm[1]. However the production ratio of DWNT in all produced CNT with by-produced single-wall carbon nanotube (SWNT) is not high ($\sim 10\%$) and diameter of DWNT cannot be controlled so far. Recently, however, we have found that the ratio is enhanced up to 30% with low pressure (~ 300 Torr) operation[2]. Even in this low pressure condition, the diameter is still unchanged. To control the diameter and to achieve further enhancement of the ratio, here we present the effect of flow rate of Ar. The flow rate has been utilized to control the structures of carbon nanotubes, especially with laser vaporization (LV) method, where thick single-wall carbon nanotubes are produced in the low flow rate conditions[3].

The HTPAD system consists of a furnace with a ceramic tube inside, an Ar gas flow and pressure control system, an HV pulse voltage controller, and a water cooling trap. Electrodes made of graphite containing catalytic metals (Ni/Y 4.2/0.5 at. %:Toyo Tanso Co. Ltd.) were located in the ceramic tube. The pulsed arc discharges (0.6 ms, 50 Hz, and 100 A) vaporized the electrodes and produced nanotubes in the Ar gas at the temperature of 1250 °C and at the pressure of 300 Torr. The flow rate was change from 200 ml/min to 400 ml/min. The products were collected on the trap and were characterized by TEM and Raman spectroscopy.

Figure 1 shows the diameter distribution of SWNT and DWNT. Both of them shift to the larger diameters as the flow rate is decreased. This flow effects are very similar to those found in LV experiments[3]. Even though the diameter enlargement of SWNT is much more prominent than that of DWNT, the DWNTs produced in the condition of 200 ml/min with the average diameter of 2.3 nm is the thickest DWNT ever produced by HTPAD. This distribution change was also confirmed by Raman spectra. Not only the diameter, but also the production ratio of DWNT is enhanced up to 60% in the 200 ml/min condition. These flow effects can be interpreted as that nascent production process of DWNT with HTPAD and that of SWNT with LV have some similarity.

References

- 1 T. Sugai *et al.*, *Nano Lett.* **3**, 769 (2003).
- 2 H.Kikuchi *et al.*, *44th Fulluerene-nanotue-graphene conference*. 1P-24
- 3 R. Sen *et al.*, *Chem. Phys. Lett.* **332**, 467 (2000).

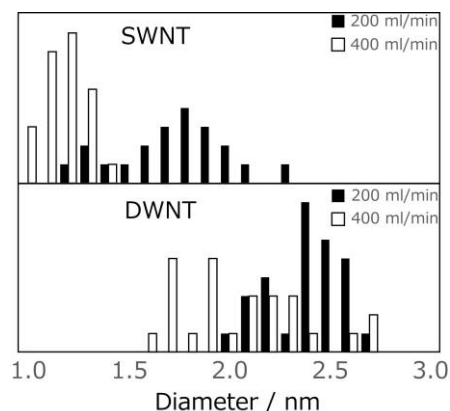


Fig. 1 Diameter dependence on flow rate

Production and characterization of graphene quantum dots

H. Morita, and T. sugai

Department of Chemistry, Toho University, Miyama 2-2-1, Funabashi 274-8510, Japan

Keywords: Fluorescent graphene quantum dots,

Graphene quantum dots (GQD) are nanometer-size graphene fragments derived from various carbonaceous materials, such as graphite and carbon nanotubes.[1] They are promising materials especially because of their unique fluorescent properties. The emission should be independent of excitation like fluorescent molecules for the applications such as biomarkers. However, the emission wavelength of GQD depend on excitation wavelength.[2] Here we present production of GQD with molecule-like fluorescence by chemical oxidation from various carbon materials.

GQD was prepared from CoMoCAT-SWNTs (Sigma-Aldrich) and graphite powder (nacalai tesque) by oxidation in a mixture of concentrated H_2SO_4 and HNO_3 . The solution was sonicated for tens of hours. The oxidized mixture was diluted with deionized water followed by centrifugation at 10000 rpm for 30 min to separate GQD. Collected supernatant containing GQD was neutralized with NaOH and re-crystallized to eliminate by-produced salt. The produced GQD was characterized by TEM, absorption, and fluorescence observation.

Fig.1 shows emission spectra of the GQD prepared from SWNTs. The emissions at 410 and 520 nm were

independent of the excitation wavelength. Those molecular like emission may come from the method utilized here, which is relatively milder than conventional ones such as reflux in concentrated H_2SO_4 and HNO_3 at high-temperature.[3] Furthermore, GQD was also derived from graphite but the production efficiency is smaller than that of GQD from SWNTs by an order of magnitude confirmed by the emission intensity. We are now enhancing the productivity of GQD and controlling the emission wavelength by changing reaction conditions.

References

1. M. Bacon, S. J. Bradly, T. Nann, *Part. Part. Syst. Charact.*, **31**, 415-428 (2014)
2. D. Pan, J. Zhang, Z. Li, M. Wu, *Adv. Mater.*, **22**, 734-738 (2010)
3. R. Sekiya, Y. Uemura, H. Naito, K. Naka, & T. Haino, *Chem. Eur. J.*, **22**, 1-10 (2016).

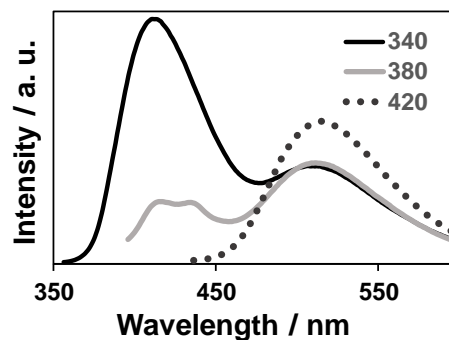


Fig.1 Emission spectra of GQD. The peak positions of 410-510 nm are independent of excitation wavelength of 350-380 nm

Coulomb Interaction in Hole-Doped Molecular Dirac Fermion Systems

Y. Akita¹, E. Tsuboi¹, S. Hayashi¹, K. Ogawa¹, N. Tajima^{1,2}, Y. Kawasugi²,
M. Suda³, H. M. Yamamoto^{2,3}, R. Kato², Y. Nishio¹ and K. Kajita¹

¹Department of Physics, Toho University, Miyama 2-2-1, Funabashi, Chiba 274-8510, Japan.

²RIKEN, Wako, Saitama, 351-0198 Japan.

³Institute for Molecular Science, Okazaki, Aichi, 444-8585 Japan.

Keywords: Dirac fermion system, Organic conductor α -(BEDT-TTF)₂I₃, Hole-doping,
Quantum transport phenomena

A massless Dirac fermion system was realized in α -(BEDT-TTF)₂I₃ under high pressure [1-6]. The Dirac fermion phase neighbors a charge-ordered insulating phase in the temperature-pressure phase diagram. Because the origin of the charge-order is nearest neighbor Coulomb interaction, massless Dirac fermion system in α -(BEDT-TTF)₂I₃ also seem strongly correlated [7, 8]. Thus, we have demonstrated that the valley polarization of zero-mode Landau level played an important role to the transport in a magnetic field at low temperatures [9].

In this work, the Coulomb interaction was examined from the detection of the valley polarization of other Landau levels. To detect this effect, magnetic field angle dependent Shubnikov-de Haas (SdH) oscillations in the hole-doped thin crystals were investigated.(Fig.1)

The valley polarization of other Landau levels were not detected. However, we found that the Zeeman effect gave rise to the crossing between Landau levels in the tilted magnetic field.

References

- [1] N. Tajima, et al., JPSJ 69 543 (2000).
- [2] A. Kobayashi, et al., JPSJ 73 3135 (2004).
- [3] S. Katayama, et al., JPSJ 75 054705 (2006).
- [4] N. Tajima, et al., EPL 80 47002 (2007).
- [5] N. Tajima, et al., PRL 102 176403 (2009).
- [6] K. Kajita, et al., JPSJ 84 072002 (2014).
- [7] D. Liu, et al., PRL 116 226401 (2016).
- [8] M. Hirata, et al., arXiv:1607.07142 (2016).
- [9] S. Hayashi, et al., private communication.

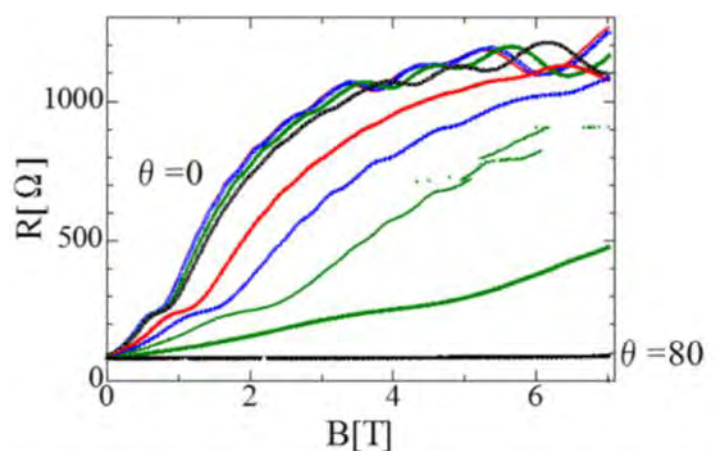


Fig.1 : Magnetic field dependence of R_{xx} for the several field angles between 0 and 80 degree at 0.5 K. We find SdH oscillations.

Angle dependent interlayer magnetoresistance in multilayered Dirac fermion systems

K. Ogawa¹, S. Hayashi¹, Y. Akita¹, N. Tajima^{1,2}, Y. Kawasugi², M. Suda³,
H. M. Yamamoto^{2,3}, R. Kato², Y. Nishio¹ and K. Kajita¹

¹Department of Physics, Toho University, Miyama 2-2-1, Funabashi, Chiba 274-8510, Japan.

²RIKEN, Wako, Saitama, 351-0198 Japan.

³Institute for Molecular Science, Okazaki, Aichi, 444-8585 Japan.

Keywords: Dirac, organic, transport, magnetoresistance

Massless Dirac fermion systems was realized in an organic conductor α -(BEDT-TTF)₂I₃ under high pressure[1]. In contrast to graphene, this is the first bulk (multilayered) system. Thus, we have established the physic of inter-layer transport in multilayered massless Dirac fermion systems. One of the characteristic transport in this system is the large negative magnetoresistance originate from the degeneracy of zero-mode (N=0) Landau level that is expected to appear at the Dirac point in the magnetic field normal to the two-dimensional plane[2].

Another important fact is that the Dirac cones are highly tilted. Thus, this system provides us a suitable testing

ground for the transport of the multilayered Dirac fermion system with tilted cones. In this work, the inter-layer transport in the magnetic field parallel to 2D plane was investigated at low temperature (Fig. 1). A focus is the peculiar coherence peak of the inter-layer magnetoresistance as shown Fig. 1. It appears over the whole of azimuthal angle in 2D plane.

References

1. N. Tajima, S. Sugawara, M. Tamura, Y. Nishio and K. Kajita, J. Phys. Soc. Jpn. **75**, 051010, (2006).
2. N. Tajima, S. Sugawara, R. Kato, Y. Nishio and K. Kajita, Phys. Rev. Lett. **102**, 176403, (2009).

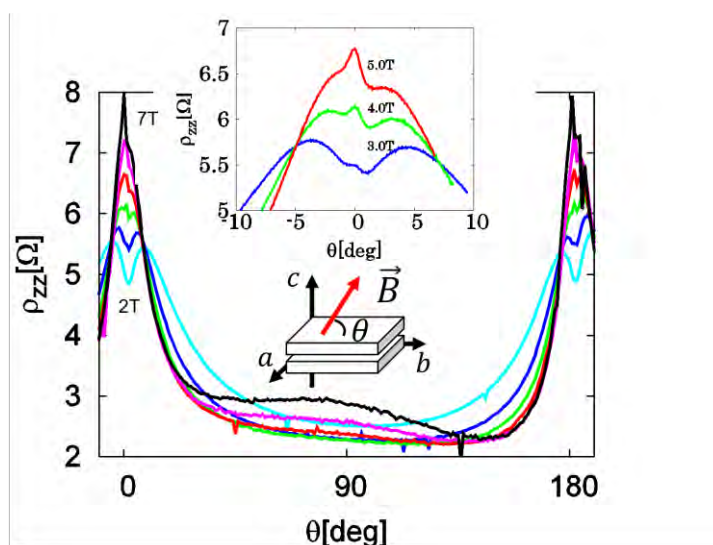


Fig.1 Angle dependent inter-layer magnetoresistance (ρ_{zz}) in the field from 2 to 7T at 4.2K.

Polyimides derived from Novel Cycloaliphatic Tetracarboxylic Dianhydride.

Hiroki SATO, Shuichi TAKAHASHI, Junichi ISHII, Masatoshi HASEGAWA

Department of Chemistry, Faculty of Science, Toho University, 2-2-1 Miyama, Funabashi, Chiba 274-8510

Keywords: Polyimides, Linear coefficient of thermal expansion, Transparency, Solubility

Recently, optically transparent high-temperature polymeric materials are strongly demanded for optoelectronic applications (in particular, as plastic substrates for flat panel display devices). If current fragile inorganic glass substrates were replaced by plastic substrates, flat panel displays could become significantly light and flexible. However, it is not easy to develop practically useful plastic substrates simultaneously possessing excellent optical transparency (non-coloration), sufficiently high heat resistance ($T_g > 300$ °C), and high ductility.

Colorless polyimides (PIs) are the promising candidates, and they can be produced by the combinations of cycloaliphatic tetracarboxylic dianhydrides and aromatic diamines without a salt formation problem during the polymerization [1]. However, mass-producible and practically useful cycloaliphatic tetracarboxylic dianhydrides are limited to hydrogenated pyromellitic dianhydride (H-PMDA). However, H-PMDA often leads to brittle PI films on the basis of its insufficient polymerizability (the resultant insufficient molecular weights), particularly when aromatic diamines with rigid/linear structures were used. Another problem is that the H-PMDA-based PI films usually do not show low coefficients of thermal expansion (CTE), because of a non-planar/non-linear steric structure at the H-PMDA-based diimide moieties. To solve these problems, in this work, we synthesized a

novel cycloaliphatic tetracarboxylic dianhydride and attempted to prepare novel low-CTE colorless PIs with good solution-processability by combining with proper aromatic diamines. The structures of the monomers used in this work are shown in Fig. 1.

We also examined the effect of the polymerization processes: the conventional two-step process (method-1), chemical imidization (method-2), and one-pot polymerization (method-3). Method-3 was most effective in enhancing the molecular weight of the PIs, consequently, in obtaining ductile PI films. As listed in Table 1, the obtained H-PMDA-based PIs (#1 and #2) provided high-quality films with very high T_g s and suppressed coloration. However, these PIs did not show low CTE property. On the other hand, the use of amide-linked diamines (#3 and #4) somewhat contributed to an appreciable decrease in the CTE.

The polyaddition of H-PMDA and 4,4'-ODA led to a relatively low inherent viscosity (η_{inh}), reflecting low reactivity of H-PMDA, whereas a novel cycloaliphatic tetracarboxylic dianhydride (X) provided a much higher η_{inh} value as listed in Table 1. This result suggests that X is superior to H-PMDA in obtaining the PI precursors with higher molecular weights. We will report the detailed properties of X-based PIs.

Reference

1. M. Hasegawa *et al.*, *Polym. Int.*, **65**, 1063 (2016).

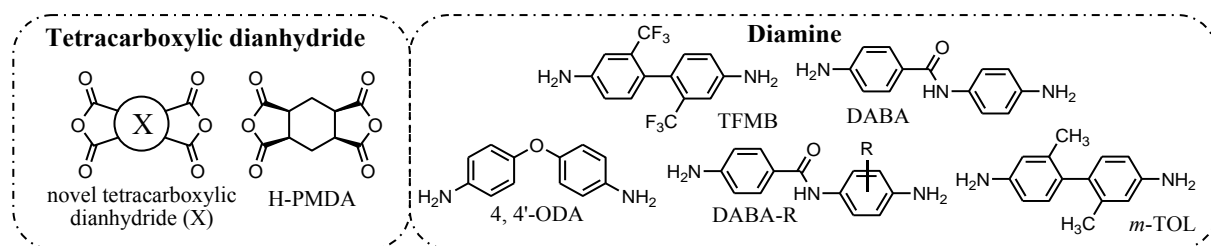


Fig.1 Molecular structures of monomers used in this work.

Table 1 Properties of PIs from cycloaliphatic tetracarboxylic dianhydrides and aromatic diamines.

系	Tetracarboxylic dianhydride	Diamine	Polym. process	η_{inh} (PI) [dL/g]	T_{400} [%]	YI	Δn	CTE [ppm/K]	T_g [°C]	ε_b (%) [Av/Max]
1	H-PMDA	TFMB	③	0.54	89.6	0.7	0.015	59.4	349	5.2/6.5
2		<i>m</i> -TOL	③	0.52	87.7	0.9	0.014	61.9	380	3.4/4.8
3		DABA(70) TFMB(30)	③	0.44	79.1	3.0	0.022	41.0	357	6.9/12.0
4		DABA-R	③	0.94	63.5	6.2	0.028	44.1	333	16.3/36.7
5		4,4'-ODA	③	0.48	86.1	1.3	0.0085	51.6	316	25.0/69.7
6		4,4'-ODA	①	0.57	83.3		0.0007	51.4	335	36.2/100.2
7		X	4,4'-ODA	①	0.88			0.0039	53.5	304

In-plane Orientation in Colorless Polyimides as Induced by Solution Casting from Polyimide Varnishes (20)

Shinya TAKAHASHI, Soichi TSUKUDA, Junichi ISHII, Masatoshi HASEGAWA

Department of Chemistry, Faculty of Science, Toho University, 2-2-1 Miyama, Funabashi, Chiba 274-8510

TEL & FAX: 047-472-1869, E-mail: mhasegaw@chem.sci.toho-u.ac.jp

Keywords: Colorless Polyimides, Coefficient of Thermal Expansion (CTE), Birefringence, Spiro-type diamine

Colorless polyimides (PI) can be key materials as heat-resistant plastic substrates alternative to heavy/fragile current inorganic glass substrates in image display devices. However, most of colorless PIs possess insufficient dimensional stability against thermal cycles in the device fabrication processes. The dimensional stability can be enhanced by decreasing the linear coefficients of thermal expansion (CTE) along the X-Y direction. However, the molecular design for reducing the CTE of colorless PI films by enhancing the main chain linearity/stiffness inevitably causes an increase in the thickness (Z)-direction birefringence ($\Delta n_{th} = n_z - n_{xy}$), which is unfavorable for applications to liquid crystal displays. In this work, we challenged to decrease both CTE and Δn_{th} by using novel spiro-type diamine monomers while keeping excellent heat resistance, transparency, and solution-processability.

The reaction schemes of PI synthesis and the molecular structures of the monomers used are shown in Fig. 1. In this work, PIs were mainly prepared via not the conventional two-step process (PI precursor casting and successive thermal imidization), but solution casting after chemical imidization in homogeneous solution, because the latter is superior to the former in obtaining lower CTE and higher transparency of the resultant PI films [1].

The properties of the PIs are shown in Table 1. A conventional PI system, CBDA/TFMB (#5), possessed excellent transparency (very high light transmittance at 400 nm: $T_{400} > 80\%$ and a low yellowness index: $YI < 4$), a relatively low CTE, but an undesirably relatively high Δn_{th} . In addition, this system was difficult to apply the chemical imidization process because of gelation during the reaction. Then we attempted a structural modification of CBDA//TFMB using novel diamine monomer, i.e., diamines incorporating a spiro structure. Copolymerization with spiro-type diamine-I (#3) permitted the formation of a colorless PI film via chemical imidization without gelation, which results from enhanced solubility, with a positive effect [an increased glass transition temperature (T_g) and a decreased Δn_{th} of the resultant PI film]. However, this approach inevitably caused a slight increase in CTE, which is probably attributed to the structure of spiro-type diamine-I. To solve this issue, we developed a modified structure of spiro-type diamine II. As shown in Table 1, the use of this diamine for copolymerization (#4) was effective in lowering CTE. We will show an effect of a spiro-type tetracarboxylic dianhydride on the properties in this report.

References

1. M. Hasegawa *et al.*, *Polym. Int.*, **65**, 1063 (2016).

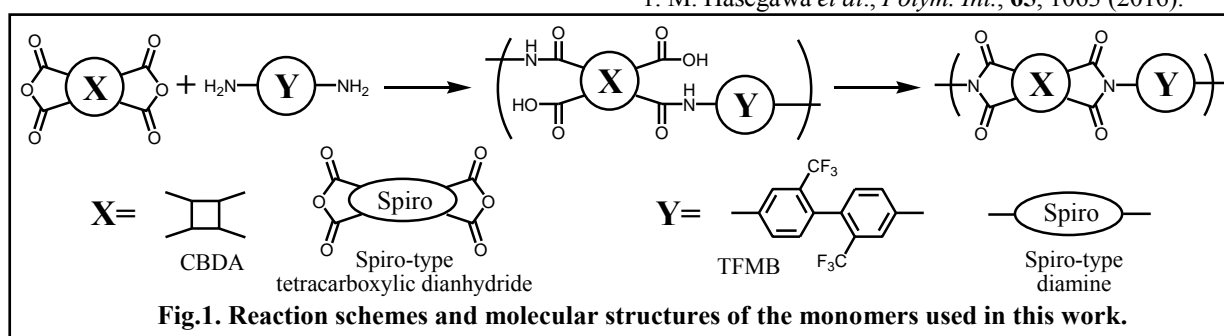


Table 1 Properties of CBDA-based PI films.

No	Diamine	Cure	η_{red} (PAA) [dL/g]	T_g [°C]	CTE [ppm/K]	Δn_{th}	T_{400} [%]	YI	Haze [%]
1	Spiro-diamine I	C	1.53	371	39.0	0.0300	79.2	5.66	1.20
2	Spiro-diamine II	C	0.94			0.0348	83.8	1.74	0.81
3	TFMB(50) Spiro diamine-I (50)	C	1.07	364	26.0	0.0378	82.8	3.67	2.29
4	TFMB(50) Spiro diamine-II (50)	C	1.26	316	17.9	0.0632	77.3	4.66	2.68
5	TFMB	T	1.63	345	22.9	0.0477	84.2	3.97	0.87

Polyalkylfluorene incorporating azomethine units for OLED applications

Yoshifumi KURIHARA, Junichi ISHII, Masatoshi HASEGAWA

Department of Chemistry, Faculty of Science, Toho University, 2-2-1 Miyama, Funabashi, Chiba 274-8510

Keywords: Polyalkylfluorene / Polyazomethine / Solubility

Polyfluorenes (PFLs) are the key materials as the emission layers in organic light-emitting diode (OLED) displays and organic thin film transistors[1,2]. However, there are some problems in PFLs, i.e., their complicated manufacturing processes involving careful purification (residual catalyst removal) procedures and an undesirable large energy gap between the PFL layer and an ITO electrode, by which the applied voltage for operating the OLED devices needs to be increased.

In contrast, another π -conjugated polymeric system, polyazomethines (PAzMs) can be easily prepared by the conventional low-temperature polycondensation process from aromatic dialdehydes and diamines, although PAzMs tend to be poorly soluble in common organic solvents because of the chain rigidity based on the $-C=N-$ linkages in the PAzM backbones [3]. To solve these problems, we designed di-*n*-octyl-substituted PFLs incorporating azomethine (AzM) units. In this work, we propose AzM-modified PFLs and an approach for ensuring their high solubility in common non-polar solvents such as toluene. PFLs are usually polymerized by the Suzuki-Miyaura cross coupling reaction between the dioxaborolan derivatives and aryl dibromide compounds under the presence of palladium(0) as a catalyst. In this work, first of all, we attempted the coupling reaction from

3-bromo-*N*-(3-bromobenzylidene)aniline with 2,7-bis(4,4,5,5-tetramethyl-1,3,2-dioxaborolan-2-yl)-9,9-di-*n*-octylfluorene as shown in **Fig.1(a)**, whereby distorted meta-linkages are introduced into the main chains, as a result, good solubility can be maintained. As expected, the obtained PAzMs showed excellent solubility in toluene and tetrahydrofuran (THF). However, this conventional process was less effective to obtain sufficiently high molecular weights as suggested from the resultant low weight-average molecular weight ($M_w = 2.8 \times 10^3$). The result is probably attributed to the low reactivity of the *meta*-type dibromide. As an alternative approach, we synthesized new monomers for the formation of AzM linkages: alkylfluorene-based dialdehyde (*m*-OFDAL) and diamine counterpart (*m*-OFDA) as shown in **Fig.1(b)**. In this work, we report the reactivity of the improved polymerization process and the properties of the resultant AzM-modified PFLs, i.e., solubility, photoluminescence properties, and the HOMO/LUMO energy levels.

References

1. D. Neher, *Macromol. Rapid. Commun.*, **22**, 1365–1385 (2001).
2. H. Sirringhaus *et al.*, *Appl. Phys. Lett.*, **77**, 406–408 (2000).
3. P. W. Morgan *et al.*, *Macromolecules*, **20**, 729–739 (1987).

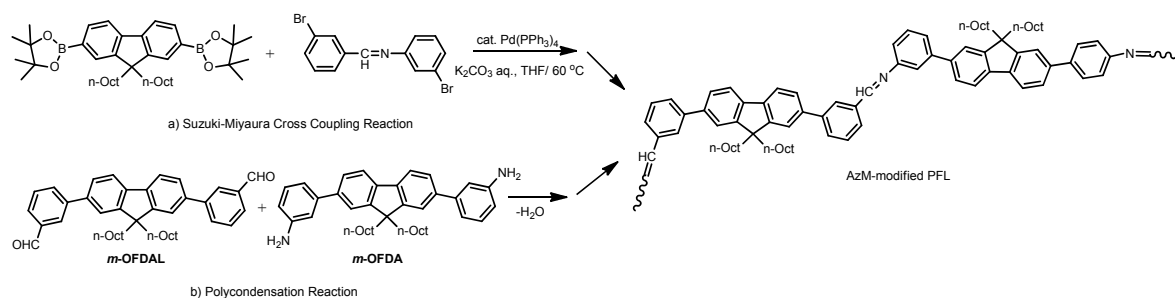


Figure 1 Polymerization schemes for AzM-modified PFLs: (a) Suzuki-Miyaura cross coupling and (b) Polycondensation of dialdehyde and diamine.

Polybenzoxazoles with Low Coefficient of Thermal Expansion. Effect of Amide-containing Bis(*o*-aminophenol)

Ryosuke WATANABE, Junichi ISHII, Masatoshi HASEGAWA

Department of Chemistry, Faculty of Science, Toho University, 2-2-1 Miyama, Funabashi, Chiba 274-8510

Keywords: Polybenzoxazoles / Coefficient of thermal expansion / Solubility / Amide-containing Bis(*o*-aminophenol)

The progress of recent semiconductor technologies requires the use of thinner silicon wafers for LSI chip fabrications. Such trend causes a forthcoming serious problem, i.e., wafer deformation arising from the coefficient of thermal expansion (CTE) mismatching between the Si wafers ($\text{CTE} = 3 \text{ ppm K}^{-1}$) and polybenzoxazole (PBO) buffer-coat films ($\text{CTE} \sim 60 \text{ ppm K}^{-1}$) formed on them as a protection layers for LSI chips [1]. To solve this problem, in this work, we attempted to develop a low-CTE PBO system using an amide-containing bis(*o*-aminophenol) as a monomer for PBO precursors (polyhydroxyamide; PHA).

Fig.1 shows the molecular structures of monomers and the reaction schemes of PHA polycondensation through the silylation method using trimethylsilyl chloride [2] and thermal cyclodehydration of PHAs toward PBOs. **Table 1** lists the reduced viscosities of PHAs, the light transmittance (T_{365}) of PHA films (18–21 μm thick) at 365 nm (*i*-line of a high-pressure mercury lamp as a standard light source for fine patterning), and basic properties of PBO films (#3) together with comparative systems (#1 and #2). PHA

(#3) derived from the amide-containing bis(*o*-aminophenol) and *trans*-1,4-cyclohexanedicarboxylic acid dichloride (t-CHDOC) possessed a high molecular weight as suggested from its high reduced viscosity at 0.5 wt% (2.0 dL g^{-1}), and the PHA powder sample (#3) isolated from the as-polymerized PHA solution showed good solubility of 14.5 wt% in *N*-methyl-2-pyrrolidone (NMP) at room temperature, although a significant decrease in the transparency at 365 nm was observed. The thermally cured amide-containing PBO film (#3) displayed a high glass transition temperature ($T_g = 354 \text{ }^\circ\text{C}$) and low CTE value of 34.4 ppm K^{-1} in comparison with conventional 6FAP-based PBO films (#1 and #2). The relatively low CTE value is attributed to a linear/rigid chain structure of PBO (#3) by the combination of the amide-containing bis(*o*-aminophenol) and t-CHDOC.

References

1. T. Bamba, *J. Chem. Eng. Jpn.*, **75**, 58–60 (2011) (in Japanese).
2. Y. Maruyama *et al.*, *Macromolecules*, **21**, 2305–2309 (1988).

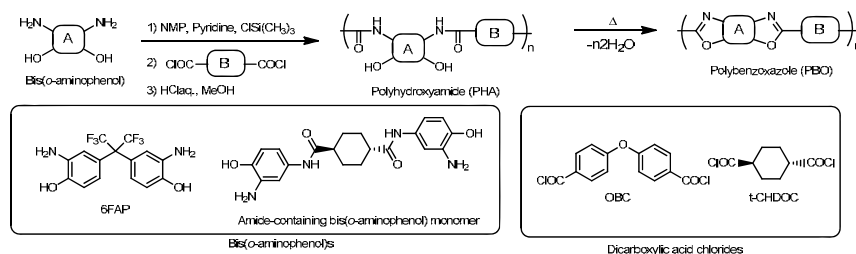


Fig.1 Polymerization scheme and molecular structures of monomers used in this work.

Table 1 The reduced viscosities of PBO precursors (PHAs) and film properties of PHAs and PBOs.

System No.	Bis(<i>o</i> -aminophenol)	Dicarboxylic acid chloride	Solubility of PHA in NMP [wt%]	η_{red} (PHA) [dL g^{-1}]	T_{365} (PHA) [%]	PBO films		
						T_g [$^\circ\text{C}$]	CTE [ppm K^{-1}]	$T_d^{5\%}$ [$^\circ\text{C}$]
1	6FAP	OBC	23.0	0.40	84.8	298	58.2	542
2	6FAP	t-CHDOC	26.2	0.35	70.5	254	80.9	496
3	Amide-containing bis(<i>o</i> -aminophenol)	t-CHDOC	14.5	2.0	29.3	354	34.4	457

Effect of chemical substitution on the relaxation time distribution for a spin ice compound $\text{Dy}_2\text{Ti}_2\text{O}_7$

Akira Horikawa*, Masaki Azuma*,

Eiji Wada*, Daisuke Akahoshi***, and Toshiaki Saito***

* Dept. Phys., Toho Univ.

** Research Center for Materials with Integrated Properties, Toho Univ.

Keywords: Frustration, Spin ice, Magnetic relaxation

Both A-site and B-site of pyrochlore oxide $\text{Dy}_2\text{Ti}_2\text{O}_7$ form the pyrochlore sub-lattices. The pyrochlore structure is composed of tetrahedral units sharing their vertexes. $\text{Dy}_2\text{Ti}_2\text{O}_7$ has a magnetic frustration originating from the competition between the effective ferromagnetic interaction and the uniaxial anisotropy. The four spins in a A-site tetrahedral unit are located on the vertexes of the tetrahedron and the easy axes of the uniaxial anisotropy are directed from the each vertex to the center of the tetrahedron. In the ground state, two Dy spins in a tetrahedron point into the center of the tetrahedron, and the other two spins point out, which is called “ice rules”. The frustration arised from the ice rules generates huge degeneracy in the ground state of spin ice network, that is, “spin ice state”. It was reported [1] that the magnetic relaxation process in the spin ice state of $\text{Dy}_2\text{Ti}_2\text{O}_7$ is represented by the Davidson-Cole (DC) model with a wide distribution of relaxation time. Recently, the relaxation process in the spin ice state is interpreted by the monopole model [2]. However, the distribution of relaxation time in the spin ice state cannot be explained by such a monodispersive model. So, the origin of the distribution of relaxation time observed in $\text{Dy}_2\text{Ti}_2\text{O}_7$ has not be revealed. To clarify the origine, we have investigated the effect of chemical substitution of A-site and B-site atoms (disorder) on the magnetic relaxation of $\text{Dy}_2\text{Ti}_2\text{O}_7$, and discussed the effect of disorder in the spin ice on the distribution of relaxation time. We prepared six series polycrystal samples, $(\text{Dy}_{2-x}\text{Y}_x)\text{Ti}_2\text{O}_7$, $(\text{Dy}_{2-x}\text{La}_x)\text{Ti}_2\text{O}_7$, $(\text{Dy}_{2-x}\text{Ho}_x)\text{Ti}_2\text{O}_7$, $\text{Dy}_2(\text{Ti}_{2-x}\text{Sn}_x)\text{O}_7$, $\text{Dy}_2(\text{Ti}_{2-x}\text{Zr}_x)\text{O}_7$, and $\text{Dy}_2(\text{Ti}_{2-x}\text{Dy}_x)\text{O}_{7-x/2}$. Their structures were determined by

X-ray diffraction, and the AC susceptibilities were measured by Magnetic Properties Measurement System (MPMS). The Cole-Cole plots obtained by the AC susceptibility results were analysed by the Havriliak-Negami model which includes the DC model. From the results, we found that (1) the relaxation time becomes shorter with increasing x (the amount of substitution) for all series, (2) the distribution of relaxation time, however, is not almost changed by any substitution (until 2 %) in all series samples. These results suggest that (1) the relaxation time is shortened by the distortions due to the substitution, and (2) the spin ice network, however, holds until 2 % substitution, which implies that the distribution of relaxation time is essential even in the pure spin ice state and independent of the disorder.

References

- [1] K. Matsuhira *et al.*: J. Phys. Cond. Mat. **13** (2001) L737
- [2] for instance, H. M. Revell *et al.*: Nat. Phys. **9** (2013) 34

Effect of random anisotropy on critical lines in H-T plane for a RKKY Heisenberg-type spin glass amorphous GdSi system

Koki Kato*, Ryosuke Motoki*, Hiroshi Kobayashi*, Kazuya Nakazawa*,
Eiji Wada**, Daisuke Akahoshi*,** and Toshiaki Saito*,**

*Dept. of Phys., Toho Univ.,

**Research Center for Materials with Integrated properties, Toho Univ.

Keywords: spin glass, amorphous, anisotropy, thin film

Spin glass (SG) is a random magnet in which both ferromagnetic and antiferromagnetic interactions coexist and compete, thereby giving frustration. Typical SG materials are dilute magnetic alloys such as AuFe and CuMn, which are called canonical SG. These systems have the RKKY interaction which couples spins through conduction electrons, and the SG magnetic transition occurs by this interaction.

Up to now, pure Heisenberg SG with no random anisotropy has not yet been found experimentally because some anisotropy in the alloys affects the critical phenomena. Thus, purpose of our study is to find experimentally the pure H-T phase diagram in Heisenberg SG with no anisotropy. The H-T phase diagram is very important to discuss the phase transition in SG. If we will find such a new SG material with pure H-T phase diagram, the material will become a standard system to investigate the effect of anisotropy on the SG phase transition. We selected amorphous (a-)GdSi as a candidate of such a material with no anisotropy. The a-GdSi system was firstly investigated by F. Hellman *et al.* and they found that this material shows SG transition due to the RKKY interaction in a range of $3.6 \leq x \leq 19$ [1]. But, further SG property such as magnetic behavior in dc field is not known. Therefore we research dc properties and the H-T phase diagram for a-Gd_xSi_{100-x}. We deposited thin films using the sputtering method and measured magnetic properties by MPMS.

It is theoretically reported that the H-T phase diagram has only single critical line (AT-line) in a low field region for the Heisenberg SG materials with random anisotropy [2]. On the other hand, in the case of no

anisotropy, the H-T phase diagram has the two critical lines (GT-line and AT-line). As seen in Fig.1, our experimental result of H- τ phase diagram in a-Gd₁₅Si₈₅ has two critical lines even in the low field region. This result indicates that a-Gd₁₅Si₈₅ is pure Heisenberg SG system with no influence of random anisotropy, which has not been reported until now as far as we know. In our poster presentation, we will report result of ac and dc susceptibility measurements and the H-T phase diagram in other compositions of a-Gd_xSi_{100-x} ($10 \leq x \leq 60$).

References

- [1] F. Hellman *et al.*: Phys. Rev. Lett. **84** (2000) 5411.
- [2] G.G. Kenning *et al.*: Phys. Rev. Lett. **66** (1991) 2923.

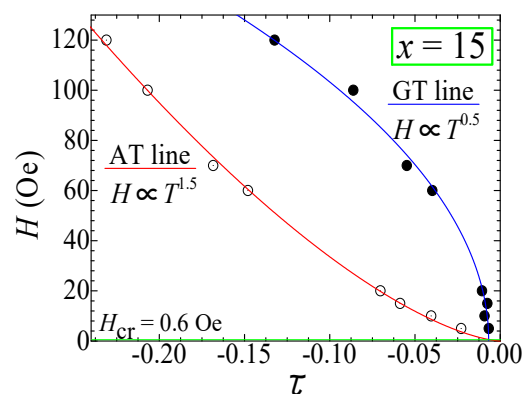


Fig.1 H- τ ($\tau \equiv (T-T_g)/T_g$) phase diagram
in a-Gd₁₅Si₈₅

T_g : transition temperature in zero field

Effect of R -site randomness on the physical properties near the multicritical point in ordered $R\text{BaMn}_2\text{O}_6$

N. Tanikawa*, H. Takada*, M. Hori*, E. Wada**, R. Oda***, H. Kuwahara***, D. Akahoshi***, and T. Saito***

*Dept. of Phys., Toho Univ., **Research Center for Materials with Integrated Properties, Toho Univ.,

***Dept. of Phys., Sophia Univ.

Keywords: Perovskite manganite, Colossal magnetoresistance (CMR) effect, Strongly correlated electron system

Mn oxides with perovskite structure have attracted much interest because of a gigantic reduction in the resistivity by application of magnetic fields, called colossal magnetoresistance (CMR) effect [1]. In the case of perovskite manganites with small randomness, the FM and CO/OO phases tend to form the bicritical region in the electronic phase diagram, where the CMR effect, *i.e.*, field-induced transition from the CO/OO to FM states, is observed. $R\text{BaMn}_2\text{O}_6$ (R = rare-earth) has a derivative perovskite structure, in which a regular arrangement of RO and BaO layers are sandwiched with MnO_2 layer (Fig.1). In $R = \text{Nd}$, there exists a multicritical point around room temperature, where the CO/OO phase, the FM phase, and the A-type antiferromagnetic (AF(A)) phases meet [2]. Thus,

$R\text{BaMn}_2\text{O}_6$ is a candidate material for potential application using the CMR effect. Structural randomness is one of the effective tools for electronic phase control. It is well-known that near the multicritical point, structural randomness largely affects the physical properties and enhances large phase fluctuation, which is indispensable for the CMR.

In this study, we have investigated the effect of R -site randomness on the physical properties of $R\text{BaMn}_2\text{O}_6$ near the multicritical point. We introduce randomness into R -site by employing a large mismatch in the ionic radii between two different R^{3+} ions (Fig.2).

References

1. Y. Tokura, Rep. Prog. Phys. **69**, 797 (2006).
2. D. Akahoshi, *et al.*: Phys. Rev. B **70**, 064418 (2004).

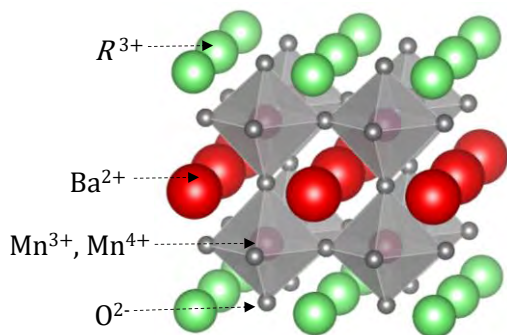


Fig.1. Crystal structure of $R\text{BaMn}_2\text{O}_6$.

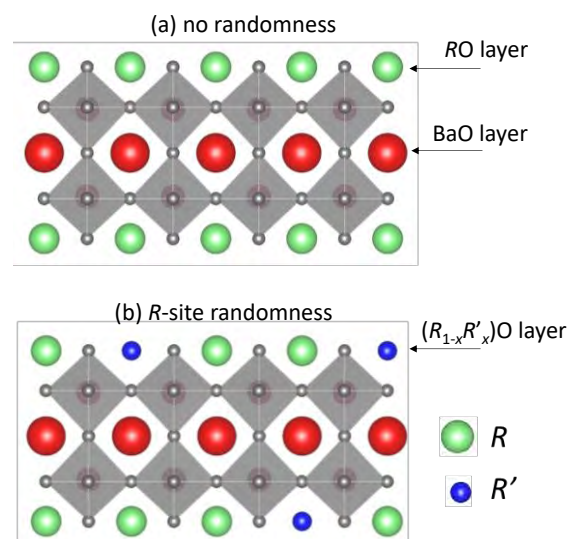


Fig.2. Schematic structure of $R\text{BaMn}_2\text{O}_6$ (a) without and (b) with R -site randomness.

Magnetolectric properties for perovskite-type oxide

$\text{EuTi}_{1-x}\text{Al}_x\text{O}_3$ ($0 \leq x \leq 1$)

S. Koshikawa*, T. Nagase*, E. Wada**, K. Nishina***, R. Kajihara***,
H. Kuwahara***, D. Akahoshi***, and T. Saito***

* Dept. of Phys., Toho Univ.

** Research Center for Materials with Integrated Properties, Toho Univ.

*** Dept. of Phys., Sophia Univ.

Keywords: Perovskite oxide, Magnetic properties, Magnetolectric effect

Perovskite-type Eu titanate EuTiO_3 (ETO) has attracted much interest because of strong coupling between electric and magnetic properties. *B*-site cation Ti^{4+} is surrounded by six-oxygen atoms to form TiO_6 octahedron. TiO_6 octahedra are connected with each other through oxygen atoms. Eu^{2+} is located at *A*-site that is coordinated with 12-oxygen atoms. Since Ti^{4+} is non-magnetic, the magnetic properties of ETO arise from localized *4f* spins of Eu^{2+} ($J = S = 7/2$). In spite of the positive Curie-Weiss temperature $T_{\text{CW}} = +3$ K, the ground state of ETO is an antiferromagnetic (AFM) insulator with $T_{\text{N}} = 5$ K, indicating that the AFM and ferromagnetic (FM) interactions compete with each other. At low temperatures, large magnetocapacitance is observed [1].

Recently, we reported that the effect of substitution of Ti^{4+} with non-magnetic ions such as Al^{3+} , Ga^{3+} , and Zr^{4+} on the magnetic properties of ETO [2]. As a result, we have revealed that $\text{EuTi}_{1-x}\text{Al}_x\text{O}_3$ (ETAO) is a FM insulator with the mixed valence state of $\text{Eu}^{2+}/\text{Eu}^{3+}$ and

that the mixed valence state plays a crucial role in the FM behavior. In this study, we have prepared heavily-doped ETAO with $0.1 < x \leq 1$ by an arc-melting method, and investigated the magnetic properties, and the magnetic phase diagram has been established from the present results.

Figure 2 shows the temperature dependence of the magnetization of ETAO. The ground state of ETO ($x = 0$) is an AFM insulator. Substitution of Al^{3+} creates FM domains in the AFM matrix. With increasing x , the FM domains are developing, and the FM correlation is most enhanced around $x = 0.2 - 0.25$.

References

1. T. Katsufuji, *et al.*: Phys. Rev. B **64**, 054415 (2001).
2. D. Akahoshi, *et al.*: Appl. Phys. Lett. **103**, 172407 (2013).

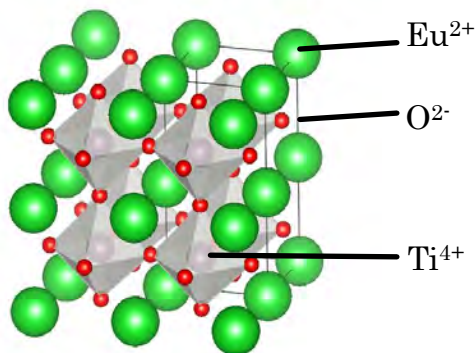


Fig.1 Crystal structure of ETO.

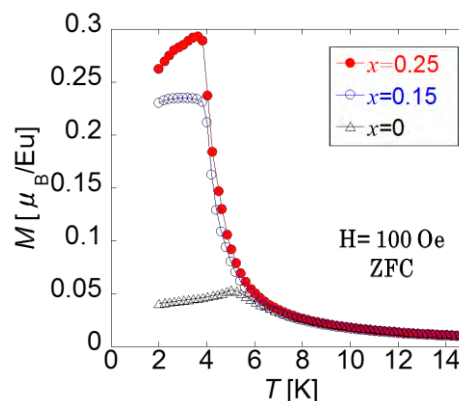


Fig.2 Temperature dependence of magnetization of ETAO.

Effect of random uniaxial anisotropy on critical lines in H-T plane for a RKKY Heisenberg spin glass amorphous GdDySi system

Ryosuke Motoki^{**}, Koki Kato^{**}, Hiroshi Kobayashi^{*}, Kazuya Nakazawa^{**},
Masaya Mitsuishi^{**}, Eiji Wada^{*}, Daisuke Akahoshi^{***}, and Toshiaki Saito^{***}

^{*}Research Center for Materials with Integrated Properties, Toho Univ.

^{**}Dept.Phys., Toho Univ.

Keywords: spin glass, amorphous, anisotropy, thin film

In the canonical spin glasses (SG) such as AuFe and CuMn, the Ising-like critical line (AT line) in the H - T plane is observed [1], which arises from the effect of “random unidirectional anisotropy” originating from Dzyaloshinskii-Moriya interaction. With increasing dc magnetic field, H , two critical lines are observed in the H - T plane (AT line and GT line). On the other hand, it has not yet examined experimentally how “random uniaxial anisotropy” influences the SG phase transition. Thus, we investigated the influence of the “random uniaxial anisotropy” by substituting anisotropic Dy for Gd in amorphous (a-)Gd₂₇Si₇₃ [2] Heisenberg SG.

We prepared the thin films of a-Gd_{27-x}Dy_xSi₇₃ by using the RF magnetron sputtering method. The amorphous structure is confirmed by X-ray diffraction. The composition is determined by EPMA and magnetization is measured by MPMS.

For the a-Gd₂₇Si₇₃ parent material, we found a thermal hysteresis between Field-cooling magnetization and Zero-field cooling magnetization below the

transition temperature (T_g). Furthermore, $\text{Re } \chi$ of ac susceptibility exhibits a cusp at T_g and the inverse susceptibility $1/\text{Re } \chi$ is linear down to just T_g . Therefore, a-Gd₂₇Si₇₃ shows the feature of canonical SG. In the H - T plane, only the AT line is observed in low field region (Fig.1). This behaviour may be responsible for the effect of weak “random unidirectional anisotropy” as well as CuMn [1].

For $x=1$ (a-Gd₂₆Dy₁Si₇₃), the AT transition is observed only for the extremely low field region in the H - T plane. For $x=3$ (a-Gd₂₄Dy₃Si₇₃), the space of two critical lines in the H - T plane opens for $H=0$ (Fig.2). This behaviour seems to be the effect of the “random uniaxial anisotropy” or the effect of a coherent anisotropy in the thin film.

Reference

- [1]G.G.Kenning *et al*:Phys.Rev.Lett. **66**(1991)2923
[2]F.Hellman *et al*:Phy.Rev.Lett. **84**(2000)5411

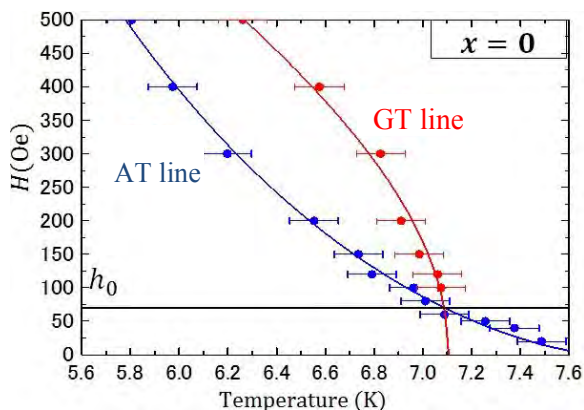


Fig.1 The critical lines for H - T plane of Gd₂₇Si₇₃

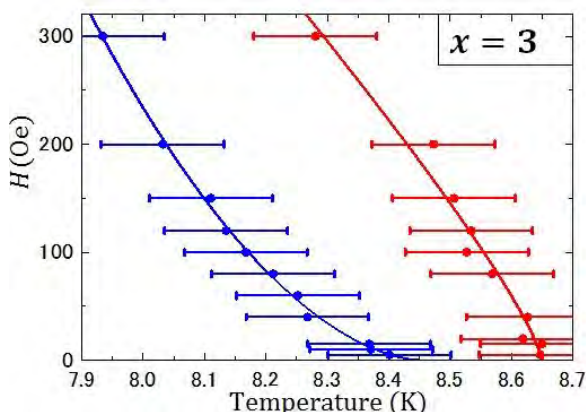


Fig.2 The critical lines for H - T plane of Gd₂₄Dy₃Si₇₃

Dependence of Ag/Cr interfacial frustration on the growth temperature for epitaxial Fe/Ag/Cr trilayers

K. Yokoyama*, E.Wada**, K.Kato*, R.Onodera*, D.Akahoshi*** and T.Saito***

* Research center for Materials with Integrated Properties, Toho Univ.

** Dept. Phys., Toho Univ

Keywords: interfacial frustration, magnetic viscosity, quantum well, epitaxial film

We have investigated the Fe/Cr interfacial frustration in epitaxial Fe/Cr bilayers by measuring the time dependence of the remanent magnetization. In the case of atomically disordered interface, not all ferromagnetic and antiferromagnetic interactions (Fe-Fe, Fe-Cr and Cr-Cr) are satisfied at the same time since they compete with each other, which is called interfacial frustration. We reported (in Ref.[1]) that the interfacial frustration and the long term relaxation (slow dynamics) are related each other.

Recently, we found the slow dynamics for epitaxial Fe/Au/Cr and Fe/Ag/Cr trilayers in spite of the separation between ferromagnetic Fe layer and antiferromagnetic Cr by nonmagnetic Au or Ag. We proposed a model that these phenomena arise from Au/Cr or Ag/Cr interfacial frustration originating from Au or Ag quantum well formation. To confirm the mechanism of such phenomenon, we examined the growth temperature (T_s) dependence of the slow dynamics for Fe/Ag/Cr (the atomic disorder at the interface can be partly controlled by T_s). We prepared epitaxial Fe/Ag/Cr trilayers at various Ag thicknesses and at various growth temperatures by using Molecular Beam Epitaxy (MBE) method. The relaxation of magnetization was measured by magnetic property measurement system (MPMS).

The slow dynamics is represented as following equation, $M_{TRM}(t)=M_0-S\ln t$, where S is a degree of slow dynamics and called magnetic viscosity, and M_0 is magnetization at the start of measurement. Fig.1 and Fig.2 show S of Fe/Ag/Cr as a function of Ag thickness for $T_s=100^\circ\text{C}$ and 50°C , respectively. For both samples, S is oscillated for Ag thickness with almost the same period (12.9Å for $T_s=100^\circ\text{C}$ and 11.8Å for $T_s=50^\circ\text{C}$).

This oscillation is responsible for the “Ag/Cr interfacial frustration originating from Ag quantum well formation”. Since only minority spins contribute the Ag quantum well, spin polarization of Ag occurs, and it is varied by Ag thickness[2], changing the degree of Ag/Cr frustration. Therefore, the period of spin polarization may correspond to that of S . On the other hand, the amplitude of the oscillation of S for $T_s=100^\circ\text{C}$ is about four times larger than that for $T_s=50^\circ\text{C}$, which may arise from enhancement of atomic disorder in the Ag/Cr interface, that is, enhancement of frustration.

In our poster presentation, we discuss them in details.

References

[1]. M. Nomura, T. Koba, R. Nakamura, C. Kanadani, D. Akahoshi, and T. Saito, J. Phys. : Conf. **320** (2011) 012042

[2] J. E. Ortega et al. Phys. Rev. B **47** (1993) 1540

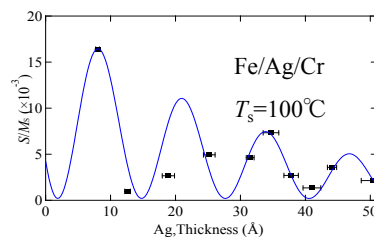


Fig.1 Ag thickness dependence of S/M_s for Fe/Ag/Cr trilayers ($T_s=100^\circ\text{C}$)

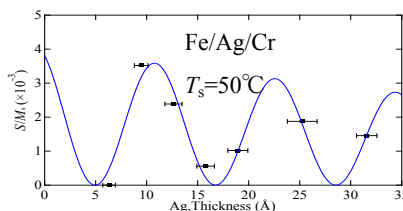


Fig.2 Ag thickness dependence of S/M_s for Fe/Ag/Cr trilayers ($T_s=50^\circ\text{C}$)

Sponsors



あなたはThemisを見たか？ Zとの遭遇

軽元素までの容易な分析、通常では困難なビーム脆弱材料のSTEM観察、
FEI Themis Zは周期律表のすみずみまで、あなたの探求のお手伝いをいたします。

Discover more at FEI.com





Spartan'16

For Windows, Macintosh and Linux



iSpartan

WAVEFUNCTION



米国法人 **Wavefunction, Inc.**
日本支店

〒102-0083 東京都千代田区麹町3-5-2
BUREX麹町

TEL : 03-3239-8339
FAX : 03-3239-8340
Email : japan@wavefun.com
URL : <http://www.wavefun.com/japan>

D8 VENTURE, D8 QUEST

Large Area CPAD Single Crystal Diffraction System



**Shutterless
CPAD!!**

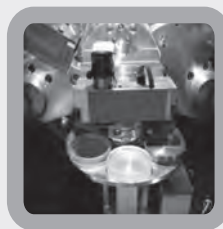
CPAD leads to new SC-XRD world !

- PHOTON II Large Area, High Speed Shutterless
140 mm x 100 mm, Air-cooled, Monolithic sensor
- I μ S 3.0 3rd Generation High Brilliance Microfocus X-ray Generator
Air-cooled, Very Low Power Consumption, Long Life Time
- METALJET New Liquid Metal Very High Brilliance X-ray Generator
Low Power Consumption, Highest Brilliance Source in Laboratory
- APEX3 Suite Most Suitable Structure Analysis Software
SHELX based, All-in-One Software



D2 PHASER 2nd Generation

All-in-One Tabletop X-ray Diffraction System



High Speed 1D detector mounted XRD system !

- LYNXEYE Silicon Stripped 1 Dimensional High Speed Detector
- θ / θ Vertical Goniometer
- Utility : 100-250V AC only. No Water supply.
- No Alignment, No Instrument Configuration.
- Single position / Motorized 6 position sample stage

DIFFRAC.EVA

- Phase Analysis
 - ICDD PDF2, PDF4
 - User defined database
 - XRD-XRF combined analysis
- Quantitative Analysis
 - RIR method
 - Report Function

Bruker AXS K.K.

URL : <http://www.bruker.com/jp/>
E-mail : Info.BAXS.JP@bruker.com

● YOKOHAMA office
3-9 Moriya-cho Kanagawa-ku Yokohama-shi
Kanagawa 221-0022 JAPAN
Tel.+81-45-453-1960 Fax. +81-45-453-1825

● OSAKA office
1-8-29 Nishimiyahara Yodogawa-ku Osaka-shi
Osaka 532-0004 JAPAN
Tel.+81-6-6393-7822 Fax. +81-6-6393-7824



Kanto Reagents

高純度溶媒

Primepureシリーズ

これまでにない最高品位を誇る新しい試薬の誕生です。

Primepure
の特徴

30項目を超える
保証スペック

- ◆ 金属不純物 (20元素以上) をppbレベルで保証
- ◆ 有機不純物を低減

最高品位

▶ 製品例

	包装	純度
アセトン	1L	>99.9% (GC)
アセトニトリル	1L	>99.9% (GC)
ジクロロメタン	1L	>99.9% (GC)
N,N-ジメチルホルムアミド	1L	>99.9% (GC)
エタノール	1L	>99.9% (GC)
ヘキサン	1L	>96.0% (GC)
2-プロパノール	1L	>99.9% (GC)
トルエン	1L	>99.9% (GC)



関東化学株式会社 試薬事業本部

〒103-0022 東京都中央区日本橋室町2-2-1 (03) 6214-1090

〒541-0048 大阪府中央区瓦町2-5-1 (06) 6231-1672

〒812-0007 福岡市博多区東比恵2-22-3 (092) 414-9361

<< <http://www.kanto.co.jp> E-mail: reag-info@gms.kanto.co.jp >>